

***In vivo* and *in vitro* characterization of annexin-3
from *Brassica juncea* L. Czern & Coss (*BjAnn3*)
concerning oxidative stress response**

Thesis submitted for the award of the degree of
Doctor of Philosophy

By

Ahan Dalal

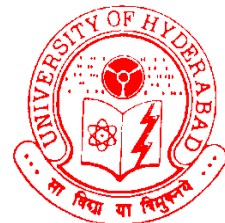


**Department of Plant Sciences,
School of Life Sciences
University of Hyderabad,
Hyderabad-500 046
Andhra Pradesh, India**

August 2013

University of Hyderabad

Department of Plant Sciences, School of Life Sciences,
P.O. Central University, Gachibowli, Hyderabad-500 046, INDIA



Declaration

This is to certify that I, Ahan Dalal, have carried out the research work embodied in the present thesis entitled “*In vivo and in vitro* characterization of annexin-3 from *Brassica juncea* L. Czern & Coss (*BjAnn3*) concerning oxidative stress response” and submitted for the degree of Doctor of Philosophy under the supervision of Prof. P. B. Kirti, Department of Plant Sciences, School of Life Sciences, University of Hyderabad, Hyderabad-500046. I declare to the best of my knowledge that no part of this thesis was earlier submitted in part or in full, for the award of any research degree or diploma from any University.

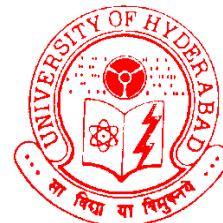
Date:

Ahan Dalal

(Regd. No.: 06LPPH07)

University of Hyderabad

Department of Plant Sciences, School of Life Sciences,
P.O. Central University, Gachibowli, Hyderabad-500 046, INDIA



Certificate

This is to certify that the present thesis entitled “*In vivo and in vitro* characterization of annexin-3 from *Brassicajunceal. Czern & Coss (BjAnn3)* concerning oxidative stress response” is a bonafideresearch work done by **Mr. Ahan Dalal**, Ph.D Scholar, Department of Plant Sciences, School of Life Sciences, University of Hyderabad. This thesis has beensubmitted by Mr. Ahan Dalal for the degree of Doctor of Philosophy in Plant Sciences and has not been submitted previously in part or in full or by any other University or Institution for the award of any degree or diploma.

Prof. P B Kirti

(Supervisor)

Head

Department of Plant Sciences

Dean

School of Life Sciences

***Dedicated to My
Beloved Grandparents
& Parents***



Acknowledgments

With great pleasure I express my deep sense of gratitude to my supervisor Prof. P.B. Kirti for his constant guidance, encouragement and support during the course of my research work which helped me to complete my Ph. D successfully.

My sincere thanks to Prof. R.P. Sharma, Dean of School of Life Sciences; Prof. M. Ramanadham and Prof. A.S. Raghavendra, former Deans of School of Life Sciences, for allowing me to use the school facilities for my research work.

Thanks are due to Prof. Ch. Venkat Ramana, Head of Department of Plant Sciences; Prof. Attipalli R. Reddy, Prof. Appa Rao Podile and Prof. P.B. Kirti former Heads of Department of Plant Sciences, for all common research facilities and administrative support concerning my research work.

I am grateful to Dr. J.S.S. Prakash and Dr. G. Padmaja, my doctoral committee members, for their valuable suggestions and kind support.

I take this opportunity to thank Dr. Mrinal Kanti Bhattacharyya, Department of Biochemistry and Dr. Sunanda Bhattacharyya, Department of Biotechnology, University of Hyderabad, for guiding me in my research work concerning yeast genetics and yeast molecular biology.

I am highly grateful to Prof. Karl-Josef Dietz and Dr. Andrea Viehhauser, Department of Plant Biochemistry and Physiology, Faculty of Biology, University of Bielefeld, Germany, for providing me scholarship along with research facilities to work with their group and helping me with their expert guidance.

My sincere thanks to Prof. Karl-Heinz Kogel, Dr. Jafargholi Imani and Dr. Gregor Langen, Department of Phytopathology, University of Giessen, Germany, for providing me research facilities to work with their group and helping me with their expert guidance.

I am grateful to Dr. Mohan Rao, Dr. T. Ramakrishna Murthy, Centre for Cellular and Molecular Biology and their research scholar Mr. Kranthi Kiran Akula for

providing me research facilities and guiding me with biophysical experiments for my research work.

My sincere thanks to Dr. KPMSV Padmasree, Department of Biotechnology, University of Hyderabad and her research scholar Mr. Abhay Pratap Vishwakarma for helping and guiding me with oxygraph experiments for my research work.

I thank all the faculty members and research scholars of School of Life Sciences, University of Hyderabad, for providing the necessary help in several aspects throughout my Ph. D tenure.

I thank Dr. Syed Maqbool Ahmed, Principal Scientific Officer and Ms. Nalini, Technician, Central Instrumentation Laboratory (CIL), for their help with confocal microscopic studies.

I express my heartfelt thanks to my former and present lab members Rajesh, Srinivasan, Sravan, Swathi, Sudar,Vijayan, Ashraf, Pushyami, Srinivasa Reddy, Naveen, Pawan, Dilip, Moin, Israr, Deepanker, Satish, Upender, Uday, Beena, Divya, Jinu, Triveni, Akanksha, Jyostna, Trishla, Achala, Kumari and Sakshi for their support and timely help.

I extend my heartfelt appreciation to Lab attendants Mr. Kishan, Mr. Abuzer and Mr. Satish for their help in lab and in greenhouse.

I also thank all the non-teaching staff members of Department of Plant Sciences and School of Life Sciences for their help in official works during my research period.

I am grateful to the University of Hyderabad; DAAD; DST-DAAD; DST-PURSE; DWIH; DFG; The Collaborative Research Center SFB (613), Bielefeld University; UoH-DBT-CREBB and Keystone Symposiafor providing financial assistance in the form of fellowship and/or travel grants.

I acknowledge UGC, CSIR, DBT, DST, DBT-CREBB, DST-FIST, UGC-SAP, ICAR for research funding to laboratory, all departments in/and School of Life Sciences.

I am highly grateful to my friends Esha, Abhay Kumar, Triveni, Suresh, Subha Narayan, Prateek, Rakesh, Anirban, Kapil and Ajay for their affection and support throughout my research tenure and also for making my stay in University of Hyderabad a wonderful memory.

I sincerely thank Late Ms. Avantika Verma for her memorable company and support. I am also grateful to Late Mr. Chandramouli for his help in protein modeling studies.

My special thanks to my grandmother and my parents for their love, patience, support and confidence on me.

Last but not the least I am highly grateful to Almighty for his blessings and strength which has helped me to successfully achieve this goal.

Ahan Dalal

TABLE OF CONTENTS

Content	Page No.
List of figures	i–iii
List of tables	iv–iv
Abbreviations	v–v
Introduction & Review of Literature	01–21
Objectives	22–22
Materials and Methods	23–47
Objective 1: Attenuation of hydrogen peroxide-mediated oxidative stress by <i>Brassica juncea</i> annexin-3 which complements thiol-specific antioxidant (TSA1) deficiency in <i>Saccharomyces cerevisiae</i>	
Introduction	49–50
Results and discussion	51–60
Conclusion	61–62
Objective 2: Alleviation of methyl viologen-mediated oxidative stress by <i>Brassica juncea</i> annexin-3 in transgenic <i>Arabidopsis</i>	
Introduction	64–65
Results and discussion	66–76
Conclusion	77–77
Objective 3: Role of AtAnn3 under methyl viologen-mediated oxidative stress in <i>Arabidopsis thaliana</i> AtAnn3-knockout plants	
Introduction	79–80
Results and discussion	81–86
Conclusion	87–87
Objective 4: Role of BjAnn3-cysteines in redox modulation and oligomerization	
Introduction	89–91
Results and discussion	92–96
Conclusion	97–97
Summary and conclusion	98–100
Literature cited	101–119

LIST OF FIGURES

- Figure 1 Alignment of plant annexin amino acid sequences.** The conserved residues for heme-binding (histidine) and S₃ cluster are marked (*). Sequence data are available in NCBI with the following accession numbers: At1g35720 (AtAnn1), ABB59550 (BjAnn1), CAA10210 (CaAnn24), ADO32900 (CkANN), AAB67993 [Anx(Gh1)], AAR13288 (GhAnx1), CAA66900 (ZmAnn33), CAA66901 (ZmAnn35), ABD47520 (BjAnn3).
- Figure 2 Recombinant expression of BjAnn3 in yeast and functional effects on cell growth and respiration.** (A) Confirmation of BjAnn3 expression in lane 1, INVSc1-pYES; 2, ADY1-pYES; 3, INVSc1-BjAnn3; 4, ADY1-BjAnn3 cells. (B) Normalized cell growth with respect to untreated cells in the presence of different concentrations of H₂O₂. (C) Mitochondrial respiration in percent of untreated cells.
- Figure 3 Restoration of cell viability by BjAnn3 expression during H₂O₂-mediated oxidative stress.** Sensitivity of yeast strains INVSc1-pYES, INVSc1-BjAnn3, ADY1-pYES and ADY1-BjAnn3 to H₂O₂ was analyzed by spotting (A) or was analyzed by use of fluctuation assay (B).
- Figure 4 Effect of BjAnn3 expression on membrane permeability upon H₂O₂-mediated oxidative stress.** (A) Propidium iodide (PI) fluorescence was observed under a confocal microscope (scale bars: 5 µm) quantified from more than 100 cells in each sample by using Image-J. (B) Values are expressed as a fraction of the control (Untreated INVSc1-pYES cells).
- Figure 5 Modulation of H₂O₂-mediated ROS accumulation by BjAnn3.** ROS was detected by DCF fluorescence using a confocal microscope; scale bars: 10 µm (A). DCF fluorescence was quantified from more than 100 cells in each replicate by using Image-J and expressed as a fraction of the control (Untreated INVSc1-pYES cells) (B).
- Figure 6 qPCR analysis of mRNA transcripts of some antioxidant enzymes.** All strains showed BjAnn3-mediated regulation upon treatment with 2.5 mM H₂O₂. *SOD1*(A), *SOD2*(B), *GPX2*(C) and *TSA2*(D) transcripts were quantified as described above. The expression patterns were compiled in a heat map (E). *ACT1* was used as reference gene.
- Figure 7 Molecular analyses of *A. thaliana* lines expressing BjAnn3 and functional effects of BjAnn3 expression on growth under stress.** (A) Confirmation of transgene insertion in T₁ plants is shown by PCR analysis of genomic DNA. +ve, -ve and 1-8 represent positive control (*BjAnn3*-pCAMBIA 2300 plasmid), negative control (wild type plants) and transgenic lines numbered 1-8 respectively. (B) *BjAnn3*

expression levels were analyzed by qPCR in transgenic plants. All expression levels are shown with respect to the lowest expression line which is considered as 1-fold. (C) Tolerance of the transgenics was assessed by MV-mediated stress on 7 d old seedlings. Wt, *BjAnn3* L4 and *BjAnn3* L6 represent wild type, *BjAnn3* transgenic line 4 and *BjAnn3* transgenic line 6 respectively.

Figure 8 Effect of MV on PSII activity and lipid hydroperoxide levels in wild type and transgenic plants. The maximal quantum yield [Fv/Fm] was recorded after the first SP (A). Effective photochemical quantum yield [Y(II)] (B), coefficient of photochemical fluorescence quenching [qP] (C) and Stern-Volmer type non-photochemical fluorescence quenching [NPQ] (D) was measured every 20 s over a period of 5 min. Filled and open symbols in line graphs represent untreated and treated samples respectively. Lipid peroxidation was assessed as MDA content (E). Wt, *BjAnn3* L4 and *BjAnn3* L6 represent wild type, *BjAnn3* transgenic line 4 and *BjAnn3* transgenic line 6 respectively.

Figure 9 Subcellular localization of BjAnn3-GFP using confocal laser scanning microscopy. In contrast to the more diffuse localization of GFP (A), the BjAnn3-GFP signal was brighter and localized in more narrow regions of tobacco epidermal cells (B). Scale bar: 35S::GFP=10 μ m and BjAnn3-GFP=20 μ m.

Figure 10 Estimation of H₂O₂ level and total peroxidase activity in *Arabidopsis* seedlings.(A) H₂O₂ content was measured in both wild type and transgenics upon MV-treatment. (B) Total peroxidase activity was determined in both wild type and transgenics by measuring the rate of guaiacol tetramerization. Wt, *BjAnn3* L4 and *BjAnn3* L6 represent wild type, *BjAnn3* transgenic line 4 and *BjAnn3* transgenic line 6 respectively.

Figure 11 Protein purification profile. M- Marker. PE- Pellet; SU-Supernatant; FT-Flow-through; W1,W2,W3-Washes (10mM,20mM,30mM); E1 TO E7 – Elutions in 100mME8,E9,E10 - Elutions in 250mM; E11,E12,E13 - Elutions in 400mM.

Figure 12 Titration of the E_m value and quantification of peroxidase activity of BjAnn3 wild type protein.(A) The redox midpoint potential of the recombinant protein was titrated by incorporation of monobromobimane after equilibration with varying ratios of DTT_{reduced}/DTT_{oxidized}. Data from four experimental repeats were fitted to Nernst equation with n=4 using OriginPro 8. (B) Peroxidase activity of the recombinant protein was quantified by measuring the rate of guaiacol tetramerization. HRP, BSA, BjAnn3 and BjAnn3 (d) represent horseradish peroxidase, bovine serum albumin, native BjAnn3 and heat-denatured BjAnn3 respectively.

Figure 13 qPCR analyses of mRNA transcripts of some antioxidant enzymes. Both lines showed BjAnn3-mediated regulation upon MV treatment. *sAPX*(A), *tAPX*(B), *APX1*(C), *CSD1*(D) and *FSD1*(E) transcripts were quantified as described above.

The expression patterns were compiled in a heat map (F). *18S rRNA* (TAIR: AT2G01010) was used as reference gene. Wt, *BjAnn3* L4 and *BjAnn3* L6 represent wild type, *BjAnn3* transgenic line 4 and *BjAnn3* transgenic line 6 respectively.

Figure 14 Multiple Sequence Alignment of *BjAnn3* and *AtAnn3*.

Figure 15 Functional effects of *AtAnn3* on growth under stress. Susceptibility of *AtAnn3*-KO seedlings was assessed by MV-mediated stress on germination after 10 days. Wt and *AtAnn3*-KO represent wild type and *AtAnn3* mutant line respectively.

Figure 16 Effect of MV on PSII activity and lipid hydroperoxide levels in wild type and mutant plants. The maximal quantum yield [Fv/Fm] was recorded after the first SP (A). Effective photochemical quantum yield [Y(II)] (B), coefficient of photochemical fluorescence quenching [qP] (C) and Stern-Volmer type non-photochemical fluorescence quenching [NPQ] (D) was measured every 20 s over a period of 5 min. Filled and open symbols in line graphs represent untreated and treated samples respectively. Lipid peroxidation was assessed as MDA content (E). Wt and *AtAnn3*-KO represent wild type and *AtAnn3* mutant line respectively.

Figure 17 qPCR analysis of mRNA transcripts of some antioxidant enzymes. *sAPX*(A), *tAPX*(B), *APX1*(C), *CSD1*(D) and *FSD1*(E) transcripts were quantified as described above. *18S rRNA* (TAIR: AT2G01010) was used as reference gene. Wt and *AtAnn3*-KO represent wild type and *AtAnn3* mutant line respectively.

Figure 18 Western blot of recombinant *AnnBj3_{WT}* protein and its variants. M- Marker; I-*BjAnn3_{C114S}*; II- *BjAnn3_{C129S}*; III- *BjAnn3_{C129S}* and *C226S*; IV- *BjAnn3_{C114S}* and *C242S*; V- *BjAnn3_{C114S}*, *C226S* and *C242S*; VI- *BjAnn3_{C114S}*, *C129S*, *C226S* and *C242S*; Wt-*BjAnn3_{WT}*.

Figure 19 Redox dependent electro-phoretic mobility of proteins under oxidizing and reducing conditions. *AnnBj3_{WT}* and its variants were incubated with different concentrations of either hydrogen peroxide or DTT_{Reduced} and the samples were resolved in SDS/PAGE and blotted. All experiments were repeated at least 3 times.

Figure 20 Determination of redox midpoint potential of *BjAnn3_{WT}* and its variants. The redox midpoint potential of recombinant proteins was determined after equilibration with varying ratios of DTT_{reduced}/DTT_{oxidized}. The samples were resolved in 12% SDS/PAGE and then blotted. All experiments were repeated at least 3 times.

Figure 21 FPLC gel filtration profiles of wild-type and variants on a Superose-12 10/300 GL column. *BjAnn3_{WT}* profile is compared with that of each variant in each figure. The peaks in each figure are marked with respective protein name. All experiments were repeated at least 3 times.

LIST OF TABLES

Table 1. Primers used for *S. cerevisiae* studies.

Table 2. *Saccharomyces cerevisiae* strains used.

Table 3. Primers used for *Arabidopsis thaliana* studies.

Table 4. List of primers for mutation studies.

Table 5. The temperature profile and cycling condition of qPCR.

ABBREVIATIONS

ANOVA	Analysis of variance
DMRT	Duncan's multiple range test
DTT _{Oxidised}	<i>trans</i> -4,5-Dihydroxy-1,2-dithiane
DTT _{Reduced}	1,4-Dithiothreitol
EDTA	Ethylenediaminetetraacetic acid
F _v /F _m	Maximal PSII quantum yield
FW	Fresh weight
MDA	Malondialdehyde
MV	Methyl Viologen
O ₂ ^{•-}	Superoxide radical
OH [•]	hydroxyl radical
PAM	Pulse Amplitude Modulation
PSI	Photosystem I
PSII	Photosystem II
qP	Coefficient of photochemical quenching
PMSF	Phenylmethylsulfonylfluoride
ROS	Reactive oxygen species
SDS-PAGE	Sodium dodecyl sulfate polyacrylamide gel electrophoresis
-SH	Thiol group
TBA	Thiobarbituric acid
TCA	Trichloroacetic acid
TEMED	N,N,N',N'- Tetramethylethylenediamine
Y(II)	Photochemical quantum yield of PSII
NPQ	Non-photochemical quenching

Introduction & Review of Literature

Introduction and Review of Literature

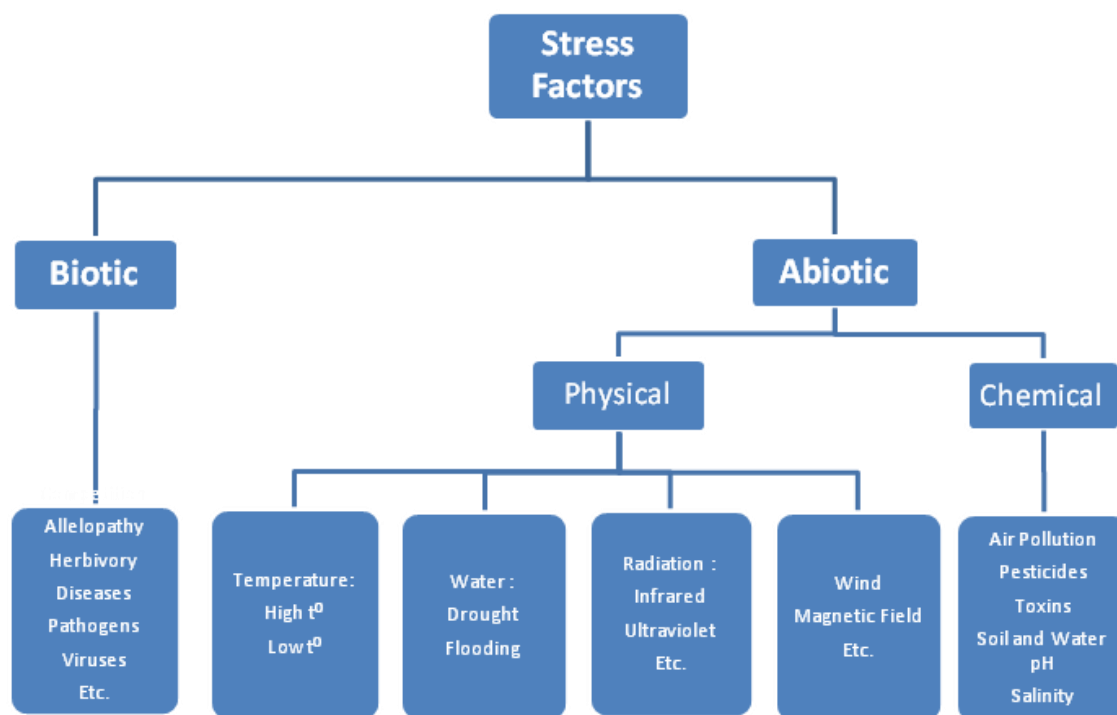
Stress and annexins

Stress as defined by scientists based on physiological and ecological requirements of an organism throughout its lifecycle (Chapin et al. 1991) is the reaction of a biological system to extreme external factors that may cause significant perturbations depending on their intensity and duration (Görling et al. 1982, Nilsen and Orcutt 1996; Godbold et al. 1998). Along with the term “stress” Levitt (1980, 1982) used the term “strain”, which might be used where the physiological changes due to extreme environmental conditions do not result in significant inhibition of plant growth or reproduction. Larcher (1980) named the responses of plants to stressors of adapting or protective nature as “alarm reactions”.

Stressors or stress factors induce functional changes in plants to an extent that results in inhibited growth, reduced bio-production, physiological acclimatization, and adaptation of species or little combination of these changes (Schubert et al. 1985; Grime et al. 1993; Nilsen and Orcutt 1996). Stressors comprise a complex set of biotic and abiotic factors. Those which are concerned with the mechanism of interaction between populations are known as biotic stressors, whereas abiotic stressors may constitute both physical and chemical factors. In abiotic stress, physical factors of the environment can affect physiological patterns in both positive and negative ways, whereas, many chemical factors can act as stressors if they are not normally in the environment (e.g. pesticides) or if their levels are relatively high (e.g. pH) (Nilsen and Orcutt 1996). Plants respond to the environment in an equally complicated manner. Combining the fact of huge number of cells each with multiple interacting organelles along with cell differentiation and interactions with the environment, we see an infinite number of permutations to this complexity (Cramer et al. 2011). According to Boyer (1982), crop production may be limited by environmental factors up to as much as 70%. Only 3.5% of the global land area is not affected by few environmental constraints according to 2007 FAO report.

On the basis of percentage of land area affected and the number of scientific publications on various abiotic stresses, it is evident that abiotic stress makes a significant impact on plants. A strong specific component in individual stress response is essential due to the

diversification of abiotic stresses (Jaspers and Kangasjärvi 2010). However, the striking common component involved in all abiotic stresses (Vaahtera and Brosché 2011) is reactive oxygen species (ROS), notwithstanding different forms and in different sub-cellular compartments (Jaspers and Kangasjärvi 2010). The metabolic processes such as photosynthesis and respiration also results in ROS formation. ROS generation in all aerobic species might result in oxidative stress. Oxidative stress may be defined as the disproportion between induction and elimination of reactive oxygen species.



[The sources of environmental stress in plants (Schubert 1985; Nilsen and Orcutt 1996)]

Chemical reactions involving transfer of electrons or hydrogen atoms among molecules are named as redox reactions. Oxidation is the loss of electrons from an electron donor or an increase in oxidation state of a molecule, atom or ion. Reduction involves gain of electrons by an electron acceptor or decrease in oxidation state of a molecule, atom or ion. The redox state represents the balance between oxidized and reduced state of the molecule concerned, in a biological system such as a cell or an organ. Furthermore, redox control is

determined by how a molecular response depends on the redox state of one or more of its constituent molecules in a cell.

Reduction of molecular oxygen by the electron flux flowing through photosynthetic and respiratory electron transport chain, leads to the generation of ROS. ROS may be hydrogen peroxide (H_2O_2), hydroxyl radical (OH^\bullet) or superoxide radical ($\text{O}_2^{\bullet-}$). Singlet oxygen which is an activated derivative of molecular oxygen is another oxidant that is formed during photochemistry and light capture by interaction between the ground state oxygen and the triplet chlorophyll of Photosystem II reaction centers (Foyer and Noctor 2006). This oxidative challenge is infringed by the antioxidative systems within the cell and helps the organism to maintain active metabolism. Thus, redox homeostasis is demonstrated as the ability to maintain a balance between the ROS generated and the activity of the antioxidative system.

Till date, among all other identified functional proteins responsible for stress-resistance, annexins have been shown to play a significant role. The term annexin is derived from the Greek word “*annex*” meaning “bring/hold together” which characterize the principal property of nearly all annexins, i.e., binding to certain biological structures, particularly membranes. The term *annexin* was named with various unrelated names according to their biochemical properties. They are calmodulins (proteins mediating Ca^{2+} signals), synexin (granule aggregating protein), lipocortins (steroid-inducible lipase inhibitors), chromobindins (proteins binding to chromaffin granules), and calpactins (proteins binding Ca^{2+} , phospholipid, and actin).

Two defining criteria of annexins are known: (i) it must be capable of binding to negatively charged phospholipids in a Ca^{2+} -dependent/independent manner (Mortimer et al. 2008; Dabitz et al. 2005) and (ii) it has to have highly conserved repeats of 70 amino acid residues known as annexin repeats (Gerke and Moss 2002).

Annexins are multigene family of Ca^{2+} , phospholipid and cytoskeleton-binding proteins ubiquitously present in animals, plants and fungi. They may exist in both soluble and membrane-bound state. Plant annexins (32–36 kDa) are abundant proteins (0.1% of total cell protein) and are widespread in Plant Kingdom (Morgan and Fernandez 1997; Hofmann et al. 2004; Mortimer et al. 2008).

The main structural features of the plant annexins distinct from those of vertebrates, are two dysfunctional canonical calcium binding sites, direct interactions of side chain residues for membrane binding on the convex side, and propensity for oligomer formation (Konopka-Postupolska et al. 2011). The protein core consists of four domains, each comprising five α -helices, of which four are arranged parallel and anti-parallel to each other (helices A, B, D and E) and the fifth (helix C) one lying nearly perpendicular to the four-helix bundle (Hofmann et al. 2000).

Discovery of plant annexins

Being ubiquitous across kingdoms, plant annexins represent 0.1% of the total protein. From past almost two decades research on plant annexins have revealed that they are expressed in many tissues and at different developmental stages. First plant annexin was identified in tomato based on amino acid sequence identity, antibody cross-reactivity and functional similarity with mammalian annexins (Boustead et al. 1989). Later, they were identified at mRNA and/or protein level in model and crop plants such as *Arabidopsis* (Lee et al. 2004, Clark et al. 2001), barley (Clarke et al. 2008), celery (Seals et al. 1994), corn and lily (Blackbourn et al. 1991, 1992; Zhou et al. 2013), alfalfa (Kovacs et al. 1998), rice (Hashimoto et al. 2009; Jami et al. 2012), potato (Riewe et al. 2008), tobacco (Seals et al. 1994; Tang et al. 2003; Baucher et al. 2011), wheat (Breton et al. 2000), pea (Clark et al. 1998), cotton (Andrawis et al. 1993; Zhou et al. 2011; Huang et al. 2013; Li et al. 2013), pepper (Hoshino et al. 1995; Proust et al. 1996; Hofmann et al. 2000), rhizoids of fern (Clark et al. 1995), tomato (Lu et al. 2012), *Cynanchum komarovii* (Zhang et al. 2011), *Mimosa* (Hoshino et al. 2004), lotus (Chu et al. 2012), soybean (Feng et al. 2013), *Brassica* (Jami et al. 2008, 2009).

Plant annexins are encoded by multigene families

Initially, annexins were discovered in animal cells with at least thirteen distinct members of the family (Raynal and Pollard 1994). In plants, southern hybridization data from *Arabidopsis* (Gidrol et al. 1996), bell pepper (Proust et al. 1996), tobacco (Proust et al. 1999) unfolded the presence of at least two different annexins in the family. Later from last

13 years, few more annexin families have been identified from *Arabidopsis*, *Brassica*, rice, tomato and soybean with 8, 7, 12, 9 and 23 members respectively (Clark et al. 2001; Cantero et al. 2006; Jami et al. 2009, 2012; Lu et al. 2012; Feng et al. 2013).

Developmental regulation of expression and distribution

Plant annexins have been identified in all organs (reviewed by Laohavisit et al. 2010). Transcript levels of annexins in *Arabidopsis* and *Brassica* differ at different tissues at different stages of life-cycle (Clark et al. 2001, 2005b; Bianchi et al. 2002; Cantero et al. 2006; Jami et al. 2009). Differential expression of plant annexins has been noted in the cell cycle (Proust et al. 1999), embryogenesis (Gallardo et al. 2003), pollen and seed germination (Buitink et al. 2006; Dai et al. 2006; Yang et al. 2007), tuber enlargement (Sheffield et al. 2006), vasculature development (Clark et al. 2001, 2005b), primary root growth and lateral root formation (Clark et al. 2001, 2005a; Bassani et al. 2004), fruit ripening (Bianco et al. 2009), cotton fibre elongation (Yang et al. 2008; Li et al. 2013; Huang et al. 2013; Andrawis et al. 1993; Shin and Brown 1999), cork formation (Soler et al. 2007) and senescence of petals (Bai et al. 2010). Annexins have been detected in the root elongation zone in *Arabidopsis* (Clark et al. 2005a,b) and maize (Carroll et al. 1998; Bassani et al. 2004). *NnANN1* was identified predominantly in flower and stem tissues of *Nelumbo nucifera* while roots and leaves showed lower transcript levels (Chu et al. 2012). *GmANN1*, *10*, *11*, *12*, and *14* from soybean showed different organ-specific expression patterns (Feng et al. 2013). Expression of rice and tomato annexins was shown to be tissue specific and developmentally regulated (Jami et al. 2012; Lu et al. 2012). *CkANN* from *Cynanchum komarovii* also showed tissue specific expression (Zhang et al. 2011).

They are also found to be associated with expansion of tomato pericarp (Faurobert et al. 2007) and tobacco cells (Proust et al. 1999; Seals and Randall 1997). They have also been detected immunologically at the apex of cells exhibiting polar growth such as fern rhizoids, pollen tubes and root hairs (Blackbourn et al. 1992; Blackbourn and Battey 1993; Clark et al. 2001, 2005a; Dai et al. 2006). MYB98 has been identified to regulate *Arabidopsis thaliana* Annexin8 (AtAnn8) expression in synergid cells (Punwani et al. 2007). AtAnn1 abundance is found to increase in *ntm1*-Dmutant (NAC with transmembrane motif 1; Lee et

al. 2008). According to Proust et al (1999), cytokinin possibly stabilizes NTM1 during cell division and it will be interesting to see whether this relates to the accumulation of the tobacco annexins (Ntp32.1 and Ntp32.2) at the cytokinin regulated G1/S and G2/M cell cycle stages. Plant growth regulators are also known to influence expression, for example, zeatin positively regulates AtAnn2 and AtAnn4 (Kiba et al. 2005).

Sub-cellular localization

Besides being cytosolic, through proteomic or immunological analyses, plant annexins have also been detected at the plasma membrane (Thonat et al. 1997; Santoni et al. 1998; Breton et al. 2000; Alexandersson et al. 2004; Marmagne et al. 2007; Carletti et al. 2008), tonoplast (Seals and Randall 1997; Lin et al. 2001), chloroplast envelope (Seigneurin-Berny et al. 2000), stroma (Rudella et al. 2006), thylakoid (Friso et al. 2004), mitochondria (Ito et al. 2006), Golgi and Golgi-derived vesicles (Shin and Brown 1999), nucleus (Clark et al. 1998; Kovacs et al. 1998), glyoxysome (Fukao et al. 2003) and peribacteroid membrane (Wienkoop and Saalbach 2003). Albeit from different tissues, AtAnn1 has been recovered from plasma membrane, mitochondria, glyoxysome, vacuole, stroma and thylakoid, indicating multiple sub-cellular localization of any given annexin (reviewed by Laohavisit and Davies 2009). The only plant annexins that are detergent-resistant microdomains (DRM) associated is MtAnn2 (Lefebvre et al. 2007).

Highly local conditions might regulate the annexin-membrane interaction where a classical targeting sequence is absent (Laohavisit et al. 2011) as in spinach annexin (Seigneurin-Berny et al. 2000). An important ER export signal (a C-terminal diacidic motif D/E-X-D/E- where X denotes any amino acid) to the plasma membrane has been identified (Mikosch and Homann 2009) and is found in several plant plasma membrane K⁺ channels and aquaporins (Mikosch and Homann 2009). This motif is present in AtAnn1, ZmAnn33 and ZmAnn35 and they have been detected at the plasma membrane (Santoni et al. 1998; Alexandersson et al. 2004; Benschop et al. 2007; Carletti et al. 2008). AtAnn1 has been found to be cell wall associated as well as apoplastic while AtAnn2 have been identified in the cell wall (Kwon et al. 2005; Bayer et al. 2006; Bindschedler et al. 2008). A *Phytophthora ramorum* annexin has also been identified in the cell wall (Meijer et al. 2006).

Stimulus-dependent localization

Like animal annexins (Babiychuk et al. 2009), plant annexins are evidenced to undergo stimulus-dependent relocation from cytosol to membrane. With stress MsAnn2 localizes to the nucleolus (Kovács et al. 1998). Cold results in wheat annexin p39 accumulation (as integral proteins) in shoot PM (Breton et al. 2000). Salt stress is found to trigger Ca^{2+} -dependent reversible relocation of AtAnn1 from cytosol to root cell membranes based on immunological analysis of cell fractions (Lee et al. 2004). *Mimosa* annexins are largely cytosolic at night but during daytime accumulate at the periphery of motor cells of pulvinus (Hoshino et al. 2004). Pea annexin changes localization below the plumule apical meristem for more even peripheral distribution by gravitational stimulus for even distribution at the periphery (Clark et al. 2000). Mechanical stress causes Ca^{2+} -dependent relocation of *Bryonia dioica* annexin from the cytosol to the parenchyma PM (Thonat et al. 1997). Subcellular localization pattern of NnANN1 was found to be affected by heat stress (Chu et al. 2012).

Stimulus-dependent transit-time for localization

Transit time to membrane due to stimulus was determined by Ca^{2+} affinity of an animal annexin (Gerke et al. 2005). Membrane association and function are subjective by local $[\text{Ca}^{2+}]$, phospholipid head-group specificity, membrane curvature, pH and voltage (Hofmann et al. 1997; Maffey et al. 2001; Fischer et al. 2007; Babiychuk et al. 2009). In plant annexins, the range of $[\text{Ca}^{2+}]$ required for half-maximal binding varies from sub-millimolar (CaAnn24, GhAnn1; Dabitz et al. 2005) to nano-molar (VCaB42, Seals et al. 1994; AtAnn1, Gorecka et al. 2005).

Environmental response

Response to biotic stimulus

Multiple environmental signals are likely to regulate plant annexin expression and its abundance. Annexin abundance in pea roots is increased by mycorrhizal infection and has synergistic effect upon cadmium treatment (Repetto et al. 2003). MtAnn1 from *Medicago*

truncatula is transcriptionally activated specifically in roots only upon application of Nod factor to root tissue (de Carvalho-Niebel et al. 1998, 2002). In contrary to *Pseudomonas syringae* infection (Truman et al. 2007), *AtAnn4* is negatively affected by *Pseudomonas fluorescens* or cucumber mosaic virus (CMV)-Y infection (Marathe et al. 2004; Wang et al. 2005). Tomato annexin *LeAnn34* is upregulated after pathogenic challenges (*Pto* expression) (Xiao et al. 2001). *AtAnn1* transcription is activated at the site of infection of an obligate biotroph *Golovinomyces orontii* (Chandran et al. 2010). *Ntann12* expression was found to be induced in tobacco BY-2 cells by *Rhodococcus fascians* infection (Vandeputte et al. 2007).

Wounding activates *AtAnn4* downstream of jasmonic acid production (Yan et al. 2007). Wounding positively regulates *AtAnn1* and *BjAnn3* expression possibly via H_2O_2 production in *BjAnn3* (Jami et al. 2009; Konopka-Postupolska et al. 2009). Tomato annexins were also found to be induced by wounding (Lu et al. 2012). **Jasmonic acid** induces *AtAnn2* in *Arabidopsis* (Kiba et al. 2005). Maize annexins are also found to be induced by jasmonic acid (Zhou et al. 2013). Expression of *CkANN* from *Cynanchum komarovii* was shown to be induced by methyl jasmonate treatment (Zhang et al. 2011). **Salicylic acid** both positively regulates *AtAnn1* (Gidrol et al. 1996; Konopka-Postupolska et al. 2009) and down-regulates *AtAnn2* and *AtAnn4* expression in *Arabidopsis* (Kiba et al. 2005). Expression of *CkANN* from *Cynanchum komarovii* was shown to be induced by salicylic acid (Zhang et al. 2011). *Ntann12* expression is induced by **auxin** in tobacco roots and is linked to the perception of a signal in the aerial part of the plant that is transmitted to the root (Baucher et al. 2011). Tomato annexins were found to be induced by **gibberellic acid** (Lu et al. 2012).

Response to abiotic stimulus

Much more evidences have been gathered with respect to **abiotic stress** response which potentially regulates different plant annexins. **Cold stress** induces abundance of rice and wheat annexins (Hashimoto et al. 2009; Breton et al. 2000), up-regulates *AtAnn1*, 3, 4, 5, 7 and 8 expression on contrary to *AtAnn2* and 6 in *Arabidopsis* (Clark et al. 2005b, Cantero et al. 2006) and regulates expression in poplar leaves (Renault et al. 2006). *GmANN1*, 11, 12, and 14 from soybean was induced by cold (Feng et al. 2013). Expression

of rice and tomato annexins was found to be regulated by cold (Jami et al. 2012; Lu et al. 2012). **Heat** induced NnAnn1 (both at transcript and protein level) was identified in *Nelumbo nucifera* (Chu et al. 2012). Expression of rice and tomato annexins was found to be regulated by heat (Jami et al. 2012 and Lu et al. 2012). **Salinity stress** transcriptionally activates *BjAnn3* and *BjAnn7* in *Brassica* (Jami et al. 2009), *AtAnn4–8* in *Arabidopsis* (Cantero et al. 2006), *NtAnn12* in tobacco (Vandeputte et al. 2007), *CkANN* in *Cynanchum komarovii* (Zhang et al. 2011) and *MsAnn2* in *Medicago* (Kovács et al. 1998). An acute salinity stress up-regulates *AtAnn1* expression but salt-adapted roots show suppressed expression (Lee et al. 2004, Cantero et al. 2006, Konopka-Postupolska et al. 2009, Katori et al. 2010). Expression of rice and tomatoannexins was found to be regulated by salt (Jami et al. 2012; Lu et al. 2012). Expression of *GmANN1*, *11*, and *12* from soybean responded to high salinity (Feng et al. 2013). Variance in annexin expression and /or abundance due to **drought** is observed in *Medicago* (Buitink et al. 2006), *Arabidopsis* (Bianchi et al. 2002, Cantero et al. 2006, Konopka-Postupolska et al. 2009), rice (Gorantla et al. 2005), soybean (Feng et al. 2013), Loblolly pine (Watkinson et al. 2003) and *B. juncea* (Jami et al. 2009). Expression of rice and tomato annexins was found to be regulated by drought (Jami et al. 2012; Lu et al. 2012). Expression of *CkANN* from *Cynanchum komarovii* was shown to be induced by PEG (Zhang et al. 2011). **ABA** plays prominent role in increasing expression and/or abundance of *AtAnn1* from *Arabidopsis* having an ABA responsive cis-acting element (ABRE) in its promoter (Gidrol et al. 1996; Lee et al. 2004; Kiba et al. 2005; Konopka-Postupolska et al. 2009). Absciscic acid positively regulates *BjAnn1-3*, *6*, *7* from *B. juncea* (Jami et al. 2009), *AtAnn4* from *Arabidopsis* (Kiba et al. 2005; Xinet al. 2005), tobacco annexin *NtAnn12* (Vandeputte et al. 2007) and *MsAnn2* from *Medicago sativa* (Kovács et al. 1998). *AtAnn1* participates downstream in cross-talk between auxin- and ABA-signaling (Bianchi et al. 2002; Laohavisit et al. 2011). Expression of *GmANN1*, *10*, *11*, *12*, and *14* from soybean was significantly induced by absciscic acid (Feng et al. 2013). Tomato annexins were also found to be induced by ABA (Lu et al. 2012). Expression of *CkANN* from *Cynanchum komarovii* was shown to be induced by ABA treatment (Zhang et al. 2011). Plant annexins have been implicated in **oxidative stress** response similar to mammalian annexins A1, A5 and A6 (Rhee et al. 2000; Kush and Sabapathy 2001; Sacre

and Moss 2002). Oxidative stress, which may be downstream of both biotic and abiotic challenge, also up-regulates BjAnn1–3, MsAnn2, *CkANN* and AtAnn1 (Gidrol et al. 1996; Kovács et al. 1998; Jami et al. 2009; Konopka-Postupolska et al. 2009; Zhang et al. 2011). AtAnn1 expression in *Arabidopsis* leaves is activated by **phosphate starvation** (Muller et al. 2007). **Metal stress** also triggers annexin expression, for example, zinc regulates homologues of AtAnn1 and AtAnn2 in *Thlaspi caerulescens* (Tuomainen et al. 2010); cadmium activates AtAnn1 and pea root annexin level (Repetto et al. 2003; Konopka-Postupolska et al. 2009) and copper regulates AtAnn3 and AtAnn4 expression (Weber et al. 2006). Maize annexins are also found to be induced by heavy metals (Zhou et al. 2013).

Gravity affects the expression and abundance of AtAnn1 (Clark et al. 2005a, Kamada et al. 2005; Barjaktarović et al. 2007). Effect of **light** on the expression of certain *Arabidopsis* and tobacco annexins were studied (Tang et al. 2003; Cantero et al. 2006) where AtAnn1 and AtAnn4 displayed opposite response downstream of the photo-morphogenesis transcription factor HY5 (Lee et al. 2007).

Structural properties of plant annexins

Structural information on plant annexins is available as crystal structures of bell pepper annexin 24 (Ca32) (Hofmann et al. 2000), cotton annexin Anx(Gh)1 (Hofmann et al. 2003 and Hu et al. 2008) and *Arabidopsis* annexin Anx(At)1 (Levin et al. 2007). They are comprised of a four-fold repeat (I–IV) of 70 amino acid sequence that constitutes the C-terminal (core) domain. Each repeat consists of a five-helix (A–E) bundle with membrane binding sites present in the AB and DE loops. Type II or type III binding sites are responsible for canonical calcium binding. Type II is formed through the endonexin sequence G-X-G-T/{38–40}/-D/E, where G-X-G-T motif occurs in the AB loops, and the bidentate acidic side chain sits at the C-terminal end of helix D within the same repeat. The N-terminal domain is positioned at the opposite side of the molecule without facing the membrane and can vary in length from 5 to 50 amino acids. It may associate with the core domain as well as involve in allosteric regulation (Hofmann et al. 2003; Konopka-Postupolska et al. 2011).

Calcium and membrane binding

Plant annexins have up to four annexin repeats each of 70 amino acid residues. The repeats responsible for calcium binding contains a consensus endonexin sequence K-G-X-G-T-[38]-D/E. Each repeat contains five short α -helices joined together by short loops which are necessary for Ca^{2+} -annexin interaction, in particular the AB loop (i.e. the short loop connecting helix A and helix B) and DE loop (Hofmann et al. 2003; Hu et al. 2008). The majority of annexin secondary structure is made by α -helices. Based on earlier hypothesis, plant annexins are known to bind calcium ions in a canonical fashion only in repeats I and IV (Delmer et al. 1997). Later confirmation was achieved from the crystal structure of calcium bound Anx(Gh)1 (Hu et al. 2008), which remains the only structure of calcium-bound plant annexin till date. In repeat II, in place of the required acidic bidentate side chain presence of a histidine residue boils down to dysfunctional calcium-binding site. Despite the presence of the bidentate acidic residue, the absence of endonexin sequence in repeat III makes the conformation of side chains in the IIIAB loop unfavorable for calcium binding, (Konopka-Postupolska et al. 2011). X-ray crystal structures from cotton and Capsicum annexins (Hofmann et al. 2000, 2003; Hu et al. 2008) reveals formation of a slightly curved disc with type II and type III Ca^{2+} -binding sites on the convex side, similar to their animal counterparts (Hofmann et al. 2000, 2003; Hu et al. 2008). The short N-terminal domain appears to be anchored into the C-terminal core by hydrogen bonding (Hofmann et al. 2003) and remains unaffected by coordination of Ca^{2+} ions (Hu et al. 2008).

Tryptophan 35 (W35 in GhAnn1) appears to be an important residue for Ca^{2+} -dependent as well as Ca^{2+} -independent lipid binding (Hofmann et al. 2003; Dabitz et al. 2005; Hu et al. 2008). The two other tryptophan residues along several basic and hydrophobic residues on their convex side that are found exposed in crystal structures enable calcium-independent membrane interactions, which has been experimentally evidenced by mutagenesis study (Dabitz et al. 2005; Konopka-Postupolska et al. 2011; Laohavisit et al. 2011). Ca^{2+} -independent membrane binding of plant annexins at neutral and acidic pH has been experimentally proved. Up to 20% of total GhAnn1 and CaAnn24 showed Ca^{2+} independent membrane binding at neutral pH (Blackbourn et al. 1991; Breton et al. 2000; Hofmann et al.

2000, 2002; Dabitz et al. 2005; Gorecka et al. 2007; Laohavisit et al. 2009; Laohavisit et al. 2011).

The four repeats of plant annexins are different in lipid binding (Lim et al. 1998). Repeats I/IV and II/III may function as separate lipid-binding domains (Hofmann et al. 2004; Hu et al. 2008). I/IV repeat pair in GhAnn1 is responsible phospholipid binding (Hu et al. 2008) and holds three Ca^{2+} co-ordination sites. A fourth site is hypothesized to be present in the I-DE loop (Hu et al. 2008). I-AB loop may contribute to rapid phospholipid interaction due to its conformational flexibility. Plant annexins are known to exist in partially or fully membrane-inserted form (wheat p39 and p22.5, Breton et al. 2000; AtAnn1, Santoni et al. 1998; Gorecka et al. 2007).

Oligomerization

The function of plant annexin oligomerization has remained unclear; however, Hofmann et al (2003) proposed that it can constitute a structural basis of oxidative stress response (Konopka-Postupolska et al. 2009). Plant annexins oligomerization was first reported by Hoshino et al (1995) from *Capsicum annum*, Anx (Ca35), where the protein was purified from a natural source in membrane bound state. They observed the formation of homo-dimers during cross linking of the protein to phosphatidylinositol vesicles. Oligomerization state of four more recombinant plant annexins Anx23(Ca38), Anx24 (Ca32), Anx (Gh1) and Anx (Gh2) had been studied by gel filtration and equilibrium sedimentation. The former exist in monomer-trimer equilibrium in solution (Hofmann et al. 2002). Small-angle X-ray scattering results indicate the formation of high molecular mass prolate oligomers of 24(Ca32) (Hofmann and Pedersen, unpublished results). Only a small fraction of Anx(Gh2) was found to be trimeric and mainly exists in monomer-dimer equilibrium. These oligomers formation is calcium independent unlike mammalian annexins. Calcium-mediated dissolution of oligomers in cotton annexins is by reduction of trimeric or dimeric oligomers.

Peroxide induces dimerization of AtAnn1 and oligomerization of ZmAnn33/35 (Gorecka et al. 2005; Mortimer et al. 2009). In contrast to animal annexin A2, redox driven oligomerization of AtAnn1 is not via covalent S-S bonding as evidenced by Konopka-Postupolska et al (2009), but is hypothesized to be via electrostatic interactions. A conserved

tryptophan switch in repeat I apparent from the comparative crystal structures of plant annexins may play a role in oligomerization tendency of plant annexins in solution (Hofmann et al. 2002; Konopka-Postupolska et al. 2011). Although plant annexins are known to oligomerize, study by Huh et al. (2010) provides the first evidence of plant annexins to form hetero-dimers (Clark et al. 2012).

Oxidative stress response

Antioxidant property of annexins was proposed to be on the basis of two different criteria. Firstly, the histidine residue in the N-terminal region of the protein was hypothesized to bind heme and utilize in the electron transfer reactions (Gidrol et al. 1996). This hypothesis was based on the analysis of amino acid sequence of plant annexin AtAnn1 which possess a conserved histidine residue within the N-terminal region that seemed similar to a sequence observed in plant peroxidases (Gidrol et al. 1996; Konopka-Postupolska et al. 2011). Further, the same protein was also able to protect mammalian cells from oxidative stress (Kush and Sabapathy 2001). Gorecka et al. (2005) reported that the recombinant annexin AtAnn1 displayed peroxidase activity and site-directed mutagenesis of His40 to Ala40 abolished this activity. Amino acid sequence similarity in two different proteins does not necessarily suggest a three-dimensional structural resemblance (Konopka-Postupolska et al. 2011). Heme binding by plant annexins is not yet experimentally evidenced and on the basis of the structural data available, heme-binding by plant annexins seems impossible. Firstly, the heme-binding histidine residue (His-40 in Anx(Gh)1) is located near the C-terminal end of helix IB which provides an anchor point for association of N-terminal domain with the C-terminal core through hydrogen bonding in Anx(Gh)1. Therefore the histidine side chain is protected from further intermolecular contacts. Secondly, the surface of the annexin molecule in this area has no suitable place to accommodate the large porphyrin ring of heme molecule. And lastly, in a test for heme binding, Anx(Gh)1 wild-type and Anx(Gh)1-H40A did not show any shift of the Soret band of heme in the presence of the annexin proteins, when the UV/Vis spectra of myoglobin was compared (Osman and Hofmann, unpublished data) (Laohavisit et al. 2009; Konopka-Postupolska et al. 2011). However, His-40 might serve as a key residue in providing stability by anchoring of the N-

terminal domain to the core as observed in all plant annexin crystal structures till date (Konopka-Postupolska et al. 2009 and 2011). Therefore the first speculation looks inconceivable. Rather, His40 has now been proposed to be involved in maintaining the secondary structure (Konopka-Postupolska et al. 2009; Clark et al. 2010; Laohavisit et al. 2011).

Secondly, the putative S₃ cluster in the first domain is predicted to function as redox-reactive center involved in electron transfer reactions. S₃ cluster was first discovered from the crystal structure of cotton (*Gossypium hirsutum*) annexin (Hofmann et al. 2003) and later from that of AtAnn1 in *A. thaliana* (Protein Data Bank no. At1g35720; 1YCN). Despite lacking experimental validation, the second hypothesis looks promising on the ground of three dimensional crystal structures. Of the three sulfur containing residues responsible for S₃ cluster, two cysteine residues are highly conserved among plant annexins nonetheless the methionine residue has deviated rendering the S₃ cluster into an unconserved feature. The cluster is located in the lower part of the annexin core in module II/III and is accessible only from the hydrophilic cleft between both molecules. It is likely to be involved in redox reactions and might constitute the molecular basis of oxidative stress response by annexins (Konopka-Postupolska et al. 2011; Laohavisit et al. 2011).

Another possibility is that copper-associated annexin can react with peroxide. AtAnn1 has been reported to be a copper-binding protein (in common with vertebrate annexins A2, A4 and A5; She et al. 2003). The binding is possibly mediated by His- or Met-bounded motifs (Kung et al. 2006). This functional implication remained unexplored either in terms of redox activity or copper sequestration (Laohavisit et al. 2011).

Post-translational modification

Actin binding in plant annexins could be due to a conserved IRImotif (Calvert et al. 1996; Clark et al. 2001) which is not supported *in vitro* (Mortimer et al. 2008). The N-terminal region of the second annexin repeat (AVMLWT*LDPPER where T is phosphorylated) (Agrawal and Thelen 2006) in *B. napus* is phosphorylated. In AtAnn2 this sequence is fully conserved (Laohavisit et al. 2011). Plant annexin may have multiple putative phosphorylation sites as studied by Jami et al. (2009) and this phosphorylation

status is connected to the regulation of *in vitro* peroxidase activity (Gorecka et al. 2005). GhAnn1 may bind to cotton fibre PM and gets phosphorylated by a PM-associated kinase (Andrawis et al. 1993). Rice annexins can interact with several kinases, including MAPKK and Ste20-related protein kinase, suggesting their involvement in membrane-associated, Ca^{2+} -dependent MAPK signaling cascade (Rohila et al. 2006). The two conserved Cys residues of AtAnn1 may be S-nitrosylated or S-glutathionylated where the latter occurs downstream of ABA (Lindermayr et al. 2005; Konopka-Postupolska et al. 2009; Clark et al. 2010). Experimental evidence showed that these two cysteine residues are neither responsible for intra-molecular nor inter-molecular disulfide bridges under non-reducing condition in AtAnn1. However, they remain free for modifications under biological conditions. Moreover, AnxGh1 was also found to exist in thiol state though the protein was not under reducing condition. This may signify their regulation in membrane-binding via S-glutathionylation (Konopka-Postupolska et al. 2009).

Biochemical properties of plant annexins

Peroxidase activity

Peroxidase activity is attributed to certain plant annexins. Inherent peroxidase activity was originally suggested for *A. thaliana* AtAnn1 based on protection against oxidative stress to H_2O_2 -sensitive *Escherichia coli* Δoxy5 strain or mammalian cells and sequence similarity with heme peroxidases (Gidrol et al. 1996; Kush and Sabapathy 2001; Gorecka et al. 2005; Konopka-Postupolska et al. 2009; Laohavisit et al. 2009; Clark et al. 2010). *In vitro* peroxidase activity has also been observed in BjAnn1, ZmAnn33/35, CaAnn24 and NnAnn1 (Jami et al. 2008; Laohavisit et al. 2009; Chu et al. 2012). Plant annexins provide oxidative protection to cells as studied in both native (Konopka-Postupolska et al. 2009) and transgenic plants (Gorecka et al. 2005; Jami et al. 2008; Laohavisit et al. 2009; Divya et al. 2010; Jami et al. 2010; Zhang et al. 2011; Chu et al. 2012). Guard cells of *Atann1* knockout mutant accumulated more intracellular ROS when challenged with ABA or exogenous H_2O_2 than wild type. On the other hand, ROS accumulation was suppressed in AtAnn1 over-expressor lines compared to wild type (Konopka-Postupolska et al. 2009). A complex of proteins purified from *Brassica rapa* floral buds showed peroxidase activity that contains

BrAnn1 and a peroxiredoxin (Clark et al. 2010). Mustard annexin found as complex with the chloroplast RNA polymerase has been proposed to protect transcription from oxidative damage (Pfannschmidt et al. 2000).

Signal transduction

The N-terminal domain of annexins is frequently involved in interactions with other proteins. Phosphorylation in this region is likely to trigger signals and is structurally achieved by a conformational change in the secondary structure of this region of the molecule (Szilak et al. 1997; Andrew et al. 2002; Konopka-Postupolska et al. 2011). Several studies have evidenced native plant annexins to be phosphorylated (Andrawis et al. 1993; Hoshino et al. 2004; Lee et al. 2004; Konopka-Postupolska et al. 2011). Heterologously expressed AtAnn1 from *N. benthamiana* leaves showed more peroxidase activity than recombinant protein expressed in *Escherichia coli*. However, the activity was decreased by de-phosphorylation (Gorecka et al. 2005). Phosphorylation is known to clearly reduce the peroxidase activity (Konopka-Postupolska et al. 2011). In silico analysis showed potential phosphorylation sites both in the N-terminal and C-terminal domain of *Arabidopsis* annexins. These in silico data do not perfectly match with the experimentally verified phosphorylation sites. With the hypothesis that the convex (membrane binding) side or the concave (membrane distal) side are the two sides on the annexin molecule where functional (non-annexin) interactions occur, they are known locations of phosphorylation.

As far as interactions of plant annexins with components of signaling pathway is concerned, rice annexin Os05g31750 has been found to interact with any of the 23 tested kinases, namely: receptor like kinase (RLK) Os01g02580, Os10g37480 casein kinase Os01g28950, SPK-3 kinase Os01g64970 and Sterile 20 (Ste20)-like kinase. However, Os05g31750 was the only rice annexin identified as a substrate for these (de-) phosphorylating enzymes (Rohila et al. 2006; Konopka-Postupolska et al. 2011). Its interaction with casein kinase and calcium/calmodulin dependent SPK3 might suggest its involvement in calcium-dependent and independent signaling cascades. Its association with Ste20-like kinase (SLK) supports its putative involvement in plant stress responses as well as apolar growth (Konopka-Postupolska et al. 2011).

Channel gating and selectivity involves two conserved salt bridges (D92-R117 and E112-R271) located within the central pore (Liemann et al. 1996) which are conserved in plant annexins. Recombinant CaAnn24 mediates a Ca^{2+} -permeable pathway in vesicles as shown by Hofmann et al (2000a). At acidic pH, recombinant AtAnn1 inserts into planar lipid bilayers to form a K^{+} -permeable conductance (Gorecka et al. 2007). Regulation through S-nitrosylation by nitric oxide (NO) is unknown (Lindermayr et al. 2005). However, Ca^{2+} affinity of AtAnn1 is decreased by S-glutathionylation (Konopka-Postupolska et al. 2009). Maize annexins ZmAnn33/35 increase $[\text{Ca}^{2+}]_{\text{cyt}}$ (possibly as a signaling second messenger) and form a Ca^{2+} - and K^{+} -permeable conductance in planar lipid bilayers with a low selectivity for Ca^{2+} over K^{+} . This resembles nonselective Ca^{2+} -permeable cation channels (NSCC) (Laohavisit et al. 2009, 2010). The occurrence of *Medicago* annexins in nuclear membranes, and the possibility of them forming channels, has led to the hypothesis that they might be involved in symbiotic Ca^{2+} signaling (de Carvalho-Niebel et al. 2002 and Talukdar et al. 2009). Ca^{2+} -dependent membrane binding of annexins might also contribute to $[\text{Ca}^{2+}]_{\text{cyt}}$ signaling on their release. The lipid bilayer has a significant role in modulating Ca^{2+} transport by annexins. This could fine-tune a resultant cytosolic Ca^{2+} increase to encode a specific signal (Laohavisit et al. 2010).

AtAnn1 lies in the downstream of the cross-talk between auxin- and ABA-signaling (Bianchi et al. 2002; Laohavisit et al. 2010). The C-terminal diacidic motif has been shown as an important ER export signal to the PM (Mikosch and Homann 2009). Constitutive expression of BjAnn1 in tobacco resulted in reduced MDA level and the chlorophyll content was maintained. This suggests enhanced ability of the protein to sense/signal or degrades ROS at membranes and in the chloroplast (Jami et al. 2008; Laohavisit et al. 2010).

Nucleotide Phosphodiesterase activity

First ATPase activity was found to be associated with maize annexin p68 (McClung et al. 1994). Dimerization increases phosphodiesterase activity which has also been observed in cotton and tomato annexins (McClung et al. 1994; Calvert et al. 1996; Lim et al. 1998; Shin et al. 1999). While Ca^{2+} has an inhibitory effect, specificity varies between ATP and GTP along with magnesium requirement (McClung et al. 1994; Calvert et al. 1996; Shin et

al. 1999). The nucleotide phosphodiesterase activity of tomato annexin is reduced when it binds to phospholipid (Calvert et al. 1996; Lim et al. 1998). The fourth endonexin repeat is critical to GTPase activity as observed from sequence alignments and site-directed mutagenesis studies (Clark et al. 2001; Shin et al. 1999). The GTP-binding site was mapped onto carboxy-terminal of the fourth domain by domain-deletion mutants of the annexin (Shin and Brown 1999). The putative GTP binding motifs 'GXXXXGKT and DXXG' are the Walker A motif and the GTPase superfamily GTP-binding motif, respectively (Clark et al. 2001). AtAnn1 binds to ATP but the structural basis is unclear (Ito et al. 2006). Phosphodiesterase activity has not yet been observed for *Arabidopsis* annexins, but AtAnn2 and AtAnn7 have a GTP-binding motif similar to cotton annexin and are likely to be the candidates for GTP binding (Clark et al. 2001; Shin et al. 1999). Phosphodiesterase activity is also linked with exocytosis as was observed in cotton annexin (Shin and Brown 1999) as well as in maize annexin (Carroll et al. 1998).

Tomato annexin nucleotide diphosphatase activity is not affected by F-actin binding (Calvert et al. 1996). Two PM-associated annexins from zucchini (*Cucurbita pepo*), bind to F-actin in vitro (Hu et al. 2000). This suggests that annexins are part of the apparatus connecting PM and cytoskeleton. Animal annexins interact with C2 domain-containing proteins to modulate their activity (Morgan et al. 2006). C2 helps Ca^{2+} -dependent membrane binding and enhances the activity of coupled enzymatic domains. The K/RH-G-D motif present in the Ca^{2+} -binding repeats and N-terminus is considered to be the basis for annexin–C2 interaction (Morgan et al. 2006). AtAnn1, AtAnn7 and CaAnn24 harbors consensus K-R-H/G/D motif. Others contain a slightly modified version (ZmAnn33; S /G/D motif) while some lack it (AtAnn5, ZmAnn35) (Laohavisit et al. 2011).

Cytoskeletal binding

Two plasma membrane-associated annexins in zucchini (*Cucurbita pepo*) were the first plant annexins shown to bind F-actin in vitro and was released under high salt concentrations (Hu et al. 2000). This might suggest that annexins are part of the apparatus that connects plasma membrane to the cytoskeleton (Laohavisit et al. 2010). Calcium-dependency of F-actin binding was first demonstrated for tomato annexins. F-actin-binding

does not affect tomato annexin nucleotide diphosphatase activity (Calvert et al. 1996), possibly allowing actin to 'place' GTPase activity in the cell (Laohavisit et al. 2010). Hoshino et al. (2004) showed that mimosa annexin can bind to F-actin in a Ca^{2+} -dependent manner. This is the first study to prove that plant annexins can mediate calcium-induced actin bundling in vitro. Actin being ROS-sensitive (Franklin-Tong and Gourlay 2008), it is possible that actin-bound annexin peroxidase could affect the cytoskeleton's role in ROS signaling (Laohavisit et al. 2010). Actin bundling in maize coleoptiles is induced in epidermal cells during growth inhibition (Waller et al. 2002). Therefore, certain plant annexins can inhibit cell elongation by modulating actin bundling properties (Konopka-Postupolska et al. 2011). AnxGb6 was shown to have an important role in fiber elongation by potentially providing a domain for F-actin organization (Huang et al. 2013).

Exocytosis

Exocytosis is the final stage in the secretory pathway where secretory vesicles originate from golgi bodies, migrates and ultimately fuses with the plasma membrane to secrete polysaccharides. Besides mediating the secretion of newly synthesized wall materials and plasma membrane, another potential secretory role for plant annexins is to deliver a wide range of signaling molecules. These are wall-modifying enzymes like expansins and extensins, arabinogalactan proteins which are delivered to the extra cellular matrix (ECM) while receptors & transporters to the plasma membrane (Konopka-Postupolska et al. 2011). Annexins are also found to be present during cork formation indicating their role in cell proliferation and expansion, perhaps through exocytosis. This could also indicate their role in irreversible commitment to cell death (Soler et al. 2007). Association of cotton annexin with PM and dictyosome-derived coated vesicles involved in fibre elongation (Shin & Brown 1999) indicates its implication in exocytosis. AtAnn1 mutant (T-DNA Knockout) displayed a short root phenotype and the protein is implicated in gravitropic-induced root bending by stimulating oligosaccharide secretion (Clark et al. 2005a,b). It also showed stress-induced germination delay (Lee et al. 2004) indicating its role in exocytosis or cell cycle control. AtAnn2 knockouts (T-DNA knockout) have reduced hypocotyl elongation and the protein is implicated in hypocotyl oligosaccharide secretion during gravitropism. This suggests the role

of the protein in exocytosis (Clark et al. 2005a,b). Gravi-stimulated redistribution of pea annexin also indicates regulation of exocytosis for growth (Clark et al. 2000; Clark et al. 2005a,b). Lily (*Lilium longiflorum*) annexin is also known to be involved in golgi mediated secretion of polysaccharides (Blackbourn et al. 1992). ZmAnn33/35 stimulates exocytosis in root cap protoplasts (estimated by membrane capacitance) which can be prevented by non-hydrolysable GTP analogues (Carroll et al. 1998). Tobacco Ntp32.1 and Ntp32.2 involve positively with cell division and lie beneath the PM probably to contribute to exocytosis (Proust et al. 1999).

Complex carbohydrate synthesis

Plasma membranes from higher plants contain glycosyltransferases that catalyze the synthesis of 1, 3- β -D-glucan (Callose) and 1, 4- β -D-glucan (cellulose) from UDP-glucose. These enzymes are of pivotal importance in normal development, because of their necessity in cell wall biosynthesis, particularly for the plant response to mechanical wounding, environmental stresses and pathogen attack (Hofmann et al. 2004). In the endosperm of the starch synthase IIa mutant, barley annexin p33 is upregulated during seed filling (Clarke et al. 2008). AtAnn7 has no direct link with callose synthase regulation (Velloso et al. 2007). GhAnn1 showed association with cotton fibre PM callose synthase in a Ca^{2+} -dependent manner (Andrawis et al. 1993; Shin & Brown 1999; Laohavisit et al. 2011). *Saprolegnia* and cotton (GhAnn1) annexin stimulate or inhibit callose ((1 \rightarrow 3)- β -D-glucan) synthase activity, respectively. Regulation of callose synthase by annexin implicates its role in cotton and bast fibre growth, cell plate formation, growth of pollen tubes, sieve tube sealing, response to pathogens, wounding and cell death. Hence it may be noteworthy that annexins are evident in localization at polar growth points, in the cell cycle, found in phloem, and are upregulated during biotic stress responses (Laohavisit et al. 2011).

Objectives:

1. Attenuation of hydrogen peroxide-mediated oxidative stress by *Brassica juncea* annexin-3 which complements thiol-specific antioxidant (TSA1) deficiency in *Saccharomyces cerevisiae*.
2. Alleviation of methyl viologen-mediated oxidative stress by *Brassica juncea* annexin-3 in transgenic *Arabidopsis*.
3. Role of AtAnn3 under methyl viologen-mediated oxidative stress in *Arabidopsis thaliana* AtAnn3-knockout plants
4. Role of BjAnn3-cysteines in redox modulation and oligomerization.

Materials & Methods

Materials and Methods

Bacterial and yeast strains

The bacterial strain *Escherichia coli* DH5 α was used for the maintenance of plasmids and *Escherichia coli* BL21 (DE3) pLysS was used for the expression of recombinant BjAnn3 wild type and its variants.

The *Agrobacterium tumefaciens* LBA4404 cells was used for transformation in *Arabidopsis thaliana* and Agro infiltration studies in tobacco leaves.

S. cerevisiae INVSc1 strain was used for the expression of recombinant BjAnn3 wild type protein. A surrogate model of *S. cerevisiae* (Δ *tsa1*) was generated for functional characterization of the protein. In order to inactivate the thiol-specific antioxidant (*TSA1*) gene, the *KANMX* cassette with *TSA1* flanking region was amplified using pFA6a-kanMX6 plasmid as template and the primer pair as mentioned in **Table 1**. The PCR product was then transfected into INVSc1 cells and clones were selected on G418 Sulfate (Cambiochem[®], Germany)-containing YPD plates to generate the *tsa1* null strain named as ADY1 (**Table 2**). *S. cerevisiae* ADY1 cells were used for complementation studies.

Table 1. Primers used for *S. cerevisiae* studies

Gene	Primer name	Primer sequence
<i>KANMX</i> cassette	TSA1-KANMX F	5' ATGGTCGCTCAAGTTCAAAAGCAAGCTCCAAC TTTTAAGA CGGATCCCCGGGTAAATTAA 3'
	TSA1-KANMX R	5' TTATTTGTTGGCAGCTTCGAAGTATTCCTTGGAGTCTTCAG AATTCGAGCTCGTTTAAAC 3'
<i>BjAnn3</i>	BjAnn3-KpnI	5' AAAAAAAGGTACCaATGGCCACCATTAGAGTAC3'
	FBjAnn3-XhoI R	5' AAAAAA ACTCGAGTCAGATCTTGGATCCAAGG3'
<i>SOD1</i>	SOD1 F	5' TGGTTGTGTCTCTGCTGGTC3'
	SOD1 R	5' TAACGACGCTTCTGCCTACA3'
<i>SOD2</i>	SOD2 F	5' CAAGCTGGACGTTGTTCAAA3'
	SOD2 R	5' AGATCTTGCCAGCATCGAAT3'
<i>GPX2</i>	GPX2 F	5' TTTGGGGTTCCCATGTAATC3'
	GPX2 R	5' ACCTGCTTTTGGCTTTTCA3'
<i>TSA2</i>	TSA2 F	5' TTTGTCCCATTTGGCTTTTTC3'
	TSA2 R	5' ACCGTCTTTTCTGGGAAGGT3'
<i>ACT1</i>	ACT1 F	5' CGTTCCAATTTACGCTGGTT3'
	ACT1 R	5' GAAGTCCAAGGCGACGTAAC3'

Table 2. *Saccharomyces cerevisiae* strains used:

Strains	Genotype	Reference
<i>S. cerevisiae</i> INVSc1	MATa <i>his3Δ1 leu2 trp1-289 ura3-52</i> /MATα <i>his3Δ1 leu2 trp1-289 ura3-52</i>	Invitrogen™, USA
<i>S. cerevisiae</i> ADY1	MATa <i>his3Δ1 leu2 trp1-289 ura3-52 TSA1::KAN^r</i> /MATα <i>his3Δ1 leu2 trp1-289 ura3-52 TSA1::KAN^r</i>	Generated

Plant materials

Arabidopsis thaliana (ecotype Columbia, Col 0), *A. thaliana AtAnn3* knockout (Δ Atann3: (SALK_130101C)), *Brassica juncea* L. Czern & Coss and *Nicotiana tabacum* L. cv Xanthi were used in this study. *AtAnn3* knockout (T-DNA insertion line) was obtained from Nottingham Arabidopsis Stock Centre.

Chemicals

All the chemicals used were obtained from Sigma-Aldrich, USA; Invitrogen™, USA; MBI Fermentas, Germany; HiMedia®, India; Thermo Fisher Scientific Inc., USA; Cabiochem®, Germany; Qiagen, The Netherlands; Roche Applied Science, Germany and Qualigens fine chemicals, India.

Enzymes and Markers

All the enzymes, their corresponding buffers were from Sigma-Aldrich, USA; Thermo Fisher Scientific Inc., USA; or MBI Fermentas, Germany. The DNA markers (λ DNA/EcoR I + Hind III or λ DNA/ EcoR I) and pre-stained or unstained protein markers were from MBI Fermentas, Germany.

Plasmid DNA vectors

pTZ57R/T (MBI Fermentas, Germany)

This vector is used in the cloning of all cDNAs (wild type and its variants) of *BjAnn3* from *B. juncea*. It has a bacterial selectable marker gene, β -lactamase and can be selected on ampicillin.

pEXP-5-NT/TOPO® TA (Invitrogen™, USA)

This is a bacterial expression vector with T7 lac promoter used for expressing recombinant BjAnn3 wild type protein. It has a bacterial selectable marker for ampicillin.

pET-28(a) (Novagen, USA)

This is a bacterial expression vector with T7 lac promoter used for expressing recombinant BjAnn3_{WT} and its variants. It has a bacterial selectable marker for kanamycin.

pYES2A (Invitrogen™, USA)

pYES2A is a *S. cerevisiae* expression vector used for expressing BjAnn3 recombinant proteins. It has β - lactamase gene for ampicillin based bacterial selection and *URA3* gene for selection in *S. cerevisiae*.

pRT100 (Töpfer et al. 1987)

This is a plant expression vector used for cloning of *BjAnn3* cDNA. The multiple cloning site is flanked by CaMV 35S promoter and NOS terminator. pRT100 has a gene encoding for β -lactamase for bacterial selection on ampicillin.

pCAMBIA 2300 (CAMBIA, Australia)

pCAMBIA 2300 is a binary vector used to clone the 35S-*BjAnn3*-nos cassette. This binary vector has *nptII* and *kan^R* gene for selection in plants as well as in bacteria respectively on kanamycin.

pCAMBIA 1302 (CAMBIA, Australia)

pCAMBIA 1302 is a binary vector used to clone the BjAnn3 cDNA with C-terminally fused *gfp* for localization studies in tobacco leaf. This binary vector has *hptII* and *kan^R* gene for selection in plant on hygromycin as well as in bacteria on kanamycin, respectively.

Growth conditions for microorganisms

The different strains of *E.coli* were incubated and cultured either in LB broth medium (HiMedia[®], India) with continuous shaking at 200 rpm or in LB agar medium at 37 °C, while *Agrobacterium*, were incubated in LB broth medium with continuous shaking at 200 rpm or in LB agar medium at 28 °C with appropriate antibiotics for selection. *S. cerevisiae* INVSc1 and ADY1 cells were cultured either in YPD or synthetic dropout (-URA) media (Agar or broth at 200 rpm) at 30 °C.

Plant Growth conditions and stress treatments

Brassica and *Nicotiana* were grown on soil in green house for 6 weeks. *Arabidopsis* seeds were sterilized and sown on half strength of Murashige and Skoog medium (HiMedia[®], India), followed by stratification at 2–4 °C in dark for 2 d before transferring them to light. They were grown at a light intensity of 100–150 $\mu\text{mol quanta m}^{-2} \text{s}^{-1}$ (8 h light/16 h dark) at 22–24 °C for a period up to 2–12 weeks depending on experimental plans. All treatments with methyl viologen (MV; Sigma-Aldrich, USA) (in 0.05% Triton-X 100) were administered to *Arabidopsis* seedlings or mature leaf discs under continuous illumination of 100 $\mu\text{mol quanta m}^{-2} \text{s}^{-2}$. To assess stress tolerance in transgenic lines, 7 d old seedlings were transferred onto ½ MS media with 1.5 μM and 3 μM MV. Chlorophyll fluorescence was measured with leaf discs of 8–10 week old plants. They were treated with 10 μM MV for 1.5 h and acclimated to darkness for 30 min before analysis. Alternatively, 15 d old seedlings were treated with 50 μM MV for 2 h for subsequent determination of MDA levels, H_2O_2 levels and transcript analysis.

Genomic DNA Isolation and purification from plants

Genomic DNA was isolated from 4–5 days old seedlings or from the leaves of 2–3 months old *A. thaliana* plants according to the method of CTAB procedure (Doyle and Doyle 1990). The seedlings or the leaf materials (0.5 g) were ground to fine powder in liquid nitrogen using pre-chilled mortar and pestle. The powder was then suspended in 2 ml of pre-warmed DNA extraction buffer [2% (w/v) CTAB, 100 mM Tris-HCl, pH 8.0, 1.4 M NaCl, 20 mM EDTA, 0.2% (v/v) β -mercaptoethanol which should be added freshly (before

extraction)] and was incubated at 65 °C for 1 h in a water bath with occasional mixing by gentle swirling. The mixture was further suspended in one volume of chloroform: isoamyl alcohol (24:1 ratio) and gently mixed by inversion to emulsify and then centrifuged at room temperature for 15 min at 12000 rpm. The aqueous phase was carefully collected and then gently mixed with 2/3 volume of isopropanol and 0.1 volume of 3 M sodium acetate (pH 5.2) by inversion and further incubated at room temperature for 1 h. The mixture was centrifuged at room temperature for 15 min at 12000 rpm and the supernatant was carefully discarded. The pellet was rinsed in 70% (v/v) ethanol for 10 min, air-dried and then resuspended in 0.5 ml of TE (10 mM Tris-HCl, pH 8.0, 1 mM EDTA).

To the DNA sample, 5 µl of RNaseA (10 mg/ml) was added and incubated for 2 h at 37 °C. Then 0.5 ml of Phenol: chloroform: isoamyl alcohol (25:24:1) was added and mixed gently by inversion for 10 min. The suspension was centrifuged at 12000 rpm for 15 min at room temperature. The aqueous phase was carefully collected and was gently mixed with 0.1 volume of 3 M sodium acetate (pH 5.2) and 2.5 volumes of chilled absolute alcohol and further incubated at –20 °C for 2h or overnight. DNA was pelleted by centrifugation at 12000 rpm for 15 min at room temperature and washed in 70% (v/v) ethanol for 10 min. DNA pellet was air-dried and resuspended in 50–100 µl of TE buffer and stored at –20 °C.

Isolation of total RNA from plants

The plant materials (0.2) mg from treated and untreated seedlings/leaves were frozen in liquid nitrogen and ground to a fine powder using pre-chilled mortar and pestle. Total RNA was extracted using TRI Reagent[®] (Sigma-Aldrich, USA) according to the manufacturer's instructions. Finally the pellet was resuspended in 40 µl of RNase-free water and stored at –70 °C.

Isolation of total RNA from yeast

Cultures diluted to an OD₆₀₀ = 0.5 were treated with 2.5mM H₂O₂ for 75 min. RNA was isolated by acid phenol method (Schmitt et al. 1990 and Laskar et al. 2011). The culture pellet was suspended in 400 µl TES buffer (10 mM TrisHCl, [pH 7.5], 10 mM EDTA, 0.5% SDS). 400 µl phenol (pre equilibrated with DEPC water) was added and the mixture was

incubated at 65 °C for 1 hour, with intermittent vortex. The mixture was rapidly cooled on ice for 5 min followed by centrifugation at 14000 rpm for 10 min at 4 °C. The aqueous layer was mixed with 400 µl chloroform, vortexed and further centrifuged for the same time at same speed and temperature as mentioned above. The extracted aqueous phase was precipitated by adding 1/10th volume of 3 M sodium acetate [pH 5.2] and 2.2 volume of chilled ethanol. The RNA pellet was washed with 70% ethanol and dissolved in 30 µl DEPC treated water.

Estimation of nucleic acids

The quantity and quality of purified nucleic acids (DNA and RNA) in solution were determined by using nano-drop spectrophotometer (ND-1000, USA). The quantity and quality of nucleic acids was directly displayed in terms of ng/µl and OD_{260/280} respectively. Pure DNA should have the value of OD_{260/280} between 1.8 and 2.0. A value below 1.8 indicates the contamination of DNA with proteins and phenolic compounds. Pure RNA should have the value of OD_{260/280} higher than 2.0. A value below 2.0 indicates the contamination of RNA with proteins or phenolic compounds. Equal amount of RNA measured was then subjected to DNaseI (MBI Fermentas, Germany) treatment for 15 min at room temperature. The treated samples were incubated with 25 mM EDTA at 65 °C for 10 min to inactivate DNaseI.

First strand cDNA synthesis

Five µg of total RNA was used to synthesize first strand cDNA using oligo-dT₍₂₀₎ using M-MLV Reverse Transcriptase (Sigma-Aldrich, USA) according to manufacturer's protocol. After first strand synthesis, the reaction was terminated by heat inactivation at 70 °C for 10 min followed by the addition of 4 units of RNase H (InvitrogenTM, USA) to remove excess RNA.

Cloning of DNA fragments

Primer designing for cloning

For PCR amplification, specific primers were designed as listed in **Table 2 and 3**. Both manual method as well as primer3 software was used to design primers. In manual method, the melting temperature (T_M) of the primers was according to Faust rules, T_M ($^{\circ}\text{C}$) = 4 (G+C) + 2 (A+T), where G, C, A and T represent the number of corresponding nucleotides in the primer. The annealing temperature (T_A) depends on the T_M value and was calculated as, $T_A = T_M - 5$ $^{\circ}\text{C}$. The primers were designed to avoid self-complementation thereby forming a secondary structure. The forward and reverse primers of each reaction were designed to have approximately the same T_M .

Table 3. Primers used for *Arabidopsis thaliana* studies.

Gene	Primer name	Primer sequence
<i>BjAnn3</i> for cloning in to pRT 100/pCAMBIA 2300	BjAnn3 ApaI F	5' AAGGGCCCATGGCCACCATTAGAGTAC 3'
	BjAnn3 XbaI R	5' AATCTAGATCAGATCTTGGATCCAAGGAA 3'
<i>BjAnn3</i> for cloning in to pCAMBIA 1302	BjAnn3 NcoI F	5' AACCATGGATGGCCACCATTAGAGT 3'
	BjAnn3 SpeI R	5' AAAC TAGTGATCTTGGATCCAAGGAA 3'
<i>BjAnn3</i> for cloning into pEXP-5-NT/TOPO® TA sAPX	BjAnn3-F-Topo	5' ATGGCCACCATTAGAGTACCA 3'
	BjAnn3-R-Topo	5' TCAGATCTTGGATCCAAGGAAAGT 3'
	sAPX F	5' CCTCAGAAAAATGGCAGAGC 3'
	sAPX R	5' GAGGAGGAAGCGGAGAGAGT 3'
<i>tAPX</i>	tAPX F	5' TGGAGAAGCAGGAGGACAGT 3'
	tAPX R	5' GCAGCCACATCTTCAGCATA 3'
<i>APX1</i>	APX1 F	5' GCATGGACATCAAACCCTCT 3'
	APX1 R	5' AGCAAACCCAAGCTCAGAAA 3'
<i>CSD1</i>	CSD1 F	5' TGAAC TCAGCCTGGCTACTGG 3'
	CSD1 R	5' AGCCACACACCAGAAGATACACAC 3'
<i>FSD1</i>	FSD1 F	5' GCCTGGCTTGCTTATTCAA 3'
	FSD1 R	5' GGCATTACAGCTTCCCAAG 3'
<i>18S rRNA</i>	18S rRNA F	5' ATGATAACTCGACGGATCGC 3'
	18S rRNA R	5' CTTGGATGTGGTAGCCGTTT 3'

Polymerase chain reaction (PCR)

For amplification of DNA fragments, a total volume of 50 μl reaction mixture was prepared in a sterile 0.2 ml thin-wall PCR tube with 10 pmol/ μl each of both forward and reverse primers, 100–150 ng of genomic DNA or 5 ng/ μl plasmid DNA or PCR product

or 2–5 µl of first strand cDNA (20 µl reaction mix from 1 µg RNA) as a template, 200 µM of each dNTP, 1.5 mM MgCl₂ and 2.5 U of Taq DNA polymerase (Sigma-Aldrich, USA) or 1 U of Phusion High-Fidelity DNA Polymerase (Thermo Fisher Scientific Inc., USA). Each PCR aliquot was mixed and the PCR reactions were performed in Eppendorf personal cyclers or Eppendorf Mastercycler Gradient (Germany) and/or MJ Research Inc. (USA). The standard reaction conditions maintained using Taq DNA polymerase were initial denaturation at 94 °C for 4 m, followed by 30 cycles of 94 °C for 1 m, 58–60 °C for 45s, 72 °C for 1 m and a final extension of 10 m at 72 °C. Reaction conditions maintained using Phusion High-Fidelity DNA Polymerase were initial denaturation at 98 °C for 30s, followed by 30 cycles of 98 °C for 10s, 58–60 °C for 30s, 72 °C for 30s and a final extension of 5m at 72 °C. An aliquot from the amplified mix was run on 1% agarose gel to check for amplification.

Purification of DNA fragments from the agarose gel

After PCR amplification or restriction digestion, DNA bands, plasmid DNA constructs or plasmid inserts were identified using standard molecular weight marker (λ DNA/EcoR I + Hind III or λ DNA/EcoR I) in agarose gel. The bands were excised from the agarose gel and purification of DNA from the agarose gel pieces was done using GenElute™ Gel Extraction Kit (Sigma-Aldrich, USA) according to manufacturer's instructions.

Restriction endonuclease treatments

DNA digestion was carried out in a reaction volume of 20 µl, containing 1/10 of the end volume of appropriate reaction buffer (10X) and 5 U of restriction enzyme per 1 µg of DNA to be digested, while for double digestions, the restriction digestions were carried out sequentially.

Ligation

For plasmid DNA constructs, different DNA inserts were ligated in various independent experiments using T₄ DNA ligase (MBI Fermentas, Germany). The ligation reaction mixture was made in a total volume of 20 µl comprising 2 µl of ligation buffer (10 X), appropriate

volumes (in μl) each of linear digested plasmid DNA and insert DNA and finally T₄ DNA ligase (1–2 units for cohesive ends and 5 units for blunt ends). The reaction mixture was incubated for 16 h at 16 °C and at 22 °C for cohesive and blunt ends respectively.

Preparation of *E.coli* competent cells and transformation

A single colony of *E.coli* DH5 α or BL21 (DE3) pLysS cells was inoculated into 5 ml of LB broth and incubated overnight with constant shaking at 37 °C. One ml of the overnight culture was further grown in 50 ml of LB broth with vigorous shaking until OD₆₀₀ = 0.5. The cells were then cooled on ice for 10 min and pelleted by centrifugation at 4000 rpm for 5 min at 4 °C. The pellet was suspended in 40 ml of ice-cold 100 mM CaCl₂ and incubated on ice for 20 min and further centrifuged as described above. Finally, the pellet was resuspended in 2 ml ice-cold 100 mM CaCl₂ and 15% (v/v) sterile glycerol and then mixed and stored at –70 °C in aliquots of 200 μl .

One μl of the plasmid DNA (10–50 ng/ μl) or the ligated plasmid DNA construct (ligation mixture) was added to competent cells, carefully/gently mixed and incubated on ice for 30 min. The cells were subjected to heat shock at 42 °C for 90 s followed by immediate immersing into ice for 1 min. LB broth (0.8 ml) was added to the treated cells and further incubated by shaking at 200 rpm at 37 °C for 1 h. Aliquots (100–200 μl) of the transformed cells were spread on LB selective agar plates and incubated at 37 °C overnight.

Plasmid DNA isolation from *E. coli*

For plasmid mini-prep, transformed *E. coli* colonies were inoculated in 5 ml of LB broth containing appropriate antibiotics and were allowed to grow overnight with shaking at 200 rpm at 37 °C. The culture was harvested by centrifugation at 12000 rpm at room temperature for 1 min and plasmid isolation was done using GenElute™ Plasmid Miniprep kit (Sigma-Aldrich, USA) according to the manufacturer's protocol.

Preparation of *S. cerevisiae* competent cells and transformation

One yeast colony was inoculated in 5 ml of YPD broth and was incubated overnight at 30 °C with shaking at 200 rpm. Secondary inoculation was done in 40 ml of YPD broth so

that the final required OD₆₀₀ after two generation (3h) reaches 0.5. The following equation was used to calculate the volume of overnight culture to be used for inoculation:

$$V_1 * \text{O.D.}_{600} \text{ of overnight culture} * 2^{2(\text{generations})} = \text{Final Volume} * \text{Final O.D.}_{600} (\text{required})$$

$$V_1 * 3.0 * 2^2 = 40 \text{ ml} * 0.5$$

$$V_1 = 2.0 \text{ ml.}$$

Therefore, in this case we need to add 2 ml of the primary inoculum to 40 ml of YPD broth. The culture was incubated at 30 °C (200 rpm) for 3 h or more until O.D.₆₀₀ reaches 0.5 to 0.7. Immediately the culture was placed in ice and then centrifuged at 3500 rpm for 5 min at 4 °C. The harvested cells were resuspended in 10 ml of ice-cold sterile water followed by further centrifugation at 3500 rpm for 5 min at 4 °C. The pellet was finally resuspended with ice-cold freshly prepared lithium solution to make the cells competent, and kept on ice.

DNA sample (5–10 µg) was mixed with 10 µg of carrier DNA (5 µl of 2 mg/ml Salmon Sperm DNA (Sigma-Aldrich, USA) stock) to make a final volume not exceeding 20 µl and added to a 1.5 ml Eppendorf tube (transformation tube). 200 µl of freshly prepared competent cells were added to the transformation tube followed by immediate addition of 1.2 ml of freshly prepared PEG 2000 (Sigma-Aldrich, USA) solution. The mixture was incubated at 30 °C for 30 min at 200 rpm. The cells were then given heat shock at 42 °C in a water bath for 15 min and then centrifuged at a high speed for 6–7 s. The PEG supernatant was then removed carefully and the pellet was resuspended in 200 µl of 1X TE buffer followed by spreading on appropriate selection plate.

Expression of recombinant protein in yeast and immunodetection

AnnBj3 cDNA was cloned into KpnI and XhoI sites of pYES2A vector for heterologous expression of N-terminally His₆-tagged fragments. Integrity of the construct was confirmed by sequencing (eurofins mwg|operon, Germany). The construct was transfected into *S. cerevisiae* INVSc1 cells and test expression was carried out under various conditions (varying induction time) to attain optimized expression which was verified by immunoblotting. Briefly, a single colony of INVSc1 containing pYES2A construct was inoculated into 15 ml of synthetic dropout medium (SC-U) containing 2% glucose and was grown at 30 °C overnight with shaking. OD₆₀₀ of the overnight culture was taken and

amount of culture necessary to obtain OD₆₀₀ of 0.4 in 50 ml of induction medium (SC-U medium with 2% galactose) was calculated. The same amount of overnight culture was centrifuged at 3500 rpm for 5 min at 4 °C and the pellet was resuspended in 50 ml of induction medium and was incubated at 30 °C with shaking. 5 ml of the culture was collected at every 4 h of interval after addition of the cell to the induction medium and OD₆₀₀ was recorded. The cultures were centrifuged at 3500 rpm for 5 min at 4 °C and the pellets were resuspended with 500 µl of breaking buffer and then further centrifuged at 3500 rpm for 5 min at 4 °C. The pellets were resuspended again in a volume of breaking buffer to obtain an OD₆₀₀ of 50–100 and then they were repeatedly freeze/thawed in liquid nitrogen and hot water bath (95 °C) for lysis. The lysed cells were centrifuged for 10 min at maximum speed and the supernatants were run on SDS-PAGE for further immunoblotting as described below (Pabla et al. 2006; Laskar et al. 2011).

Growth in liquid media and phenotypical analysis of *S. cerevisiae*

Freshly grown cultures (OD₆₀₀ 0.7 to 1) after secondary inoculation in SC-ura media containing 2% galactose were diluted to OD₆₀₀ = 0.2 with the same media. Oxidative stress was elicited with different concentrations of H₂O₂. After 12 h, cell number was estimated at OD₆₀₀ and the percent ratio of treated to untreated samples calculated.

In addition diluted culture of OD₆₀₀ = 0.2 were treated with 2 mM and 2.5 mM H₂O₂ for 4 h and aliquots were spotted by serial dilution on YPD plates for phenotypic analysis. Viability was determined with fluctuation assay by plating 1000 cells from treated and untreated samples based on OD₆₀₀ on YPD plates. Plates were photographed and colonies counted after 48 h.

Oxygen consumption in *S. cerevisiae* under oxidative stress

Exponentially growing cultures (OD₆₀₀ 0.7 to 1) after secondary inoculation in SC-ura liquid media containing 2% galactose were sedimented and re-suspended twice for washing and finally brought to an OD₆₀₀ 20 with fresh media. 25 µl cell suspension was added to the oxygraph chamber (Hansatech Instruments Ltd., England) filled with 975 µl of minimal

medium. Respiratory oxygen consumption was measured for at least 10 min without and with H₂O₂ (modified Agrimi et al. 2011).

Plasma membrane permeabilization in *S. cerevisiae*

Cells re-suspended to OD₆₀₀ = 10 were treated with H₂O₂ for 75 min and subsequently incubated with 5 µgml⁻¹ propidium iodide (PI; Sigma-Aldrich, USA) for 30 min in dark at 30°C, washed twice and imaged under a Carl Zeiss LSM 710 NLO ConfoCor 3 laser-scanning confocal fluorescence microscope at λ_{em} 620 nm (λ_{exc} 530 nm) in order to check for viability and plasma membrane integrity (modified Li et al. 2006). DNA-bound PI fluorescence was quantified in equal number of cells of each treatment from three different experiments using Image-J 1.42 software (NIH, USA).

Intracellular reactive oxygen species (ROS) production in *S. cerevisiae*

Cells washed as before were re-suspended to OD₆₀₀=10. Cells were treated with H₂O₂ for 10 min and then incubated with 10 µM 2',7'-dichlorofluorescein diacetate (DCFDA; Sigma-Aldrich, USA) for 10 min in the dark at 25°C. The cells were washed twice with the same media for removal of unincorporated dye and immediately imaged under a laser-scanning confocal fluorescence microscope (Carl Zeiss LSM 710 NLO ConfoCor 3, Germany) at λ_{em} 529 nm (λ_{exc} 495 nm) (modified Wong et al. 2002). 2',7'-dichlorofluorescein (DCF) fluorescence was quantified in equal numbers of cells of each treatment from 3 different experiments using Image-J 1.42 software (NIH, USA).

Preparation of *Agrobacterium* competent cells and transformation

A single colony of *A. tumefaciens* (LBA4404) cells was inoculated into 5ml of LB broth and grown overnight with constant shaking (200 rpm) at 28 °C. Two ml of the overnight culture was used to inoculate in 50 ml LB broth with vigorous shaking under the same conditions until the OD₆₀₀ reaches 0.5 to 1.0. The culture was then cooled on ice for 10 min and centrifuged at 3000 rpm for 5 min at 4 °C. The pellet was resuspended in 1 ml of ice-cold 20 mM CaCl₂ and 15% (v/v) sterile glycerol, mixed and stored at -70 °C in aliquots of 100 µl.

Transformation of *Agrobacterium* with plasmid DNA was carried out by adding 1 µg of DNA to the competent cells followed by gentle mixing and immediate freezing in liquid nitrogen. The cells were thawed by incubating the eppendorf tube at 37 °C for 5 min. Subsequently, 1 ml of LB broth was added to the tube and incubated at 28 °C for 2–4 h with gentle shaking. The cells were then briefly centrifuged for 30 s and the pellet was resuspended in 100 µl of LB broth. The cells were spread on LB selective agar plate and incubated at 28 °C for 48 h.

Plasmid DNA isolation from *Agrobacterium*

A single colony of transformed *Agrobacterium* cells was inoculated in 10 ml of LB broth containing appropriate antibiotics and incubated overnight at 28 °C on shaking (200 rpm). The overnight culture was spun at 1000 rpm for 1 min and harvested in eppendorf tubes. The pellet was resuspended in 100 µl of ice-cold solution I followed by incubation at RT for 10 min. To this suspension, 200 µl of freshly prepared solution II was added, mixed thoroughly, incubated at room temperature and 30 µl of phenol (equilibrated with 2 volumes of solution II) was added. The contents were vortex mixed for a few seconds or till the suspension became viscous and to this viscous lysate, 150 µl of 3.0 M sodium acetate (pH 4.8) was added with proper mixing. The tubes were incubated at –70 °C for 15 min and centrifuged at 5000 rpm for 3 min. The supernatant was collected in a fresh tube and ice cold 100% ethanol was added to fill the tube. The content was mixed thoroughly by inversion and incubated at –70 °C for 15 min followed by centrifugation at 5000 rpm for 3 min. The pellet was suspended in 0.5 ml of 0.3 M sodium acetate (pH 7.0) and DNA was precipitated by adding ice-cold 95% ethanol. The DNA in sodium acetate and ethanol was mixed well by inversion and incubated at –70 °C for 15 min. After incubation, the tubes were centrifuged at 5000 rpm for 3 min and the supernatant was decanted. The tubes were allowed to stand in inverted position until the supernatant drained off completely. The pellet was rinsed with 1 ml of 70% ice-cold ethanol; vortex mixed briefly and was centrifuged at 5000 rpm for 1 min. The pellet was air-dried and was suspended in 50 µl of TE buffer and stored at –20 °C.

***Arabidopsis* transformation and generation of transgenic lines**

The recombinant plasmid *BjAnn3*-pCAMBIA 2300 carrying the expression cassette was transfected into *A. tumefaciens* LBA4404 cells which was further used to transform *A. thaliana* using the floral dip method as described by Clough and Bent (1998) and Bechtold et al (1993) with modifications. The first bolt was clipped for proliferation of multiple secondary bolts. *Agrobacterium* strain carrying gene of interest in a binary vector was grown in a large volume of LB medium with appropriate antibiotics at 28 °C with shaking, till mid-log or recent stationary phase. The culture was spinned down and resuspended to OD₆₀₀ around 0.8 in MS media with 5% sucrose. 0.005 to 0.01% Silwet L-77 was added to the culture, mixed well and the plant inflorescence was dipped fully for 15 to 20 min under vacuum. Further, the plants were kept in dark with high humidity for 1 day and then were exposed to light. The seeds were harvested and were selected on MS agar plates containing 50 mg l⁻¹ kanamycin (Duchefa Biochemie b.v., The Netherlands) and were confirmed by gDNA PCR using cetyl trimethyl ammonium bromide (CTAB; Sigma-Aldrich, USA) procedure (Doyle and Doyle 1990) as described above. Transgene expression was investigated by qPCR as described below.

Site-directed mutagenesis, recombinant protein expression and purification from *E. coli*

Single cysteine variants *BjAnn3*_{C114S} and *BjAnn3*_{C129S}, double cysteine variants *BjAnn3*_{C129S/C226S} and *BjAnn3*_{C114S/C242S}, triple cysteine variant *BjAnn3*_{C114S/C226S/C242S} and tetra cysteine variant *BjAnn3*_{C114S/C129S/C226S/C242S} were generated from *BjAnn3*_{WT} using PCR based site-directed mutagenesis as described by Montemartini et al (1999). Primers for mutation studies are listed in **Table 4**. *BjAnn3*_{WT} and its variants were cloned into EcoRI and SalI sites of pET-28(a) to generate N-terminally His₆-tagged fragments and integrity of the constructs was confirmed by sequencing (eurofins mwg|operon, Germany). Recombinant proteins purified from these clones were used for experiments in objective 4. For experiments in objective 2, *AnnBj3* cDNA was cloned into pEXP-5-NT/TOPO® TA expression vector (Invitrogen™, USA) to generate N-terminally His₆-tagged

BjAnn3_{WT}. Integrity of the construct was confirmed by sequencing (eurofins mwgl|operon, Germany).

Table 4. List of primers for mutation studies.

Gene	Primer name	Primer sequence
BjAnn3 for cloning into pET-28(a)	BjAnn3-EcoRI-F	5' AAGAATTCATGGCCACCATTAGAGTAC 3'
	BjAnn3-SalI-R	5' AAGTCGACTCAGATCTTGGATCCAAGGAA 3'
BjAnn3 for mutation at C114S	BjAnn3-C114S-F	5' GGAGATCTCTAGCACAACCTTCTC 3'
	BjAnn3-C114S-R	5' GAGAAGTTGTGCTAGAGATCTCC 3'
BjAnn3 for mutation at C129S	BjAnn3-C129S-F	5' GAAAGCTTACAGCTCTCTCTTTG 3'
	BjAnn3-C129S-R	5' CAAAGAGAGAGCTGTAAGCTTTC 3'
BjAnn3 for mutation at C226S	BjAnn3-C226S-F	5' TGTTGATGGATCTCCAGGAGATA 3'
	BjAnn3-C226S-R	5' TATCTCCTGGAGATCCATCAACA 3'
BjAnn3 for mutation at C242S	BjAnn3-C242S-F	5' GGTGATCTTGAGCATTGAGTCCC 3'
	BjAnn3-C242S-R	5' GGGACTCAATGCTCAAGATCACC 3'

All the constructs were transfected into *E. coli*BL21 (DE3) pLysS cells and test expression was carried out under various conditions (varying IPTG concentrations, induction time and temperature) to attain the expressed protein mostly in soluble fraction. Finally, from the overnight primary culture, secondary inoculation was carried out in 1/20th ratio of the final culture volume and were grown at 37 °C till OD₆₀₀ of 0.5 followed by induction with 0.1mM isopropyl-β-D-thiogalactopyranoside (IPTG; Sigma-Aldrich, USA) for 3 h at 28 °C. Soluble fraction of the protein was purified under native condition by nickel-affinity chromatography according to manufacturer's protocol (Qiagen, The Netherlands). Briefly, after induction, the cells were harvested by spinning them at 5000 rpm for 5 min at 4 °C and were resuspended in lysis buffer. Then they were sonicated with amplitude of 35% at a pulse of 20 sec ON and 30 sec OFF for 5 to 30 minutes at 4 °C, depending on the pellet size. The cultures were spun again at 12000 rpm for 30 min at 4 °C and the supernatant was loaded on to equilibrated Ni-NTA column (equilibrated with lysis buffer) followed by reloading of the flow-through for the second time for sufficient

binding of His₆-tagged protein with Ni-NTA. The column was washed consecutively with 10 ml and 15 ml of wash buffer followed by elution in fractions with 5 ml of elution buffer. The elution fractions were run on SDS-PAGE and were dialyzed against 50 mM NaH₂PO₄ (pH 7.5) according to their purity.

Protein assay using Bradford method

Colorimetric protein assay based on the Bradford method was used for the measurement of protein concentration. This assay is based on the shift in the absorbance maximum when Coomassie[®] Brilliant Blue G-250 dye binds with proteins. An appropriate ratio of dye volume to sample concentration is selected for quantification of protein using Lambert-Beer's Law. Dye binds to the protein and stabilizes the blue anionic dye form, detected at 595 nm. Binding of the dye requires a protein to have active basic or aromatic residues. 990 µl of Bradford reagent was mixed with 10 µl of protein sample, incubated for 5 min in dark at room temperature and absorbance was determined at 595 nm. Protein concentration was calculated according to the manufacturer's protocol.

Polyacrylamide Gel Electrophoresis (PAGE)

SDS-polyacrylamide gel (12%) was performed according to the protocol of Laemmli et al (1970). Protein samples were prepared by mixing with one-fifth volume of 5× sample buffer. Samples were boiled at 95 °C for 3 min or left uncooked and loaded on the gel. The gels were run at 50 V till the proteins was stacked properly and thereafter they were run at a constant voltage of 100–110 V in an electrophoresis and electro-transfer unit (Hoefer mini VE, Amersham Pharmacia Biotech, USA).

Coomassie blue staining of the gel

Coomassie[®] Brilliant Blue R250 staining detection limit is 300 to 1000 ng protein and is used in the experiments. The gel with electrophoretically separated proteins was incubated for staining in Coomassie solution for 30 minutes. Destaining was done with destaining solution to remove background staining. The destaining solution was replaced every 45 minutes with a fresh solution, until protein bands are visible above a clear background.

Western blotting and immunostaining

After electrophoresis, the protein samples were electro-blotted onto Polyvinylidene fluoride (PVDV)/nitrocellulose membrane (PALL[®], India) using Trans-Blot apparatus (electrophoresis and electro-transfer unit, Hoefer mini VE, Amersham Pharmacia Biotech, USA) according to the manufacturer's instruction using Towbin buffer (Towbin et al. 1979). The gel and the membrane was first equilibrated in Towbin buffer and then the membrane was kept above the gel towards the positive end of apparatus and stacked in between Whatman filter papers taking care of no trapped air bubbles. Transfer was done for 4 h at 25 V. Transferred protein onto the membrane was checked with reversible Ponceau-S staining and was removed by 3–4 washes with TBST buffer. The membrane was blocked with 1 % fat free milk powder or 3% BSA in TBS buffer for 1 h at RT followed by incubation with primary mouse monoclonal Anti-polyHistidine antibody (Sigma-Aldrich, USA) in TBS buffer containing 1% fat free milk powder or 3% BSA in 1:3000 dilutions for overnight at 4°C. The membrane was washed 3 times in TBS buffer for 5 minutes each to remove excess of primary antibody. The membrane was then transferred to goat anti-Mouse IgG-ALP secondary antibody (Merck, Germany) in TBS buffer containing 1% fat free milk powder or 3% BSA in 1:3000 dilutions for 1h at RT. The membrane was further washed 3 times in TBS buffer for 5 minutes each to remove excess of secondary antibody. 1 ml of BCIP/NBT solution (GeNei, India) was added onto the blot to develop.

For developing western blots on X-ray films, the membrane was transferred to goat anti-Mouse IgG-HRP secondary antibody (Merck, Germany) in TBS buffer containing 1% fat free milk powder or 3% BSA in 1:6000 dilutions for 1h at RT. The Western blots were developed using chemiluminescent detection system (Pierce, Thermo Fisher Scientific Inc., USA).

Oxidation-Reduction Midpoint Potential of purified protein

The redox state of recombinant BjAnn3_{WT} and its variants was assessed after equilibration with redox buffered solution at pH 7.0. 50 µg of protein was incubated in MOPS buffer (100 mM) containing 2 mM of total DTT (varying ratios of DTT_{reduced}/DTT_{oxidized}) for 3h at ambient temperature. For fluorescent labeling based assays,

the reduced fraction was labeled with monobromobimane (Sigma-Aldrich, USA) (10 mM) and analyzed for fluorescence (Hirasawa et al. 1999). Using Nernst equation with $n=4$, data were fitted with OriginPro 8 based on a value of -330 mV for the E_m of DTT at pH 7.0 similar as described in Laxa et al. (2007). For gel based assays, the samples after incubation were resolved in 12% non-reducing SDS/PAGE and then blotted as described above.

Peroxidase activity assay of purified protein and total plant protein

Peroxidase activity was assayed using guaiacol as substrate according to Choi et al (2007) and Chu et al (2012) with modifications. Fresh seedlings were homogenized in five volumes of 0.1 M sodium phosphate buffer (pH 6.0) containing 0.5 M sucrose and centrifuged at 10000 g, 4 °C for 30 min. The supernatant was used for *in vivo* total peroxidase assay. For *in vitro* peroxidase activity, purified BjAnn3_{WT} and controls were used. Either of the supernatant or purified BjAnn3 protein was added to the reaction mixture containing 0.1 M sodium phosphate buffer (pH 6.0), 0.25% guaiacol (Sigma-Aldrich, USA) and 1 M H₂O₂. The increase in absorbance at 470 nm was used to determine peroxidase activity using an extinction coefficient of 26.6 mM⁻¹ cm⁻¹.

Pulse amplitude modulation fluorometer analysis in *Arabidopsis*

The pulse amplitude modulation (PAM) fluorometer (PAM-2500, Heinz Walz GmbH, Germany) was used for measuring chlorophyll fluorescence-based photosynthetic performance in *Arabidopsis* leaf discs treated with MV or left untreated as control.

We performed dark-light induction curve analysis after a dark acclimation for 30 min. After measuring the minimum fluorescence (F_o), maximum fluorescence (F_m) was measured with a saturation pulse (SP) and maximal quantum yield (F_v/F_m) was recorded. After a time delay of 40 s, actinic light was turned on and was superimposed with SP followed by repetitive SPs at every 20 s for 5 min. Effective photochemical quantum yield [$Y(II)$], coefficient of photochemical fluorescence quenching (qP) and Stern-Volmer type non-photochemical fluorescence quenching (NPQ) were determined during the time course.

Determination of malondialdehyde levels in *Arabidopsis*

Lipid peroxidation in MV-treated versus untreated seedlings was quantified as demonstrated Heath and Packer (1968). Briefly, the samples were homogenized in 0.1% (w/v) trichloroacetic acid (TCA; Sigma-Aldrich, USA), centrifuged and one volume of supernatant was mixed with 3 volumes of 0.5% thiobarbituric acid (TBA; Sigma-Aldrich, USA) (in 20% TCA) followed by incubation at 95 °C for 25 min. The reaction was stopped on ice followed by centrifugation, and the supernatant was used to measure the absorbance at 532 and 600 nm. Malondialdehyde (MDA) concentration was measured using Lambert-Beer law with an extinction coefficient of 155 mM⁻¹cm⁻¹.

Subcellular localization of BjAnn3-GFP fusion protein in tobacco leaf epidermal cells

The recombinant plasmid *BjAnn3-gfp*-pCAMBIA 1302 carrying the *BjAnn3* gene fused C-terminally to GFP was transfected into *A. tumefaciens* LBA4404 cells for agro-infiltration into *N. tabacum* L. cv Xanthi leaves. After 48h of incubation at 24 °C, localization of the protein in epidermal cells was imaged under a laser-scanning confocal fluorescence microscope (Carl Zeiss LSM 710 NLO ConfoCor 3, Germany) at λ_{em} 515 nm (λ_{exc} 488 nm).

Quantification of H₂O₂ levels in *Arabidopsis*

MV-treated and untreated seedlings were homogenized in 5 ml cold acetone and the extract was used to quantify H₂O₂ according to Gay et al (1999) and Divya et al (2010) with modifications. Briefly, the extract was centrifuged and 200 µl of supernatant was added to 1 ml reaction mixture containing 0.25 mM FeSO₄, 0.25 mM (NH₄)₂SO₄, 25 mM H₂SO₄, 1.25 mM xylene orange (Sigma-Aldrich, USA), and 1 mM sorbitol. The mixture was incubated at 25 °C for 1 h and the absorbance at 560 nm was used to measure H₂O₂ by reference to standards.

Real Time PCR

Triplicate PCRs were performed for each gene, each cDNA sample. The following master mix was prepared accounting for one to two additional reactions per gene.

Ingredients	Per reaction (μl)	For x reactions (μl)
QPCR SYBR Green mix (2 x)	5	x * 5
Forward Primer (10 μM)	0.5	x * 0.5
Reverse Primer (10 μM)	0.5	x * 0.5
Nuclease free water	2	x * 2
Template (40ng)	2	x * 2

All the components were added to a 96 well plate (Applied Biosystems, USA) which was sealed with the optical adhesive cover using the sealing tool. The plate was spinned briefly (up to 1500 rpm) in a centrifuge equipped with a 96 well plate adapter. Real-time PCR was performed after pre-incubation at 95 °C for 10 min followed by 40 cycles of denaturation at 95 °C for 15 s, annealing at 59 °C for 30 s and extension at 72 °C for 30 s. All reactions were performed using **FastStart Universal SYBR Green Master (Rox)** (Roche Applied Science, Germany) in Mastercycler® ep *realplex4* (Eppendorf, Germany) (**Table 5**).

Table 5. The temperature profile and cycling condition of qPCR.

Cycles	Analysis mode	Target temperature	Hold time
1 (Optional)	None	50 °C	2 min
1	None	95 °C	10 min
40	Quantification	95 °C	15 sec
		59 °C	30 sec
		72 °C	30 sec

Electrophoretic Mobility

For mobility assay under different redox conditions, AnnBj3_{WT} and its variants in NaH₂PO₄ buffer (pH 7.5) were incubated with varying concentrations of either hydrogen peroxide or DTT (1, 4-dithiothreitol; Sigma-Aldrich, USA) for 30 min at room temperature (25°C). The samples were resolved in 12% non-reducing SDS/PAGE and blotted as described above.

FPLC Gel Permeation Chromatography

Molecular sizes of the wild-type and mutant proteins in NaH₂PO₄ buffer (pH 7.5) were evaluated on a Superose-12 10/300 GL preppacked column (GE Healthcare Life Sciences, USA). The column was equilibrated with two column of elution buffer before experiment. The process was executed at a flow rate of 0.5 ml/min at 25 °C. Absorbance was monitored at 280 nm.

Solutions**Coomassie staining solution**

Coomassie Brilliant Blue R-250	:	0.025%
Methanol	:	45%
Acetic acid	:	10%

Destaining solution

Methanol	:	45 %
Acetic acid	:	10%

SDS–PAGE Gel 12%**15ml Resolving Gel**

30% Acrylamide	:	6 ml
1.5M Tris pH 8.8	:	3.7 ml
DD H ₂ O	:	5.2 ml
AMPS (0.1 gm/ml)	:	100 µl
TEMED	:	14 µl

5 ml Stacking Gel (6 %)

30% Acrylamide	:	1 ml
0.5M Tris pH 6.8	:	1.25 ml
DD H ₂ O	:	2.65 ml
AMPS (0.1 gm/ml)	:	50 µl
TEMED	:	5 µl

5X SDS-PAGE Sample Buffer

Tris pH 6.8	:	0.22 M
Glycerin	:	50%
Bromophenol Blue	:	0.05%
SDS	:	5%

Towbin Buffer

Tris	:	25 mM
Glycine	:	192 mM
Methanol	:	20%

Ponceau-S Stain

Ponceau-S	:	0.1%
Glacial Acetic Acid	:	5%

TBST Buffer

Tris-HCl pH 7.4	:	10 mM
Sodium Chloride	:	150 mM
Tween-20	:	0.1%

TBS Buffer

Tris-HCl pH 7.4	:	10 mM
Sodium Chloride	:	150 mM

50 % PEG 2000

PEG 2000 in DD H ₂ O	:	50%
---------------------------------	---	-----

10 X TE

Tris	:	100 mM
EDTA	:	100 mM

10 X Lithium Acetate

Lithium Acetate	:	1 M
-----------------	---	-----

Lithium Solution (1 ml)

10 X TE	:	100 µl
10 X Lithium Acetate	:	100 µl
Double Distilled Water	:	800 µl

PEG 2000 Solution (2.5 ml)

50 % PEG 2000	:	2 ml
10 X TE	:	250 µl
10 X Lithium Acetate	:	250 µl

Breaking Buffer

Sodium Phosphate pH 7.4	:	50 mM
EDTA	:	1 mM
Glycerol	:	5%
PMSF	:	1 mM

YPD Media

Yeast Extract	:	1%
Bacterial Peptone	:	2%
Glucose	:	2%
Agar (for plates)	:	2%

Synthetic Complete Media

Yeast Nitrogen Base (w/o amino acids But with ammonium sulfate)	:	0.67%
Amino acids (Adenine, Arginine, Cysteine, Leucine, Lysine, Threonine, Tryptophan, Uracil)	:	0.01%
Amino acids (Aspartic acid, Histidine, Isoleucine, Methionine, Phenylalanine, Proline, Serine, Tyrosine, valine)	:	0.005%
Glucose	:	2%

Galactose (for induction) : 2%

Agar (for plates) : 2%

[Uracil was omitted for SC-U or SD (Synthetic Dropout) Media]

Glucose Stock

Glucose : 40%

Galactose Stock

Galactose : 20%

Amino acid Stock (5X)

Amino acids (Adenine, Arginine, Cysteine,

Leucine, Lysine, Threonine, Tryptophan,

Uracil) : 0.05%

Amino acids (Aspartic acid, Histidine, Isoleucine,

Methionine, Phenylalanine, Proline, Serine,

Tyrosine, valine) : 0.025%

[Uracil was omitted for SC-U or SD (Synthetic Dropout) Media]

Plasmid isolation solutions**Solution I**

Lysosyme : 4.0 mgL⁻¹

Glucose : 50 mM

EDTA : 10 mM

TrisHCl (pH 8.0) : 25 mM

Solution II

SDS : 1%

NaOH : 0.2 N

Objective 1

Attenuation of hydrogen peroxide-mediated oxidative stress by *Brassica juncea* annexin-3 which complements thiol-specific antioxidant (TSA1) deficiency in *Saccharomyces cerevisiae*

Introduction

Annexins represent ubiquitous proteins that are highly conserved among most kingdoms of life. They comprise a multigene family of calcium dependent or independent phospholipid-binding proteins (Dabitz et al. 2005; Mortimer et al. 2008; Laohavisit and Davies 2011). For more than a decade they are known to be transcriptionally regulated in response to various abiotic stressors and in dependence on diverse signaling pathways (Gidrol et al. 1996; Kovacs et al. 1998; Apel and Hirt 2004; Lee et al. 2004; Clark et al. 2005; Cantero et al. 2006; Konopka-Postupolska et al. 2009; Zhang et al. 2011; Chu et al. 2012; Feng et al. 2013; Zhou et al. 2013).

AtAnn1 from *Arabidopsis thaliana* was the first annexin protein that was functionally linked to oxidative stress response and protected bacterial and mammalian cells from oxidative damage (Gidrol et al. 1996; Janicke et al. 1998; Kush and Sabapathy 2001). In line with this observation, plant AtAnn1, BjAnn1, ZmAnn33/35, CaAnn24, CkANN, GhAnx1 and NnANN1 proteins could also be associated with antioxidant function (Gidrol et al. 1996; Gorecka et al. 2005; Jami et al. 2008; Laohavisit et al. 2009; Zhang et al. 2011; Zhou et al. 2011; Chu et al. 2012). Initially, the conserved histidine residue of the first annexin repeat (His-40 in AtAnn1) was associated with peroxidase activity (Clark et al. 2001; Gorecka et al. 2005). Later the concept was challenged since peroxidase activity of plant annexin was proven to be independent of the heme-binding motif when ectopically expressed in plants or bacteria (Laohavisit et al. 2009; Konopka-Postupolska et al. 2009). The initially obtained Anx(Gh1) crystal structure suggested the putative sulfur cluster as redox reactive center and its function in H₂O₂ reduction (Hofmann et al. 2003, 2004), which later on was confirmed in AtAnn1 (Konopka-Postupolska et al. 2009, 2011).

Our previous report demonstrated transcriptional up-regulation of *BjAnn3* in *Brassica juncea* upon treatment with hydrogen peroxide, NaCl, methyl viologen and wounding (Jami et al. 2009). Based on this finding, we have postulated that BjAnn3 is important for counteracting sustained oxidative stress. Further we proceeded with amino acid sequence analysis of BjAnn3 using ClustalW and Jalview (Larkin et al. 2007 and Clamp et al. 2004), which revealed the absence of both the heme-binding histidine residue and S₃ cluster (**Fig. 1**). Cysteines are known to function as structural elements, redox switches or redox buffers.

As redox buffer they play a crucial role in maintaining redox homeostasis for cell survival on oxidative stress (Guttmann 2010). The two cysteine residues which are present in BjAnn3, are highly conserved among both plant and animal annexins (Hofmann et al. 2003), and might function in modulating or sensing oxidative stress (Konopka-Postupolska et al. 2009 and Laohavisit et al. 2009). Therefore this study aimed at functional characterization of BjAnn3 with its 319 aa residues following heterologous expression in *S. cerevisiae* in connection to H₂O₂-mediated oxidative stress response.

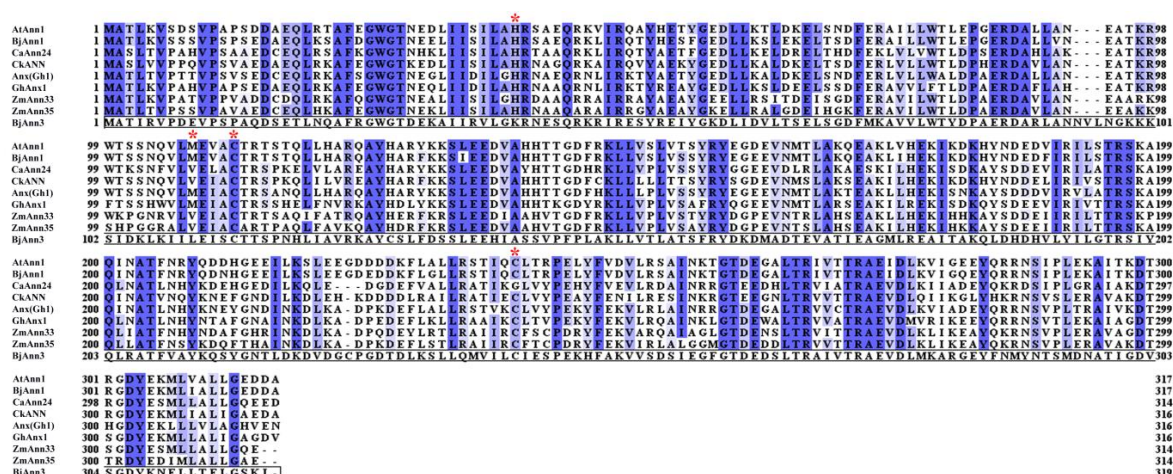


Figure 1 Alignment of plant annexin amino acid sequences. The conserved residues for heme-binding (histidine) and S₃ cluster are marked (*). Sequence data are available in NCBI with the following accession numbers: Atlg35720 (AtAnn1), ABB59550 (BjAnn1), CAA10210 (CaAnn24), ADO32900 (CkANN), AAB67993 [Anx(Gh1)], AAR13288 (GhAnx1), CAA66900 (ZmAnn33), CAA66901 (ZmAnn35), ABD47520 (BjAnn3).

Results and Discussion

The work aimed at understanding the role of BjAnn3 in H₂O₂-mediated oxidative stress. Externally applied H₂O₂ induces intracellular oxidative stress in yeast due to its water solubility and membrane permeability. Cells generate H₂O₂ both under basal and stressed growth conditions (Morano et al. 2012). TSA1, the major 2-Cys peroxiredoxin in yeast, detoxifies hydroperoxides (Demasi et al. 2001 and Garrido et al. 2002) and functions as a key regulator of intracellular ROS especially H₂O₂ in *S. cerevisiae* (Park et al. 2000). *tsa1* null mutants are viable and indistinguishable from parental wild-type under aerobic control conditions, but display a remarkable H₂O₂-sensitive phenotype (Wong et al. 2002). TSA1 was knocked out in regular INVSc1 strain to generate the *tsa1* null mutant named ADY1. Both strains were transfected either with empty vector pYES or recombinant *BjAnn3*-pYES clone to create the four different strains, INVSc1-pYES, INVSc1-BjAnn3, ADY1-pYES and ADY1-BjAnn3. BjAnn3 expression was confirmed by Western blotting in INVSc1-BjAnn3 and ADY1-BjAnn3 cells (**Fig. 2A**).

Functional effects of BjAnn3 on cell growth and respiration

To assess the role of BjAnn3 in oxidative stress, overexpressing cells were treated with H₂O₂ in liquid culture (**Fig. 2B**). Growth of all strains decreased with increasing H₂O₂ concentration. At 2 mM concentration, overexpression of BjAnn3 stimulated cell growth from 45.1 % to 63.0 % in INVSc1-BjAnn3 cells and from 16.4 % to 33.1 % in ADY1-BjAnn3 cells, when compared to the respective wild-type. ADY1-pYES showed a 28.7 % decrease in growth compared to INVSc1-pYES cells, which is in line with earlier findings (Park et al. 2000 and Demasi et al. 2001). Apparently, BjAnn3 partially complemented the lost TSA1 function in ADY1-BjAnn3 cells by up to 58.3% in the presence of 2 mM H₂O₂ (**Fig. 2B**). The data suggest a protective role of BjAnn3 in cellular defense against oxidative stress. Based on the results, H₂O₂ concentrations of 2 mM and 2.5 mM were chosen for further experiments.

We hypothesized that BjAnn3 might protect mitochondrial respiration during oxidative stress response (**Fig. 2C**). At 2 mM H₂O₂, respiration of cells overexpressing BjAnn3 showed no significant difference to wild-type. But at 2.5 mM H₂O₂ respiratory activity of

INVSc1 cells was stimulated by 28 % when overexpressing BjAnn3 and by 20% in ADY1 cells. Apparently the presence of BjAnn3 partially mitigated the oxidative stress-induced inhibition of mitochondrial respiration. ADY1-pYES cells had improved respiration compared to INVSc1-pYES cells upon treatment. TSA1 plays a prominent role in cellular protection against hydroperoxide-mediated oxidative stress in respiratory-incompetent cells compared to wild-type. In addition H₂O₂-treatment stimulates *TSA1* expression more in cells with dysfunctional mitochondria than in wild-type (Demasi et al. 2001). Based on the above studies, a possible explanation could be that compromised TSA1 resulted in compensational elevation of respiration activity in order to maintain a balanced metabolism. Our results from **Fig. 2C** suggest that BjAnn3 aids in cellular protection against oxidative stress, thereby safeguards mitochondrial respiration.

Restoration of cell viability by BjAnn3 expression during H₂O₂-mediated oxidative stress

In order to further substantiate our findings we performed growth assays on plates (**Fig. 3A**). Viability of the four strains was indistinguishable under normal aerobic conditions, while it varied in the presence of H₂O₂. INVSc1-BjAnn3 cells appeared to be slightly more tolerant than INVSc1-pYES cells when treated with 2.5 mM H₂O₂, whereas no significant difference was seen at 2 mM H₂O₂. ADY1-pYES was more sensitive to H₂O₂ at both concentrations compared with INVSc1-pYES cells, which is consistent with earlier reports (Park et al. 2000 and Demasi et al. 2001). Expression of BjAnn3 restored cell viability of ADY1-pYES cells to almost the level of INVSc1-pYES. Cell viability was quantified using the fluctuation assay (**Fig. 3B**). Survival rate of INVSc1-BjAnn3 in 2 mM and 2.5 mM H₂O₂ increased by 14.7 % and 16.5 %, respectively, compared to the control strain, and viability of ADY1-BjAnn3 cells by 20.3 % and 19.6 %, respectively. With 31.2 % and 28.4 %, observed mortalities of ADY1-pYES cells in the presence of 2 mM and 2.5 mM H₂O₂, respectively, fitted to earlier reports (Demasi et al. 2001). BjAnn3 expression in ADY1 cells efficiently complemented for the loss of TSA1 function indicating a significantly protective role of BjAnn3.

Effect of BjAnn3 expression on membrane permeability upon H₂O₂-mediated oxidative stress

Oxidative stress affects the structural integrity of phospholipids by lowering membrane lipid packing and facilitating phase separation (Megli et al. 2003 and 2005). One of the primary roles of annexins is seen in protecting cell membrane permeability by their highly conserved annexin core domain (Creutz et al. 2012). Plant annexins which respond to oxidative stress in a membrane-bound state might bind or decompose peroxidated lipids, thereby restoring membrane stability and integrity. Alternatively a protective mechanism of annexins on membranes may involve formation of two dimensional crystal patches on peroxidated membranes or fostering membrane resealing (Konopka-Postupolska et al. 2011). Therefore the next experiments investigated the capability of BjAnn3 expression to maintain membrane integrity, which may be one of the underlying mechanisms to restore cell viability upon oxidative stress. H₂O₂ treatment resulted in pronounced increase of cellular PI fluorescence in all four strains compared to the respective untreated control, indicating an increase in plasma membrane permeability (**Fig. 4A**). Loss of *TSA1* in ADY1-pYES cells further enhanced PI fluorescence upon H₂O₂-treatment. BjAnn3 overexpression counteracted the PI fluorescence increase in INVSc1-BjAnn3 and ADY1-BjAnn3. Quantification of PI fluorescence confirmed that BjAnn3 strongly quenched the fluorescence both in INVSc1-BjAnn3 and ADY1-BjAnn3 cells, compared to their respective controls (**Fig. 4B**). At both H₂O₂-concentrations BjAnn3 was able to complement the loss of TSA1 function below the level of INVSc1 cells. These data support the conclusion that annexins protect membranes against oxidative stress in line with previous findings (Konopka-Postupolska et al. 2011).

Modulation of H₂O₂-mediated ROS accumulation by BjAnn3

A role of plant annexins in improved ROS detoxification has been shown in native plants (Konopka-Postupolska et al. 2009) and transgenic plants (Gorecka et al. 2005; Jami et al. 2008; Laohavisit et al. 2009; Divya et al. 2010; Jami et al. 2010; Zhang et al. 2011; Chu et al. 2012). ROS is formed in normal yeast metabolism. Its release is enhanced in response to environmental stress (Morano et al. 2012). In order to explore the possible link between

BjAnn3 expression, increased cell viability, plasma membrane protection and ROS formation, cells were subjected to DCFDA staining and analyzed by confocal microscopy (**Fig. 5A**). The DCF fluorescence level upon H₂O₂ treatment was highest in TSA1-deficient ADY1-pYES cells. Similar results were reported by Wong et al. (2002). BjAnn3 overexpression decreased the DCF fluorescence in H₂O₂-treated INVSc1-BjAnn3 and ADY1-BjAnn3 cells (**Fig. 5B**). BjAnn3 was able to suppress ROS accumulation by a factor of 6.4 and 7.9, respectively, in INVSc1-BjAnn3 cells, and 7.9 and 8.0 in ADY1-BjAnn3 cells, compared to their respective controls, when treated with 2 mM and 2.5 mM H₂O₂. ADY1-pYES cells generated 2.3-fold more ROS in the presence of 2 mM H₂O₂ compared to INVSc1-pYES cells, while, no significant difference was observed upon 2.5 mM H₂O₂ treatment. Overexpression of BjAnn3 compensated for the loss of TSA1 function as indicated by DCF fluorescence which was lower than in INVSc1-pYES in 2 mM H₂O₂. The result is consistent with that from the PI assay. Apparently BjAnn3 lowers ROS accumulation and combats oxidative stress and increases cell viability.

qPCR analysis of mRNA transcripts of some antioxidant enzymes

In the next step, we investigated effects of BjAnn3 expression which could indirectly affect cellular ROS levels. Earlier experiments have linked plant annexins to other genes involved in improved stress response (Jami et al 2008; Divya et al 2010; Huh et al 2010). To this end transcript levels of *SOD1* (**Fig. 6A**), *SOD2* (**Fig. 6B**), *GPX2* (**Fig. 6C**) and *TSA2* (**Fig. 6D**) were quantified by qPCR. The antioxidant genes were transcriptionally up-regulated in response to H₂O₂-treatment. As described earlier, *SOD1*, *GPX2* and *TSA2* (Wong et al. 2002 and Demasi et al. 2006) were up-regulated in H₂O₂-treated ADY1-pYES cells. *SOD2* was hardly regulated. Upon treatment, BjAnn3 overexpression in INVSc1-BjAnn3 cells resulted in transcriptional activation of *SOD1*, *SOD2*, *GPX2* and *TSA2* by 2.6-fold, 17.3-fold, 20.2-fold and 48.3-fold respectively, while in ADY1-BjAnn3 cells only *SOD1* and *SOD2* got activated by 1-fold and 6.1-fold respectively, compared to their respective controls. *GPX2* showed no difference while *TSA2* got down-regulated by a factor of 32.8. Overexpression of BjAnn3 affected antioxidant expression. The compensatory activation for *TSA1* deficiency of these antioxidants are in order of *SOD2* (0-fold)

<*SOD1* (1.1-fold) < *GPX2* (23.8-fold) < *TSA2* (82.0-fold) in ADY1-pYES, cells compared to wild-type (**Fig. 6E**). This order exactly matched the progressive decrease in transcript level of *SOD2* (6.1-fold) < *SOD1* (1-fold) < *GPX2* (0-fold) < *TSA2* (-32.8-fold) in ADY1-BjAnn3 cells, compared to ADY1-pYES cells. The results from **Fig. 6** suggest that BjAnn3 functions as a key effector of *SOD1*, *SOD2*, *GPX2* and *TSA2* expression which then help to maintain cellular redox balance. On one hand, BjAnn3 positively regulates these antioxidants upon treatment whereas on the other hand BjAnn3 interacts antagonistically with other antioxidants when cells are deficient of TSA1.

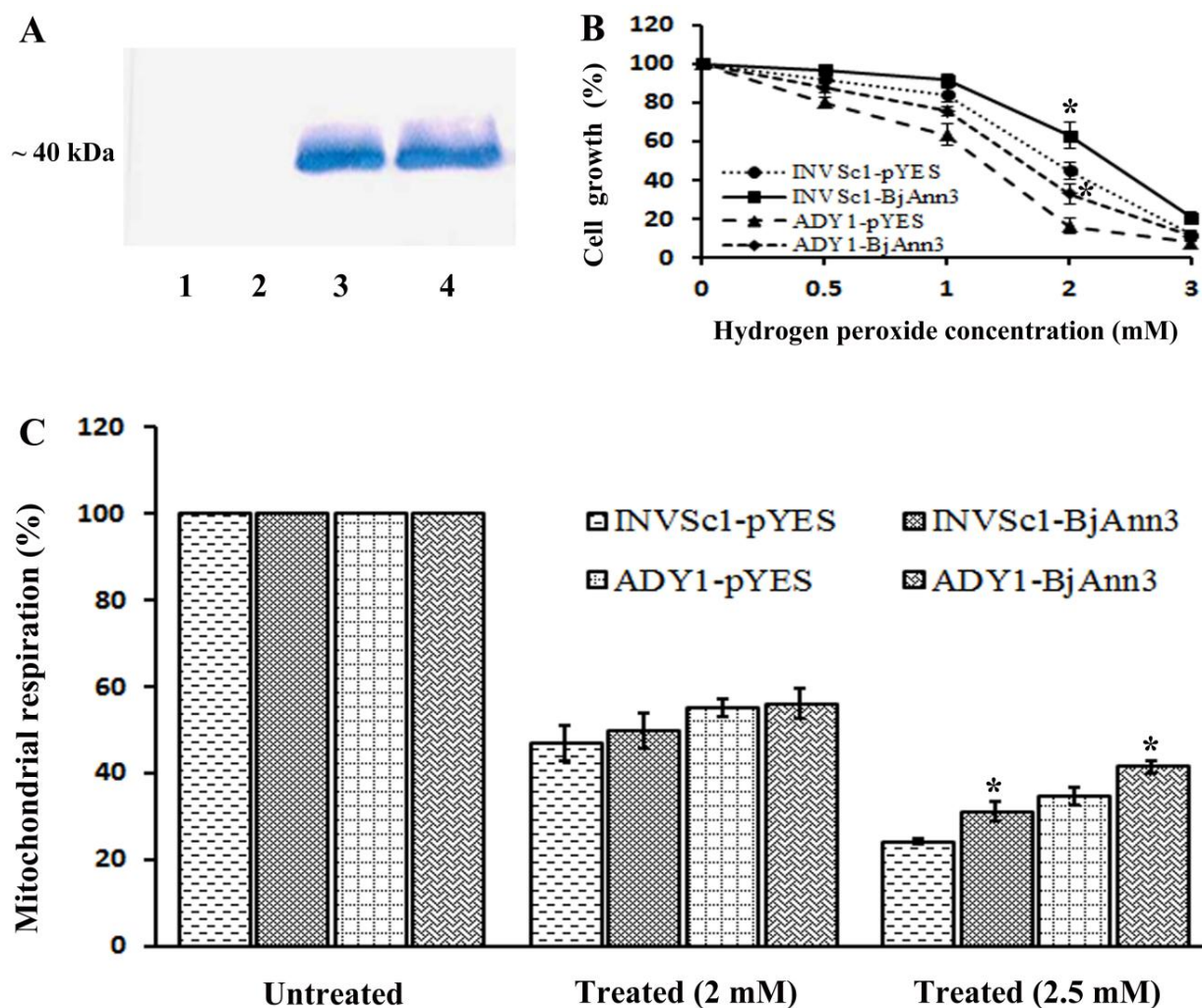


Figure 2 Recombinant expression of BjAnn3 in yeast and functional effects on cell growth and respiration. (A) Confirmation of BjAnn3 expression in *lane1*, INVSc1-pYES; 2, ADY1-pYES; 3, INVSc1-BjAnn3; 4, ADY1-BjAnn3 cells. (B) Normalized cell growth with respect to untreated cells in the presence of different concentrations of H₂O₂. (C) Mitochondrial respiration in percent of untreated cells. Data represent means \pm S.D. from 3 measurements. Statistical analysis was carried out in Sigma-Plot11.0 by One-Way ANOVA analysis with Duncan's Multiple Range Test (DMRT) (*) marks significant differences with $p < 0.05$ relative to the likewise treated wild-type.

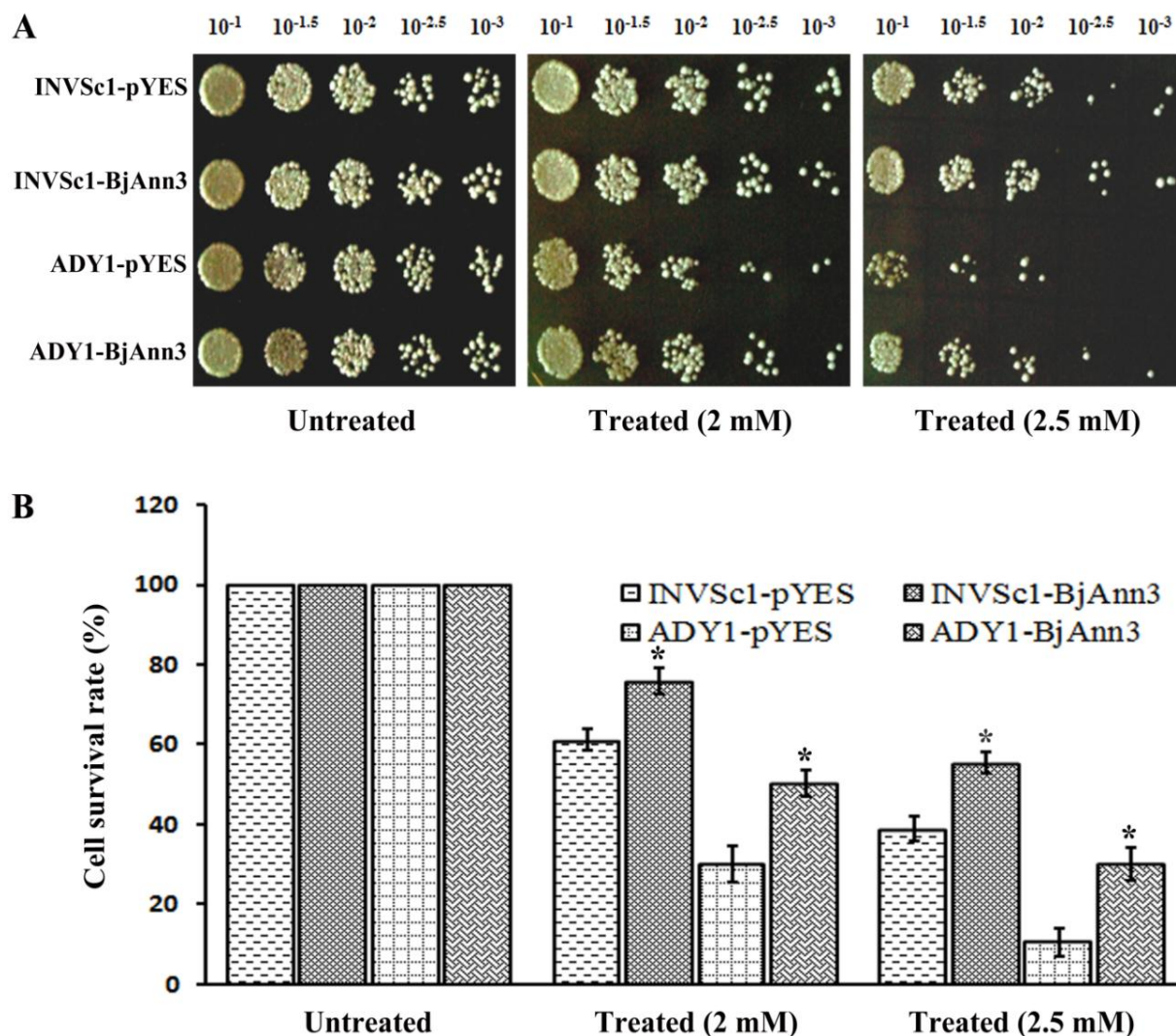


Figure 3 Restoration of cell viability by BjAnn3 expression during H₂O₂-mediated oxidative stress. Sensitivity of yeast strains INVSc1-pYES, INVSc1-BjAnn3, ADY1-pYES and ADY1-BjAnn3 to H₂O₂ was analyzed by spotting (**A**) or was analyzed by use of fluctuation assay (**B**). Data represent means \pm S.D. from 3 measurements. Statistical analysis was carried out in Sigma-Plot11.0 by One-Way ANOVA analysis with Duncan's Multiple Range Test (DMRT) (*) marks significant differences with $p < 0.05$ relative to the likewise treated wild-type.

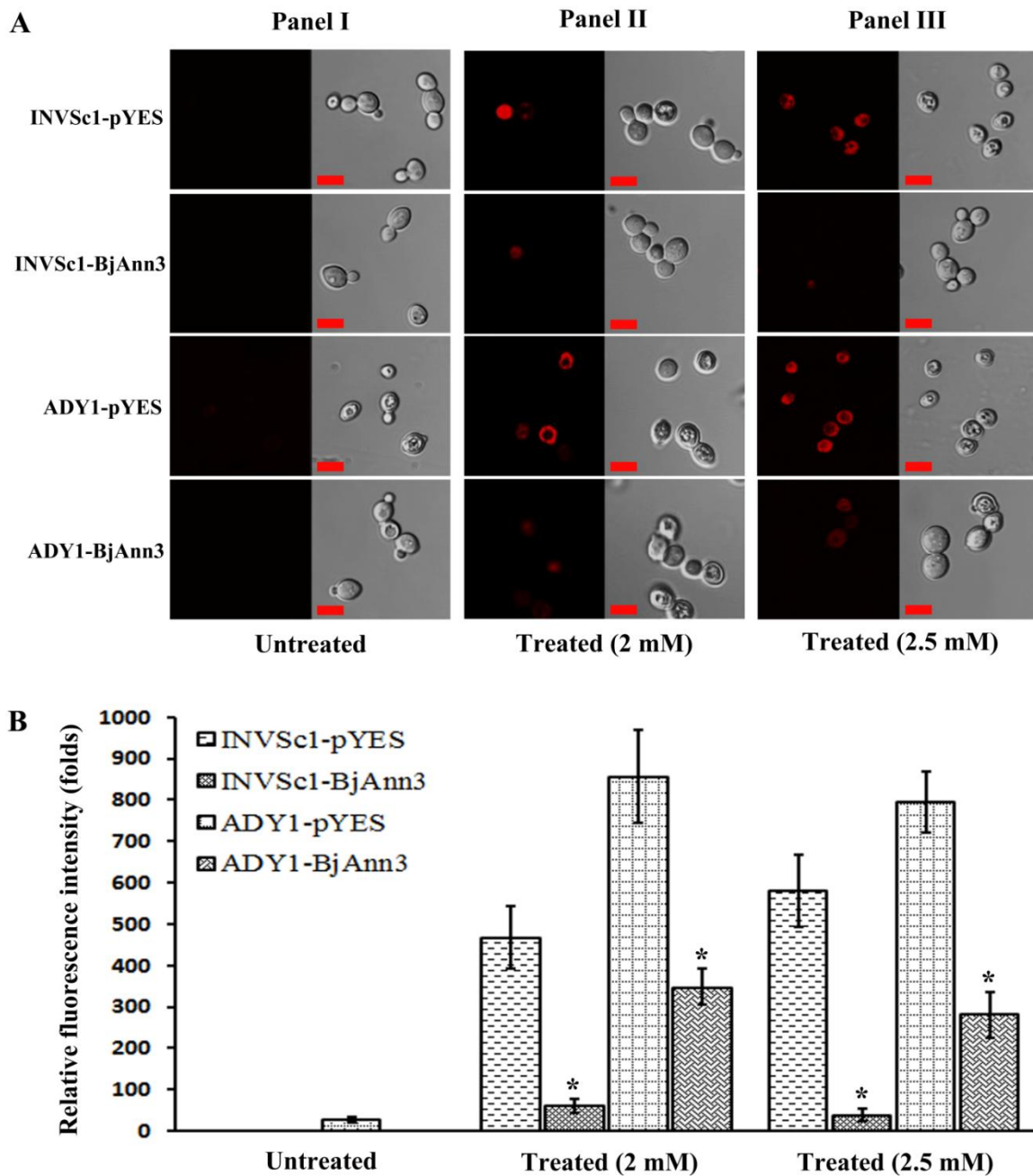


Figure 4 Effect of BjAnn3 expression on membrane permeability upon H_2O_2 -mediated oxidative stress. (A) Propidium iodide (PI) fluorescence was observed under a confocal microscope (scale bars: 5 μm) quantified from more than 100 cells in each sample by using Image-J. (B) Values are expressed as a fraction of the control (Untreated INVSc1-pYES cells). Data represent means \pm S.D. from 3 replicates. Data were analyzed for statistically significant differences using Sigma-Plot 11.0 by One-Way ANOVA analysis with Duncan's Multiple Range Test (DMRT) (*) marks significant differences with $p < 0.05$ relative to the likewise treated wild-type.

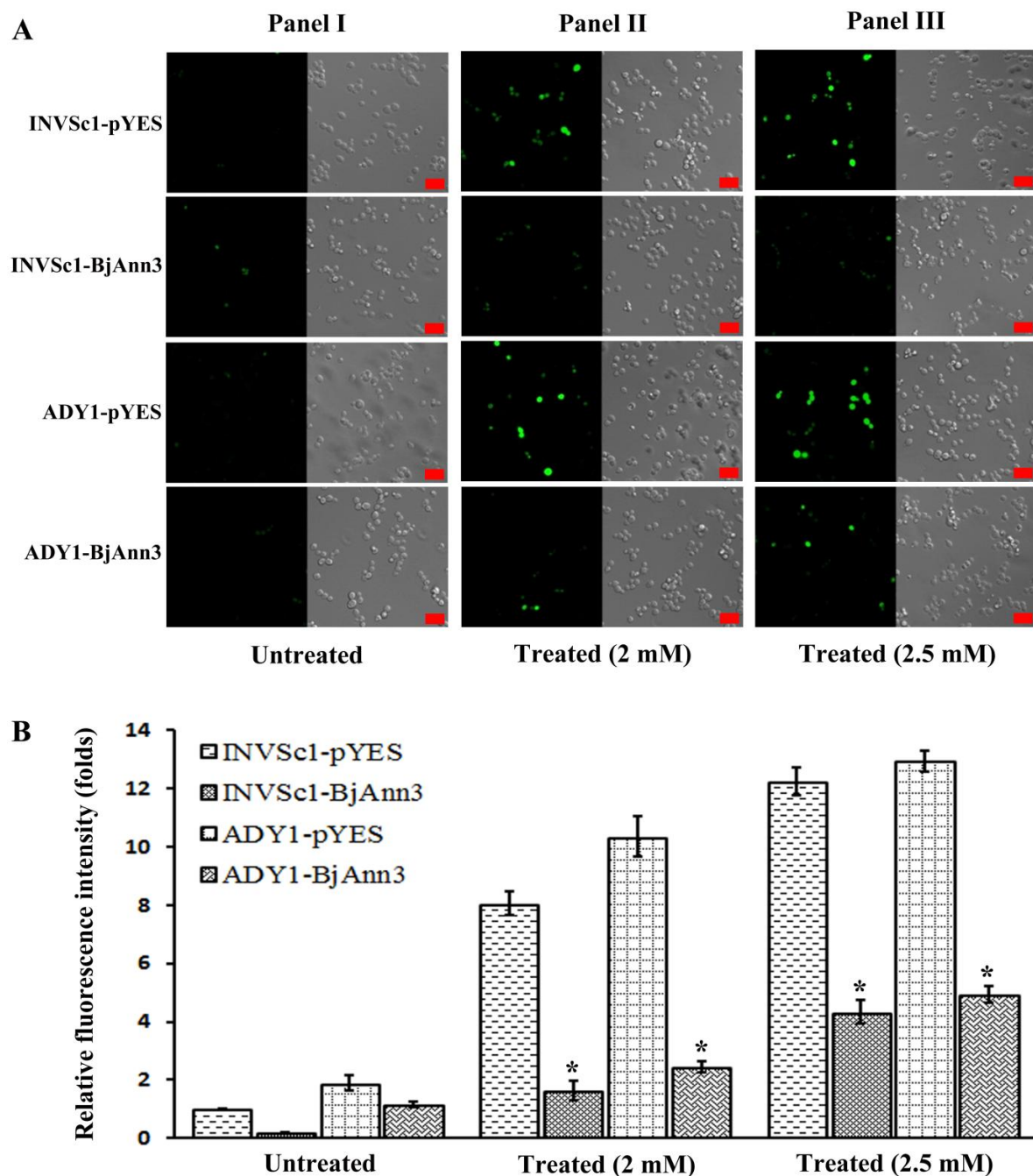


Figure 5 Modulation of H_2O_2 -mediated ROS accumulation by BjAnn3. ROS was detected by DCF fluorescence using a confocal microscope; scale bars: 10 μ m (**A**). DCF fluorescence was quantified from more than 100 cells in each replicate by using Image-J and expressed as a fraction of the control (Untreated INVSc1-pYES cells) (**B**). Data represent means \pm S.D. from 3 measurements. Statistical analysis was carried out in Sigma-Plot11.0 by One-Way ANOVA analysis with Duncan's Multiple Range Test (DMRT). (*) marks significant differences with $p < 0.05$ relative to the likewise treated wild-type.

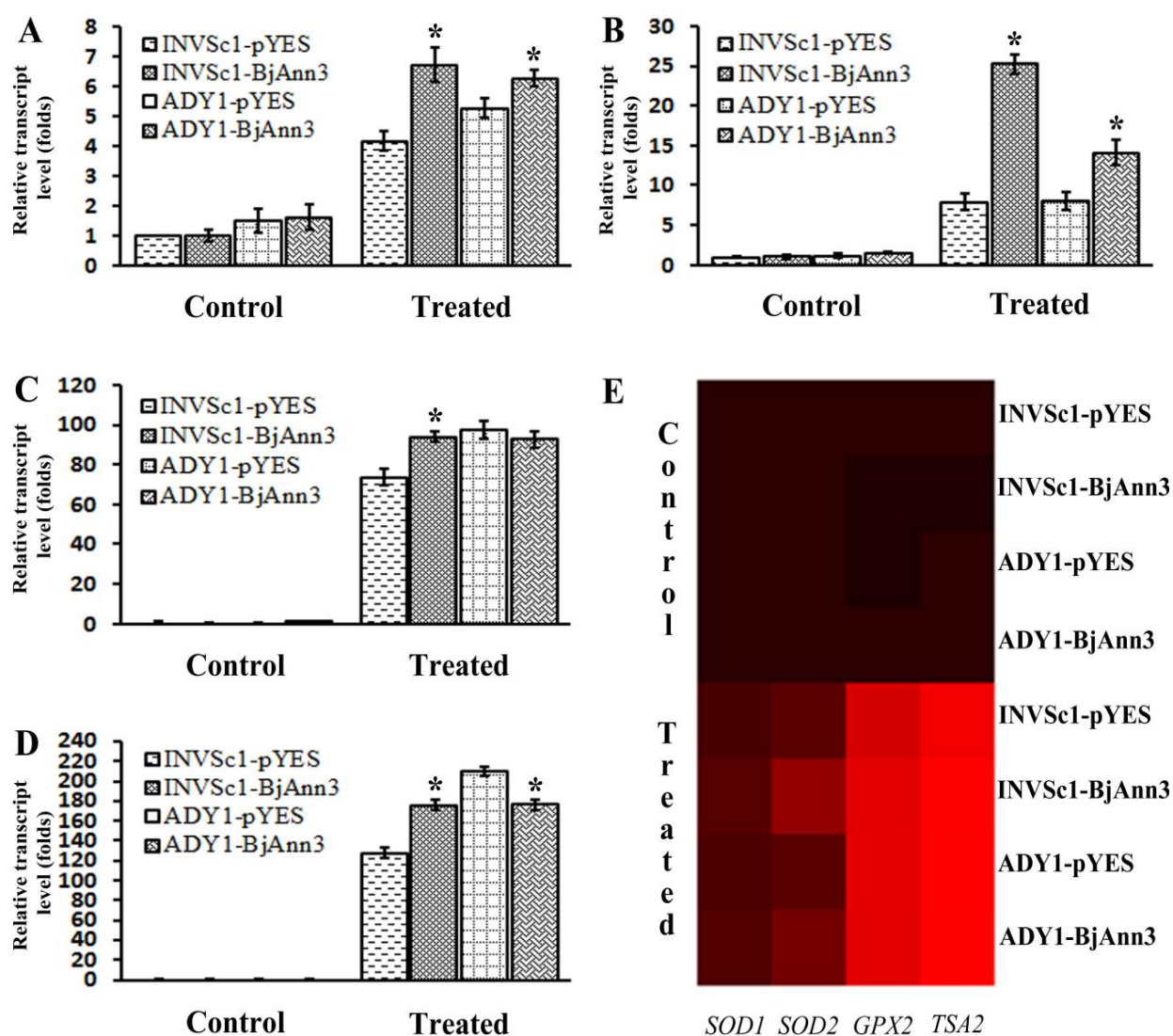


Figure 6 qPCR analysis of mRNA transcripts of some antioxidant enzymes. All strains showed BjAnn3-mediated regulation upon treatment with 2.5 mM H_2O_2 . *SOD1*(A), *SOD2*(B), *GPX2*(C) and *TSA2*(D) transcripts were quantified as described above. The expression patterns were compiled in a heat map (E). *ACT1* was used as reference gene. Data represent means \pm S.D. from 3 measurements. Statistical analysis was carried out in Sigma-Plot 11.0 by One-Way ANOVA analysis with Duncan's Multiple Range Test (DMRT). (*) marks significant differences with $p < 0.05$ relative to the likewise treated wild-type.

Conclusion

This report characterizes the effects of heterologous expression of a plant annexin in *S. cerevisiae*. *S. cerevisiae* lacks an annexin orthologue (Gerke 2002). Annexins are well known membrane binding proteins (Dabitz et al. 2005; Mortimer et al. 2008; Laohavisit and Davies 2011). They have been studied for their function in cell protection, membrane stabilization and ROS detoxification in bacteria, plants and mammalian cell lines (Gidrol et al. 1996; Janicke et al. 1998; Kush and Sabapathy, 2001; Gorecka et al. 2005; Jami et al. 2008, Laohavisit et al. 2009; Konopka-Postupolska et al. 2009; Zhou et al. 2011; Konopka-Postupolska et al. 2011). Here it is shown that BjAnn3 protects yeast cells from oxidative stress. Two scenarios are possible: (i) BjAnn3 could either directly detoxify ROS or (ii) positively modulate the endogenous antioxidants and thereby affect ROS accumulation. Expression of BjAnn3 maintained the permeability barrier which could either result from membrane stabilization by binding (Creutz et al. 2012) or from ROS detoxification in a free or membrane-bound state (Mortimer et al. 2009). Again, ROS detoxification may be due to peroxidase activity of BjAnn3 or due to an interaction with native defense system within the cell. The methionine residue is frequently mutated as in BjAnn3, but two cysteine residues of the S₃ cluster remained conserved (Konopka-Postupolska et al. 2009). The absence of both heme-binding histidine residues and S₃ cluster in BjAnn3 might suggest that the conserved Cys residues are involved in ROS detoxification. This hypothesis needs future investigation. Our results indicate that BjAnn3 interferes with other antioxidant genes for ROS modulation. Annexins are also predicted to function as heme-free glutathione peroxidase, a subgroup of peroxiredoxins, using a conserved cysteine to reduce hydroperoxides which act as electron acceptor (Rouhier et al. 2005, Laohavisit et al. 2009 and Dietz 2011). Such a thiol peroxidase activity might be the reason why BjAnn3 complements TSA1-deficient yeast. Their evolutionary significance is well concluded from our results based on their role in transcriptional activation of antioxidant genes and their cross talk with the defense system across kingdom, enabling a cooperative cellular protection. The only partial compensation of TSA1 by BjAnn3 in cell viability tests but over-complementation in ROS-related features suggests the existence of both redundant, e.g.

in ROS detoxification, and distinct features, e.g. membrane protection versus proximity-based redox regulator, of both proteins.

Objective 2

Alleviation of methyl viologen-mediated oxidative stress by *Brassica juncea* annexin-3 in transgenic *Arabidopsis*

Introduction

Plant annexins (32–36 kDa) represent about 0.1% of total cell protein and are distributed throughout the kingdom (Morgan and Fernández 1997; Hofmann 2004; Mortimer et al. 2008). The first plant annexin was identified in tomato (Boustead et al. 1989). Thereafter, they have been identified in many other plant species and studied extensively from past two decades (Blackbourn et al. 1991, 1992; Clark et al. 1998, 2005; Kovacs et al. 1998; Hofmann et al. 2003, 2004; Lee et al. 2004; Cantero et al. 2006; Konopka-Postupolska et al. 2007, 2009; Jami et al. 2008, 2009, 2012; Huh 2010; Laohavisit et al. 2009, 2012; Zhang et al. 2011; Zhou et al. 2011; Chu et al. 2012; Huang et al. 2013; Zhou et al. 2013).

The members of the evolutionarily conserved family of annexins exist in soluble form, but bind to phospholipids in a calcium dependent or independent manner (Mortimer et al. 2008; Dabitz et al. 2005; Laohavisit and Davies 2011). However these multifunctional proteins are still insufficiently characterized *in vivo*, in particular concerning their proposed peroxidase activity.

Analyses of annexins from *A. thaliana* (AtAnn1), *B. juncea* (BjAnn1), *Zea mays* (ZmAnn33/35), *Capsicum annuum* (CaAnn24) and *Nelumbo nucifera* (NnANN1) proteins point to an antioxidative function of annexins (Gorecka et al. 2005; Jami et al. 2008; Laohavisit et al. 2009; Chu et al. 2012). Two features were taken as supporting evidence for the eventual antioxidant activity of plant annexins. The first one is the heme-binding histidine residue initially identified in AtAnn1. However both experimental evidence and structural data are missing that support the concept of heme-binding in plant annexins (Laohavisit et al. 2009; Konopka-Postupolska et al. 2011). The second one is the S₃ cluster, initially identified in the GhAnn1 crystal structure. This cluster is hypothesized to function as redox reactive center and possibly in H₂O₂ reduction (Hofmann et al. 2003, 2004). Later, detailed amino acid sequence analysis of BjAnn3 confirmed that both criteria are not fulfilled (**Fig. 1**). Two Cys residues of the S₃ cluster remain highly conserved among both plant and animal annexins while the methionine residue often varies (Hofmann et al. 2003; Konopka-Postupolska et al. 2009). Generally, cysteines are known to play a crucial role in redox buffering under oxidative stress (Guttmann 2010). The two conserved cysteines of the S₃ cluster which are also present in BjAnn3 might play a role in redox homeostasis

(Hofmann et al. 2003; Konopka-Postupolska et al. 2009; Laohavisit et al. 2009). Early after their discovery, annexins were investigated for a potential role during oxidative stress in plants. Their transcript levels are regulated in response to various oxidative stressors (Gidrol et al. 1996; Kovacs 1998, Jami et al. 2008, 2009, Konopka-Postupolska et al. 2009, Zhang et al. 2011). Thus transcripts encoding annexins are up-regulated upon MV treatment (Jami et al. 2008, 2009) but their role in MV-mediated oxidative stress tolerance remained uninvestigated.

Our earlier studies validated for stressed *B. juncea* that *BjAnn3* transcripts also accumulate upon methyl viologen application and also upon other stress treatments like H₂O₂, ABA, ethephon, salicylic acid, methyl jasmonate, sodium chloride and wounding (Jami et al. 2009). We hypothesized that BjAnn3 might modulate cell acclimation responses during enduring photo-oxidative stress. Therefore this study addresses the *in vivo* role of BjAnn3 by heterologous expression in transgenic *A. thaliana* with focus on MV-mediated oxidative stress. This approach was expected to shed light on the antioxidant property of the protein.

Results and discussion

This work aimed at understanding the role of BjAnn3 in MV-mediated oxidative stress. MV has been extensively used as an oxidative stress inducer in studying tolerance and cross tolerance responses accompanied with antioxidant system responses (Lascano et al. 1998, 2001, 2003) as summarized by Jacob and Dietz (2009). In plants, photosystem I of chloroplast and complex I and III of mitochondria are the main electron donors for MV reduction resulting in oxidative stress. MV generates superoxide anions that either directly react with other molecules e.g. lipids or nitric oxide, or are converted to H₂O₂. To assess the role of BjAnn3 in MV-mediated oxidative stress, we generated transgenic *Arabidopsis* overexpressing BjAnn3. *Arabidopsis* plants were transfected with *Agrobacterium tumefaciens* carrying the *BjAnn3*-pCAMBIA 2300 construct with *BjAnn3* under the control of CaMV35S. Putative transgenics were confirmed for transgene integration by gDNA PCR (**Fig. 7A**). The expression level was analyzed by qPCR (**Fig. 7B**). All experiments were conducted with *T₃* lines. Line 4 (*BjAnn3* L4) and line 6 (*BjAnn3* L6) were chosen as low and high expression lines respectively for all subsequent experiments.

Functional effects of BjAnn3 expression on growth under stress

Aseptically grown WT, *BjAnn3* L4 and *BjAnn3* L6 seedlings were transferred to ½ MS with or without MV for stress assay (**Fig. 7C**). Transgenics showed clear resistance compared to wild type at 1.5 µM MV after 7 d. No difference was observed at 3 µM MV. This result indicated that BjAnn3 plays a role in the protection against oxidative stress.

Effect of MV on PSII activity in the leaves of wild type and transgenic plants

To assess the role of BjAnn3 in MV-induced photosynthetic performance, we measured (Fv/Fm) after the initial SP, which represents maximal quantum yield of photosynthesis (**Fig. 8A**). Fv/Fm was close to 0.8 in unstressed plants, which fits to previous findings (Björkman and Demmig, 1987; Johnson et al. 1993). Both wild type and transgenics showed no significant difference upon treatment. Photosynthetic induction was investigated for 5 min after illumination start of dark acclimated plants. The delay time of 40 s after the initial SP allows nearly complete re-oxidation of PSII acceptors before the start of repetitive firing of

SPs. We recorded Y(II) (**Fig. 8B**), qP (**Fig. 8C**) and NPQ (**Fig. 8D**) at a time interval of 20s. A fall of Y(II) in both wild type and transgenics indicated a cumulative damage and inhibited electron transport of PSII upon treatment. For more detailed presentation, we chose 308 s for measuring Y(II), which did not fall significantly for *BjAnn3* L6 below wild type, after treatment (**Fig. 8B**).

qP is a measure of the electron flow beyond PSII. Progressive increase in qP with time in transgenic lines upon treatment reflects more efficient electron flow compared to wild type. qP was significantly higher in *BjAnn3* L6 at 308 s compared to wild type after treatment (**Fig. 8C**). Plants protect themselves from high light by dissipating light energy as heat measurable as NPQ (Stepien et al. 2009). With increasing time NPQ increased progressively in both wild type and transgenics upon treatment. At 308 s, NPQ was significantly higher in wild type than in transgenics upon treatment (**Fig. 8D**). *BjAnn3* L6 showed the least change in NPQ upon treatment. Our results suggest that *BjAnn3* helps to maintain a better redox balance between light-dependent electron pressures and protects MV-treated *Arabidopsis* with better PSII performance.

Effect of MV on lipid hydroperoxide levels in the seedlings of wild type and transgenic plants

Structural integrity of membranes is widely known to be negatively affected by oxidative stress through different mechanisms (Megli et al. 2003, 2005). Plant annexins provide oxidative protection to cells by reducing lipid peroxides and/or H₂O₂ levels (Jami et al. 2008; Konopka-Postupolska et al. 2009; Divya et al. 2010; Zhang et al. 2011; Zhou et al. 2011; Chu et al. 2012; Clark et al. 2012). They interact with membranes and might counteract oxidative stress at membranes in a localized manner. Different mechanisms have been hypothesized by Konopka-Postupolska et al. (2011) which might contribute to the favorable effects of plant annexins, in particular maintenance of membrane stability and acceleration of membrane repair. Therefore, we next investigated the ability of *BjAnn3* to interfere with membrane stability and integrity. Lipid peroxidation is an established indicator of membrane damage. We estimated the amount of MDA, a secondary end product of polyunsaturated fatty acid oxidation in both wild type and transgenics upon treatment

(**Fig. 8E**). MDA content showed no difference between wild type and transgenics under control conditions. Upon treatment, MDA level increased both in wild type and transgenics. However, lipid peroxidation was lower in transgenics compared to wild type, and *BjAnn3* L6 showed least MDA accumulation. Apparently *BjAnn3* protected plant cells from $O_2^{\bullet-}$ -induced membrane damage.

Subcellular localization of BjAnn3-GFP using confocal laser scanning microscopy

Annexins are characterized to have broad tissue, cell and subcellular distribution depending on both cell type and stimuli (Mortimer et al. 2008; Laohavisit 2009, 2011). We looked for the localization of *BjAnn3*-GFP in the agro-infiltrated tobacco leaf epidermal cells. Compared to the GFP control which was more diffusely distributed and is known to localize to the cytosol and nucleoplasm, the signal from *BjAnn3*-gfp was narrowly localized and brighter, and was lacking in the nucleus. This tentatively indicates a preferred association with the plasma membrane (**Fig. 9**) in line with Huang et al. (2013), where *BjAnn3* might help to maintain the integrity of the membrane during oxidative stress. This in turn may be one of the underlying mechanisms involved in increased resistivity of the *BjAnn3* over expressing lines to MV-induced oxidative stress.

Estimation of H_2O_2 level and total peroxidase activity in *Arabidopsis* seedlings

Plasma membrane redox systems exist within lipid rafts and plant annexins have been identified to be associated with lipid raft membrane preparation (Lefebvre et al. 2007; Konopka-Postupolska et al. 2011). Plant annexins are known to detoxify ROS and have been extensively studied in both native (Konopka-Postupolska et al. 2009) and transgenic plants (Gorecka et al. 2005; Jami et al. 2008; Laohavisit et al. 2009; Divya et al. 2010; Jami et al. 2010; Zhang 2011; Chu et al. 2012). In plants ROS are produced in various compartments during normal metabolism (Asada 1999; del Rio et al. 2006; Sagi et al. 2006). MV initially produces superoxide radical which eventually gets converted into H_2O_2 . To test the direct or indirect role of *BjAnn3* in H_2O_2 detoxification, we determined H_2O_2 content in both wild type and transgenics upon treatment (**Fig. 10A**). Fe(II) is oxidized by H_2O_2 , and the generated Fe(III) together with xylenol orange forms the Fe(III)-xylenol orange complex

which is an indicator of oxidative stress measurable at A_{560} . H_2O_2 content was indistinguishable in the untreated samples. Upon treatment wild type showed significant elevation of H_2O_2 level compared to transgenics. The content was more in *BjAnn3* L4 in comparison to *BjAnn3* L6.

Further we evaluated the *in vivo* total peroxidase activity (**Fig. 10B**) in both wild type and transgenics using H_2O_2 /guaiacol assay at pH 6.0. H_2O_2 acts as electron acceptor oxidizing guaiacol to tetraguaiacol measurable at A_{470} . Transgenic lines displayed significantly enhanced total peroxidase activity in comparison to wild type which is possibly due to the ectopic expression of *BjAnn3*. Despite significant differences in peroxidase activity, the similar H_2O_2 contents of untreated samples might be due to the redox equilibrium maintained for balanced metabolism. These findings supports two conclusions, firstly, increased MV-tolerance of transgenics may be due to the restoration of membrane integrity and improved ROS detoxification and secondly, and likewise lowering of membrane damage may be linked to the physical localization of the *BjAnn3* but also to ROS detoxification.

Titration of the E_m value and quantification of peroxidase activity of *BjAnn3* wild type protein

Next we investigated a role of *BjAnn3* in redox sensing or redox-dependent regulation. *BjAnn3* has conserved Cys residues which could also be involved in thiol-specific antioxidant function. Plant annexins AtAnn1, *BjAnn1*, ZmAnn33/35, CaAnn24, CkANN, GhAnx1 and NnANN1 proteins are already known to be associated with antioxidant function (Gidrol et al. 1996; Gorecka et al. 2005; Jami et al. 2008; Laohavisit et al. 2009; Zhang et al. 2011; Zhou et al. 2011; Chu et al. 2012). We purified the recombinant *BjAnn3* protein (**Fig. 11**) and determined the redox midpoint potential (**Fig. 12A**) which characterizes the conditions under which its thiols are in the reduced form and could function in ROS detoxification or redox sensing. The E_m value of *BjAnn3* protein as determined by the monobromobimane binding assay was approximately -319 mV. This rather negative E_m -value is in the range of that of the peroxidatic thiol of peroxiredoxins (König et al. 2002). Nevertheless the thiols of *BjAnn3* will be reduced under regular

cytoplasmic redox potentials (Meyer et al. 2007) and might react with H_2O_2 . We estimated peroxidase activity of recombinant BjAnn3 (**Fig. 12B**) using H_2O_2 /guaiacol assay. Native BjAnn3 showed significantly more peroxidase activity compared to its heat denatured form. HRP and BSA were used as positive and negative controls respectively. These results suggest a direct activity of BjAnn3 in ROS detoxification and protection against oxidative stress.

qPCR analysis of mRNA transcripts of some antioxidant enzymes

There might exist an indirect role of BjAnn3 in affecting or regulating the antioxidant defense. Plant annexins have already been shown to transcriptionally regulate other genes for improved stress response (Jami et al 2008; Divya et al 2010; Huh et al 2010). We quantified the transcript levels of *sAPX* (TAIR: At4g08390, **Fig. 13A**), *tAPX* (TAIR: At1g77490, **Fig. 13B**), *APX1* (TAIR: At1g07890, **Fig. 13C**), *CSD1* (TAIR: At1g08830, **Fig. 13D**) and *FSD1* (TAIR: At4g25100, **Fig. 13E**) by qPCR. Except *FSD1*, all antioxidant genes were up-regulated in response to MV treatment in wild type as observed earlier (Rizhsky et al. 2004; Yang et al. 2012). BjAnn3 expression counteracted the MV-dependent upregulation of *sAPX*, *tAPX*, *APX1* and *CSD1*. In some cases, the transcript levels of treated and untreated transgenic lines were indistinguishable, indicating complete suppression of the involved signaling pathways, e.g. in the case of *tAPX*, *APX1* and *CSD1*. Transcript accumulation of *sAPX* was even suppressed in MV-treated BjAnn3 L6 below the level of the untreated control. *sAPX* expression is under the control of signals linked to development, light and photosynthesis (Oelze et al. 2012) and recently the transcription factor ANAC089 has been recognized to be involved in redox dependent regulation of *sAPX* expression (Klein et al. 2012). Plant annexins were suggested to play a role in ROS signaling pathways by lowering H_2O_2 level (Gidrol et al. 1996; Gorecka et al. 2005; Jami et al. 2008; Laohavisit et al. 2009; Jami et al. 2010; Divya et al. 2010; Zhang et al. 2011; Zhou et al. 2011; Chu et al. 2012).

Thus decreased antioxidant transcript accumulation can be explained by degradation of H_2O_2 through BjAnn3 or alternatively could be mediated by interference of BjAnn3 with involved signaling pathways. Apparently, independent mechanisms contribute to enhanced

tolerance to MV. In the *A. thaliana* mutant radical-induced cell death 1 (*rcd1*), MV resistance was associated with increased expression of plastidic Cu/Zn *SOD* and *APX* (Fujibe et al. 2004). In fact, chloroplast targeted overexpression of *SOD* showed MV resistance in several transgenic species (Bowler 1991, Gupta et al. 1993; Camp 1996; Arisi et al. 1998). Regulation of *FSD1* in BjAnn3-lines was opposite to the other tested antioxidants, namely with increased transcript levels in MV-treated lines. *FSD1* is found in the chloroplast as well as in the plasma membrane and mitochondrial membrane. It is regulated in response to diverse stresses including heavy metals and oxidative stress (Myouga 2008; Vanhoudt 2010). The peculiar response of *FSD1* transcript in MV-treated BjAnn3-lines hints to different regulatory mechanisms independent on ROS and/or lipid binding, possibly to a high sensitivity to redox disequilibria. The results presented in **Fig. 13** suggest that BjAnn3 functions in regulating *sAPX*, *tAPX*, *APX1*, *CSD1* and *FSD1* to maintain cell redox homeostasis.

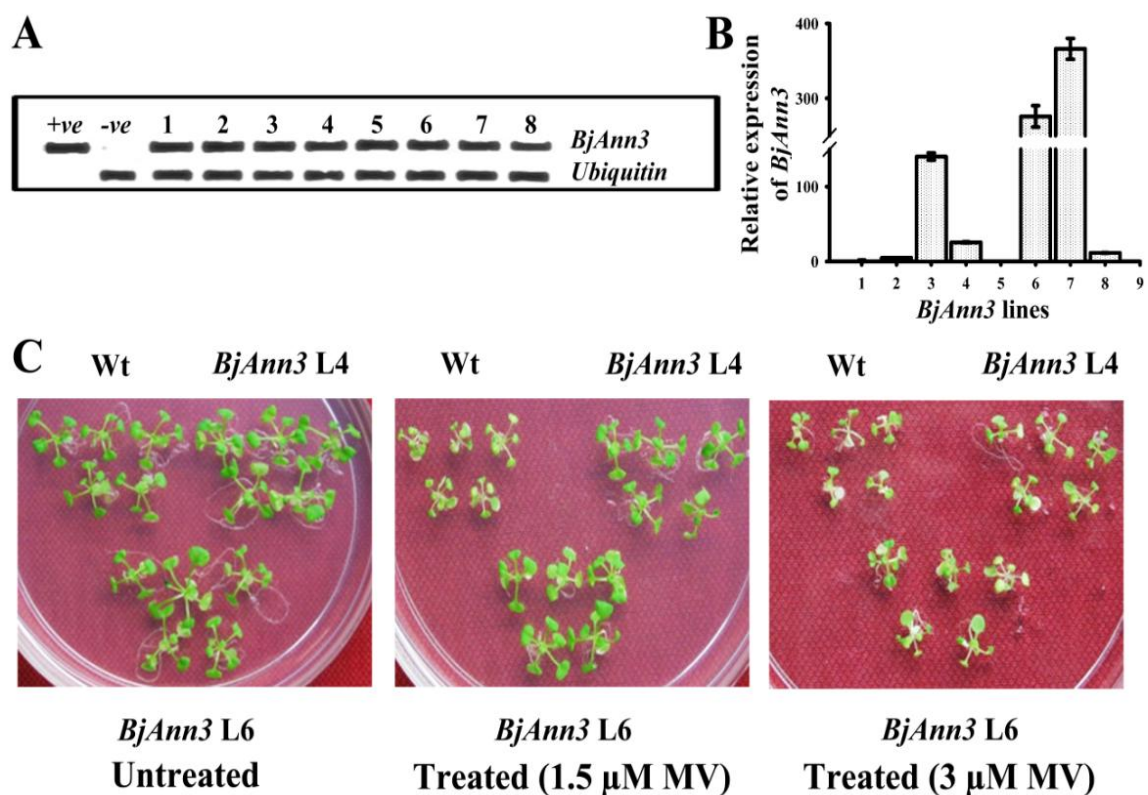


Figure 7 Molecular analyses of *A. thaliana* lines expressing BjAnn3 and functional effects of BjAnn3 expression on growth under stress. (A) Confirmation of transgene insertion in T_1 plants is shown by PCR analysis of genomic DNA. +ve, -ve and 1-8 represent positive control (*BjAnn3*-pCAMBIA 2300 plasmid), negative control (wild type plants) and transgenic lines numbered 1-8 respectively. (B) *BjAnn3* expression levels were analyzed by qPCR in transgenic plants. All expression levels are shown with respect to the lowest expression line which is considered as 1-fold. (C) Tolerance of the transgenics was assessed by MV-mediated stress on 7 d old seedlings. Wt, *BjAnn3* L4 and *BjAnn3* L6 represent wild type, *BjAnn3* transgenic line 4 and *BjAnn3* transgenic line 6 respectively.

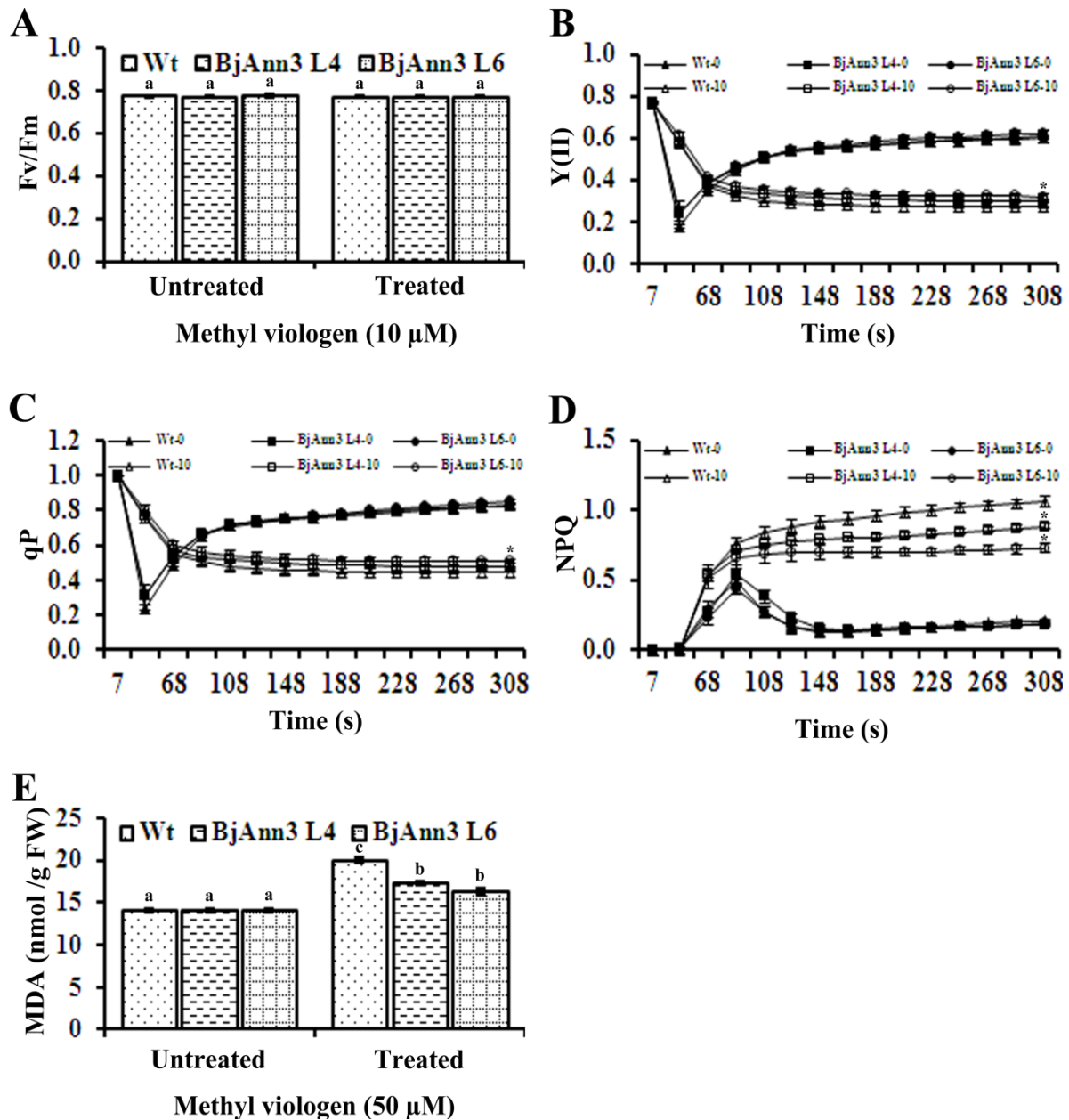


Figure 8 Effect of MV on PSII activity and lipid hydroperoxide levels in wild type and transgenic plants. The maximal quantum yield [F_v/F_m] was recorded after the first SP (A). Effective photochemical quantum yield [$Y(II)$] (B), coefficient of photochemical fluorescence quenching [qP] (C) and Stern-Volmer type non-photochemical fluorescence quenching [NPQ] (D) was measured every 20 s over a period of 5 min. Filled and open symbols in line graphs represent untreated and treated samples respectively. Lipid peroxidation was assessed as MDA content (E). Wt, *BjAnn3* L4 and *BjAnn3* L6 represent wild type, *BjAnn3* transgenic line 4 and *BjAnn3* transgenic line 6 respectively. Data represent means of $n=3 \pm SE$. Statistical analysis was carried out in Sigma-Plot11.0 by One-Way ANOVA analysis with Duncan's Multiple Range Test (DMRT). Lowercase letters

mark significance of difference ($p < 0.05$). (*) marks significant differences with $p < 0.05$ relative to the likewise treated wild type in line graphs.

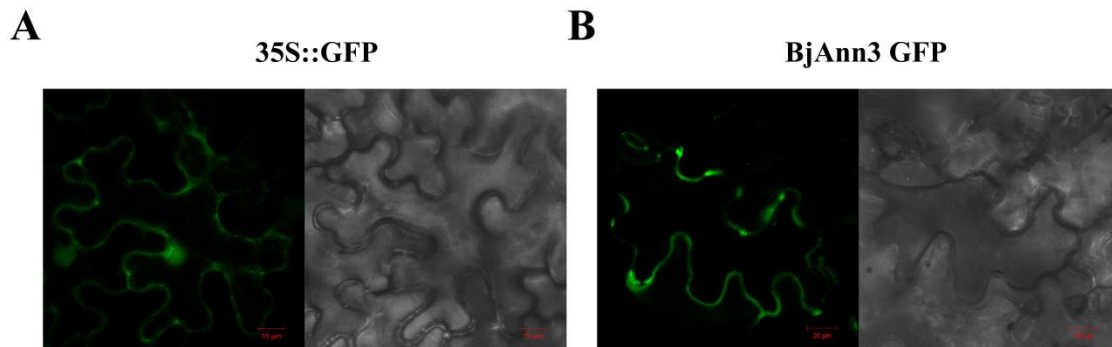


Figure 9 Subcellular localization of BjAnn3-GFP using confocal laser scanning microscopy. In contrast to the more diffuse localization of GFP (A), the BjAnn3-GFP signal was brighter and localized in more narrow regions of tobacco epidermal cells (B). Scale bar: 35S::GFP=10 μ m and BjAnn3-GFP=20 μ m.

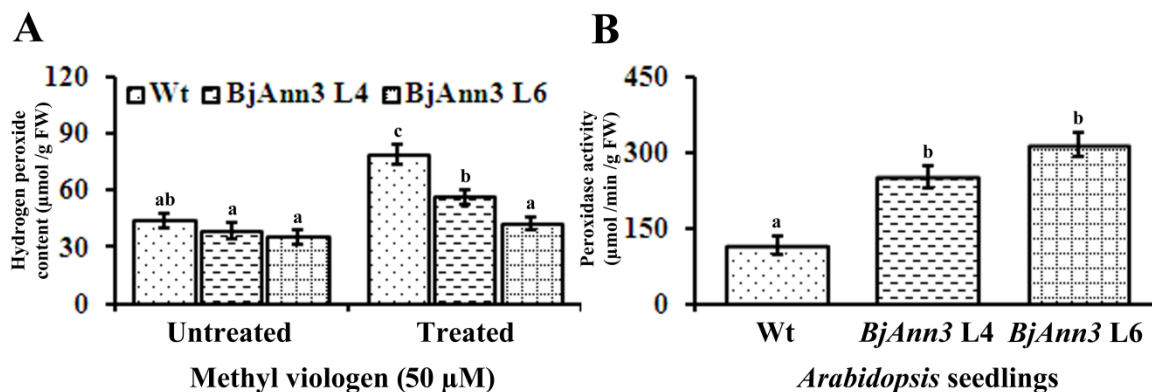


Figure 10 Estimation of H₂O₂ level and total peroxidase activity in *Arabidopsis* seedlings.(A) H₂O₂ content was measured in both wild type and transgenics upon MV-treatment. (B) Total peroxidase activity was determined in both wild type and transgenics by measuring the rate of guaiacol tetramerization. Wt, *BjAnn3* L4 and *BjAnn3* L6 represent wild type, *BjAnn3* transgenic line 4 and *BjAnn3* transgenic line 6 respectively. Data represent means of $n=5 \pm$ SE. Statistical analysis was carried out in Sigma-Plot11.0 by One-Way ANOVA analysis with Duncan's Multiple Range Test (DMRT). Letters mark significance of difference ($p < 0.05$).

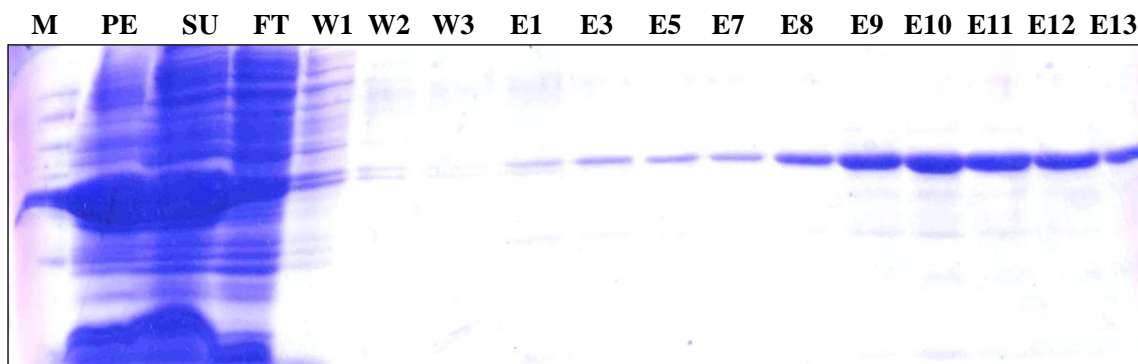


Figure 11 Protein purification profile. M- Marker. PE- Pellet; SU-Supernatant; FT-Flow-through; W1,W2,W3-Washes (10mM,20mM,30mM); E1 TO E7 – Elutions in 100mM E8, E9, E10 - Elutions in 250mM; E11, E12, E13 - Elutions in 400mM.

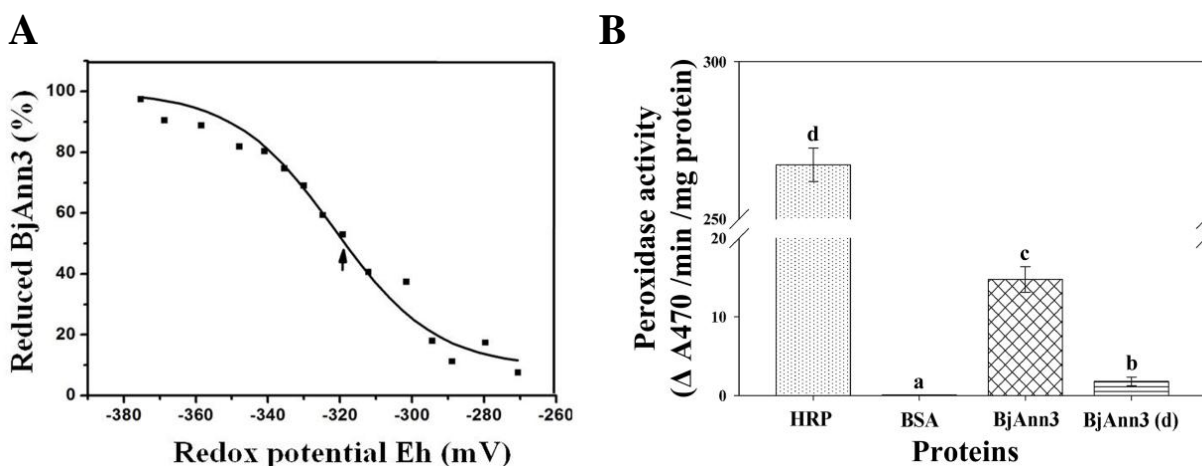


Figure 12 Titration of the E_m value and quantification of peroxidase activity of BjAnn3 wild type protein. (A) The redox midpoint potential of the recombinant protein was titrated by incorporation of monobromobimane after equilibration with varying ratios of $DTT_{reduced}/DTT_{oxidized}$. Data from four experimental repeats were fitted to Nernst equation with $n=4$ using OriginPro 8. (B) Peroxidase activity of the recombinant protein was quantified by measuring the rate of guaiacol tetramerization. HRP, BSA, BjAnn3 and BjAnn3 (d) represent horseradish peroxidase, bovine serum albumin, native BjAnn3 and heat-denatured BjAnn3 respectively. Data represent means of $n=5 \pm SE$. Statistical analysis was carried out in Sigma-Plot11.0 by One-Way ANOVA analysis with Duncan's Multiple Range Test (DMRT). Letters mark significance of difference ($p < 0.05$).

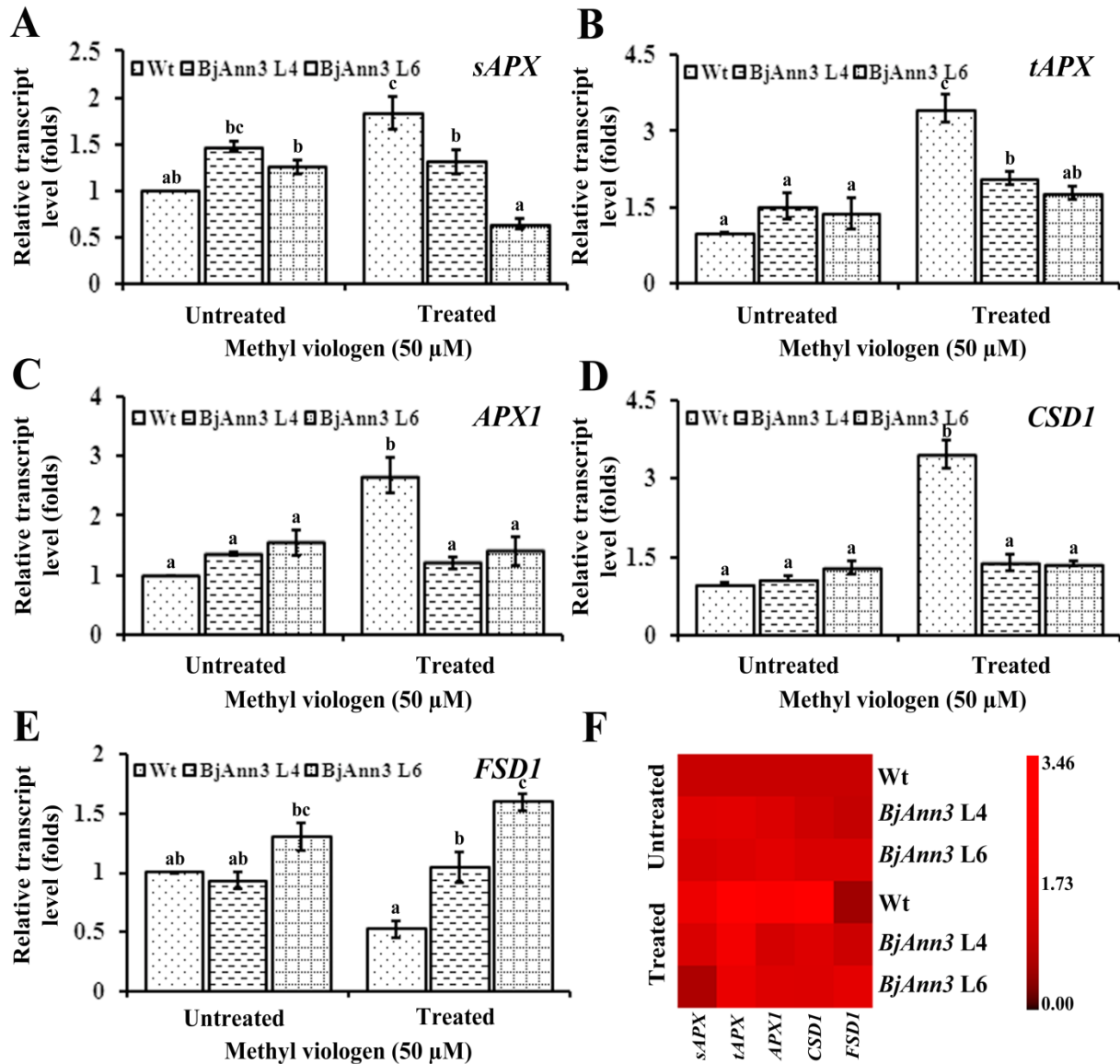


Figure 13 qPCR analyses of mRNA transcripts of some antioxidant enzymes. Both lines showed BjAnn3-mediated regulation upon MV treatment. *sAPX* (A), *tAPX* (B), *APX1*(C), *CSD1*(D) and *FSD1*(E) transcripts were quantified as described above. The expression patterns were compiled in a heat map (F). *18S rRNA* (TAIR: AT2G01010) was used as reference gene. Wt, *BjAnn3* L4 and *BjAnn3* L6 represent wild type, *BjAnn3* transgenic line 4 and *BjAnn3* transgenic line 6 respectively. Data represent means \pm S.E. from 3 measurements. Statistical analysis was carried out in Sigma-Plot11.0 by One-Way ANOVA analysis with Duncan's Multiple Range Test (DMRT). Letters mark significance of difference ($p < 0.05$).

Conclusion

This report characterizes the effect of BjAnn3 heterologously expressed in *A. thaliana*. Plant annexins have been studied for their transcriptional activation upon MV treatment (Jami et al., 2008, 2009). Here it is shown that BjAnn3 alleviates MV-mediated oxidative stress in plants. The overexpressing seedlings were more tolerant against MV compared to wild type. BjAnn3 protected photosynthesis against MV-mediated photo-oxidative damage and prevented MV-mediated plasma membrane damage. Three mechanisms may be proposed: (i) BjAnn3 localizes close to the plasma membrane and maintains membrane stability and integrity. This protection may be caused by interaction with lipids, such as direct binding to peroxidized lipids and their decomposition, formation of crystal patches on membranes or membrane resealing (Konopka-Postupolska et al. 2011). (ii) BjAnn3 counteracts ROS accumulation. This may occur either in the free or membrane bound state (Mortimer et al. 2009). ROS detoxification is likely linked to the enzymatic antioxidant property of BjAnn3 and in addition could involve cooperation with other cellular antioxidant system. The N-terminal Cys residue of annexin A2 in mammalian cells can be oxidized by H_2O_2 and reduced by thioredoxin for further availability in redox cycles (Madureira et al. 2011, Clark et al. 2012). Annexin peroxidase activity is predicted to be similar to that of heme-free glutathione peroxidase that catalyzes the reduction of lipid peroxides and H_2O_2 . There, conserved Cys residues are involved in reduction of hydroperoxides which act as electron acceptor (Laohavisit et al. 2009, Rouhier et al. 2005, Dietz 2011). BjAnn3 showed a redox potential of approximately -319 mV. This can contribute to the antioxidant property of the protein probably via thiol-based mechanisms. Peroxidase activity confirmed the antioxidant property of the protein. BjAnn3 also resulted in increase of total peroxidase activity in transgenics and showed interference with other cellular antioxidants. BjAnn3 may affect redox buffering at plasma membrane and thereby provide improved cellular protection. (iii) Alternatively BjAnn3 may interfere with cell signaling pathways by molecular interactions involving yet unknown mechanism that may also involve redox reactions (Madureira and Waisman 2013).

Objective 3

**Role of AtAnn3 under methyl viologen-mediated
oxidative stress in *Arabidopsis thaliana* AtAnn3-
knockout plants**

Introduction

Plant annexins are distributed across kingdoms and represent about 0.1% of total cell protein (Hofmann 2004; Mortimer et al. 2008). Tomato annexin was the first plant annexin that was identified and was followed by many in other plant species (Boustead et al. 1989; Blackbourn et al. 1991; Cantero et al. 2006; Konopka-Postupolska et al. 2009; Jami et al. 2012; Zhou et al. 2011; Zhang et al. 2011; Chu et al. 2012; Huang et al. 2013; Zhou et al. 2013). Annexins exist in both soluble and membrane-bound state (calcium dependent or independent manner) (Mortimer et al. 2008; Dabitz et al. 2005; Laohavisit and Davies 2011). However, these multifunctional proteins remained insufficiently characterized *in vivo*, particularly concerning the antioxidant property.

Several plant annexins showed antioxidant property (Gorecka et al. 2005; Jami et al. 2008; Laohavisit et al. 2009; Chu et al. 2012). Two criteria were suggested for the antioxidant activity of plant annexins. The first one is the heme-binding histidine residue initially identified in AtAnn1. However lack of both experimental evidence and structural data could not support the concept of heme-binding in plant annexins (Laohavisit et al. 2009; Konopka-Postupolska et al. 2011). The second feature is the S₃ cluster which was initially identified in the GhAnn1 crystal structure. This cluster is hypothesized to be involved in electron-transfer reactions and function as redox reactive center possibly involving in H₂O₂ reduction (Hofmann et al. 2003, 2004).

Detailed amino acid sequence analysis of AtAnn3 evidenced the absence of both these criteria. S₃ cluster consists of two Cys residues which are highly conserved throughout plant and animal annexins while the third one, the methionine residue, often varies (Hofmann et al. 2003; Konopka-Postupolska et al. 2009). Cysteines are known to play a pivotal role in redox buffering under oxidative stress conditions (Guttmann 2010). The two conserved Cys residues of the S₃ cluster which are also present in AtAnn3 might play a role in redox homeostasis (Hofmann et al. 2003; Konopka-Postupolska et al. 2009). Plant annexins are known to have a potential role in oxidative stress response. They are transcriptionally regulated in response to various oxidative stressors (Gidrol et al. 1996; Kovacs et al. 1998; Jami et al. 2008, 2009; Konopka-Postupolska et al. 2009, Zhang et al. 2011) including

methyl viologen (Jami et al. 2008, 2009) however; their role in MV-mediated oxidative stress tolerance remained uninvestigated.

Earlier reports from our laboratory have confirmed *BjAnn3* transcripts accumulation upon methyl viologen application and also upon other stress treatments like H₂O₂, ABA, ethephon, salicylic acid, methyl jasmonate, sodium chloride and wounding in *Brassica juncea* (Jami et al. 2009). Multiple sequence alignment of BjAnn3 and AtAnn3 using default parameters of EMBL-EBI ClustalW showed 94.7% similarity (**Fig. 14**). We assumed that similar to BjAnn3; AtAnn3 might modulate cell acclimation responses during methyl viologen-mediated photo-oxidative stress. Therefore this study unravels the loss-of-function of AtAnn3 in *AtAnn3*-knockout *A. thaliana* plants with respect to MV-mediated oxidative stress.

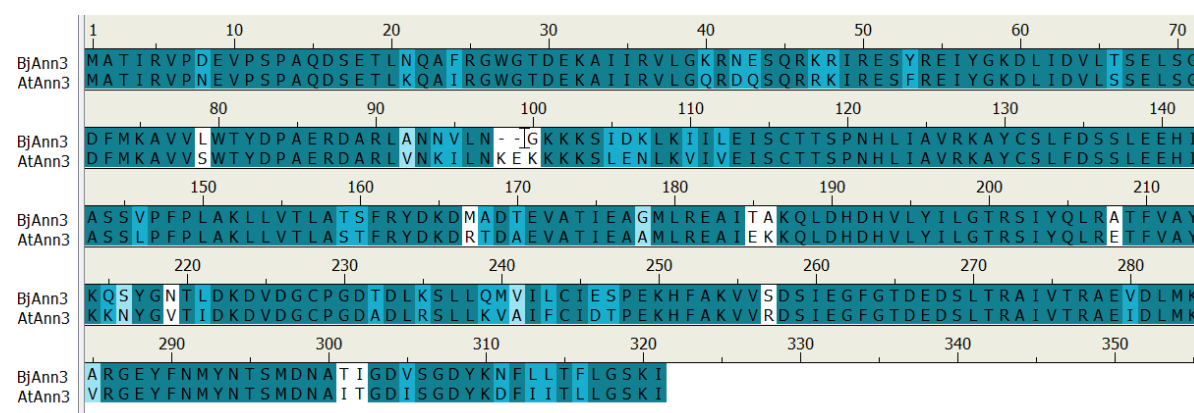


Figure 14 Multiple Sequence Alignment of BjAnn3 and AtAnn3.

Results and discussion

In this study, we tried to understand the role of AtAnn3 in MV-mediated oxidative stress. To study the tolerance and cross tolerance responses, MV has been extensively used as an oxidative stress inducer in (Lascano et al. 1998, 2001, 2003). MV accepts electrons from photosystem I of chloroplast and complex I & III of mitochondria in plants, and gets reduced resulting in oxidative stress. It generates superoxide anions that either directly react with other molecules e.g. lipids or nitric oxide, or are converted to other ROS forms. To assess the role of AtAnn3 in MV-mediated oxidative stress, we have chosen a homozygous *AtAnn3* mutant line of *A. thaliana* for all subsequent experiments.

Functional effects of AtAnn3 on growth under stress

WT and *AtAnn3*-KO seedlings were aseptically germinated on ½ MS with or without MV for stress assay (**Fig. 15**). Mutants showed clear susceptibility compared to wild type at 1.5 µM MV after 10 d of germination. Marginal or no difference was observed at 3 µM MV. This result indicated a possible role of AtAnn3 in protecting *Arabidopsis* against oxidative stress.

Effect of MV on PSII activity in the leaves of wild type and *AtAnn3*-KO plants

The role of AtAnn3 in MV-induced photosynthetic performance was studied by measuring (Fv/Fm) after the initial SP, which represents maximal quantum yield of photosynthesis (**Fig. 16A**). Fv/Fm was approximately 0.8 in unstressed plants, which is in line with earlier findings (Björkman and Demmig 1987; Johnson et al. 1993). No significant difference was observed in both wild type and mutants upon treatment. Photosynthetic induction was investigated for 5 min after illumination start of dark acclimated plants. We measured Y(II) (**Fig. 16B**), qP (**Fig. 16C**) and NPQ (**Fig. 16D**) at a time interval of 20s. In both wild type and mutants, a fall of Y(II) upon treatment indicated a cumulative damage and inhibited electron transport of PSII. For more clear understanding, we chose 308 s for measuring Y(II), which was less for *AtAnn3*-KO compared to wild type, after treatment (**Fig. 16B**).

qP represents a measure of the electron flow beyond PSII. Upon treatment, progressive decrease in qP with time in mutants indicates less efficient electron flow compared to wild type. At 308 s, qP was less in *AtAnn3*-KO compared to wild type after treatment (**Fig. 16C**).

Plants dissipate light energy as heat which can be measured as NPQ (Stepien et al. 2009). NPQ increased progressively with increasing time in both wild type and mutants upon treatment. At 308 s, NPQ was significantly higher in mutant than in wild type upon treatment (**Fig. 16D**). This study suggests that impaired *AtAnn3* has resulted in disruption of redox homeostasis in *AtAnn3*-KO plants indicating the role of *AtAnn3* in protecting MV-treated *Arabidopsis* with better PSII performance.

Effect of MV on lipid hydroperoxide levels in the seedlings of wild type and mutant plants

Oxidative stress is widely known to disrupt the structural integrity of membranes (Megli et al. 2003 and 2005). Plant annexins offer protection to cells from oxidative damage by reducing lipid peroxides and/or H₂O₂ levels (Jami et al. 2008; Konopka-Postupolska et al. 2009; Zhang et al. 2011; Zhou et al. 2011; Clark et al. 2012). They can interact with membranes and might neutralize oxidative stress at membranes in a localized manner. Konopka-Postupolska et al. (2011) postulated various mechanisms by which annexins can contribute to maintenance of membrane stability and acceleration of membrane repair. Therefore, our next study was to investigate how *AtAnn3* interferes with membrane stability and integrity. Lipid peroxidation is an established indicator of membrane damage. We measured the amount of MDA, a secondary end product of lipid peroxidation in both wild type and mutants upon treatment (**Fig. 16E**). Under control conditions, MDA content showed no difference between wild type and mutants. MV-treatment had resulted in increased MDA level in both wild type and mutants. However, lipid peroxidation was higher in mutants compared to wild type. Our result suggests that absence of *AtAnn3* in *AtAnn3*-KO plants has increased the vulnerability of membranes towards MV-mediated damage and indicates a role of *AtAnn3* in cellular protection against O₂^{•-}-induced membrane damage.

qPCR analysis of mRNA transcripts of some antioxidant enzymes

AtAnn3 might have an indirect role in regulation of antioxidant system. Plant annexins are known to transcriptionally regulate other genes for better stress response (Jami et al. 2008; Divya et al. 2010; Huh et al. 2010). We quantified the transcript levels of *sAPX* (TAIR: At4g08390, **Fig. 17A**), *tAPX* (TAIR: At1g77490, **Fig. 17B**), *APX1* (TAIR: At1g07890, **Fig. 17C**), *CSD1* (TAIR: At1g08830, **Fig. 17D**) and *FSD1* (TAIR: At4g25100, **Fig. 17E**) by qPCR. Except *FSD1*, all antioxidant genes were up-regulated in response to MV treatment in wild type as seen earlier (Rizhsky et al. 2004; Yang et al. 2012). Loss of AtAnn3 in *AtAnn3*-KO plants resulted in MV-dependent down-regulation of *sAPX*, *tAPX*, *APX1* and *CSD1*. Thus decreased antioxidant transcript accumulation can be explained by the loss of activation of antioxidant signaling pathways due to the absence of AtAnn3. In some cases the untreated mutant showed antioxidant transcript upregulation in comparison with wild type. A possible explanation could be that loss of AtAnn3 has resulted in compensational activation of those transcripts in order to maintain a redox balance. Regulation of *FSD1* in *AtAnn3*-KO was opposite to the other tested antioxidants, namely with no change in transcript levels of MV-treated mutants. FSD1 is found in chloroplast as well as in the plasma membrane and mitochondrial membrane and is regulated in response to diverse stresses including oxidative stress (Myouga 2008 and Vanhoudt 2010). The peculiar response of *FSD1* transcript in MV-treated *AtAnn3*-KO points to a different regulatory mechanism that is independent of AtAnn3-mediated regulation of antioxidant signaling pathways. The results presented in **Fig. 17** suggest that AtAnn3 functions in regulating *sAPX*, *tAPX*, *APX1*, *CSD1* and *FSD1* in order to maintain cellular redox balance.

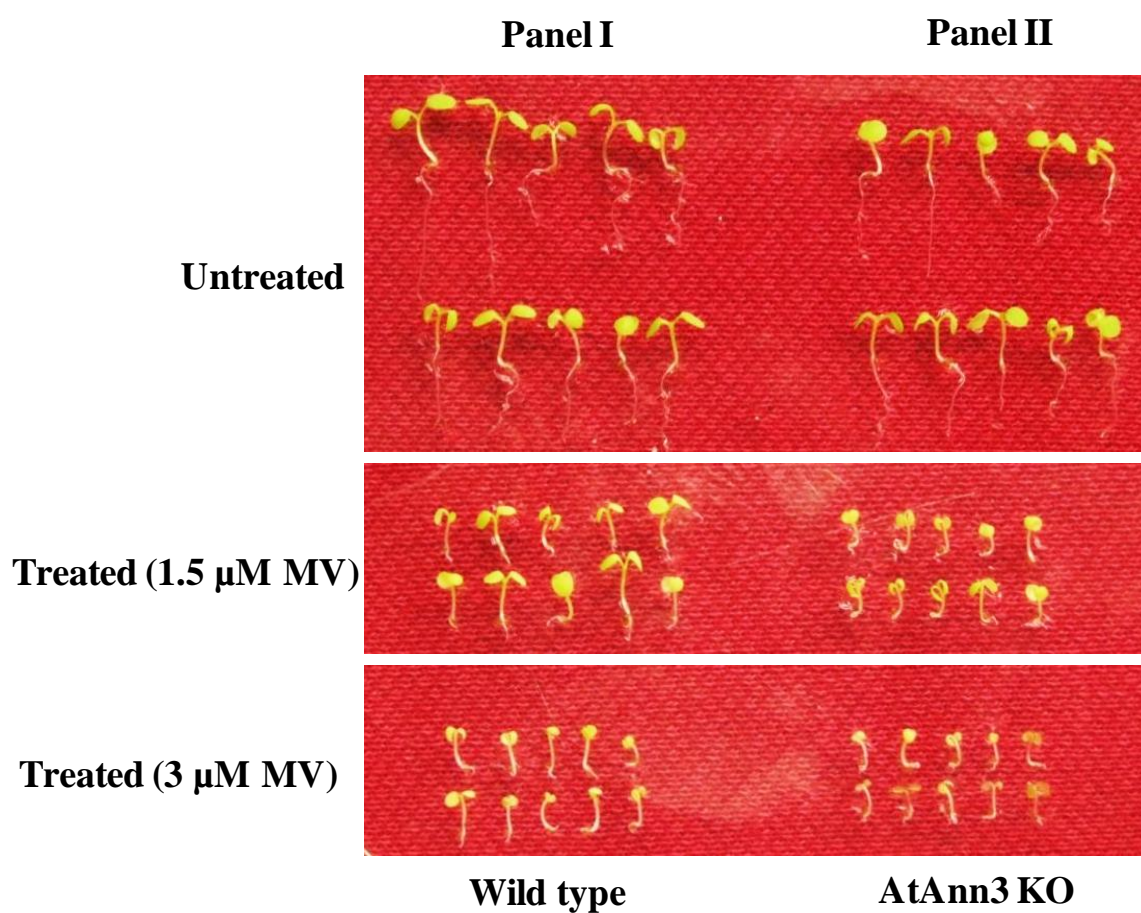


Figure 15 Functional effects of *AtAnn3* on growth under stress. Susceptibility of *AtAnn3*-KO seedlings was assessed by MV-mediated stress on germination after 10 days. Wt and *AtAnn3*-KO represent wild type and *AtAnn3* mutant line respectively.

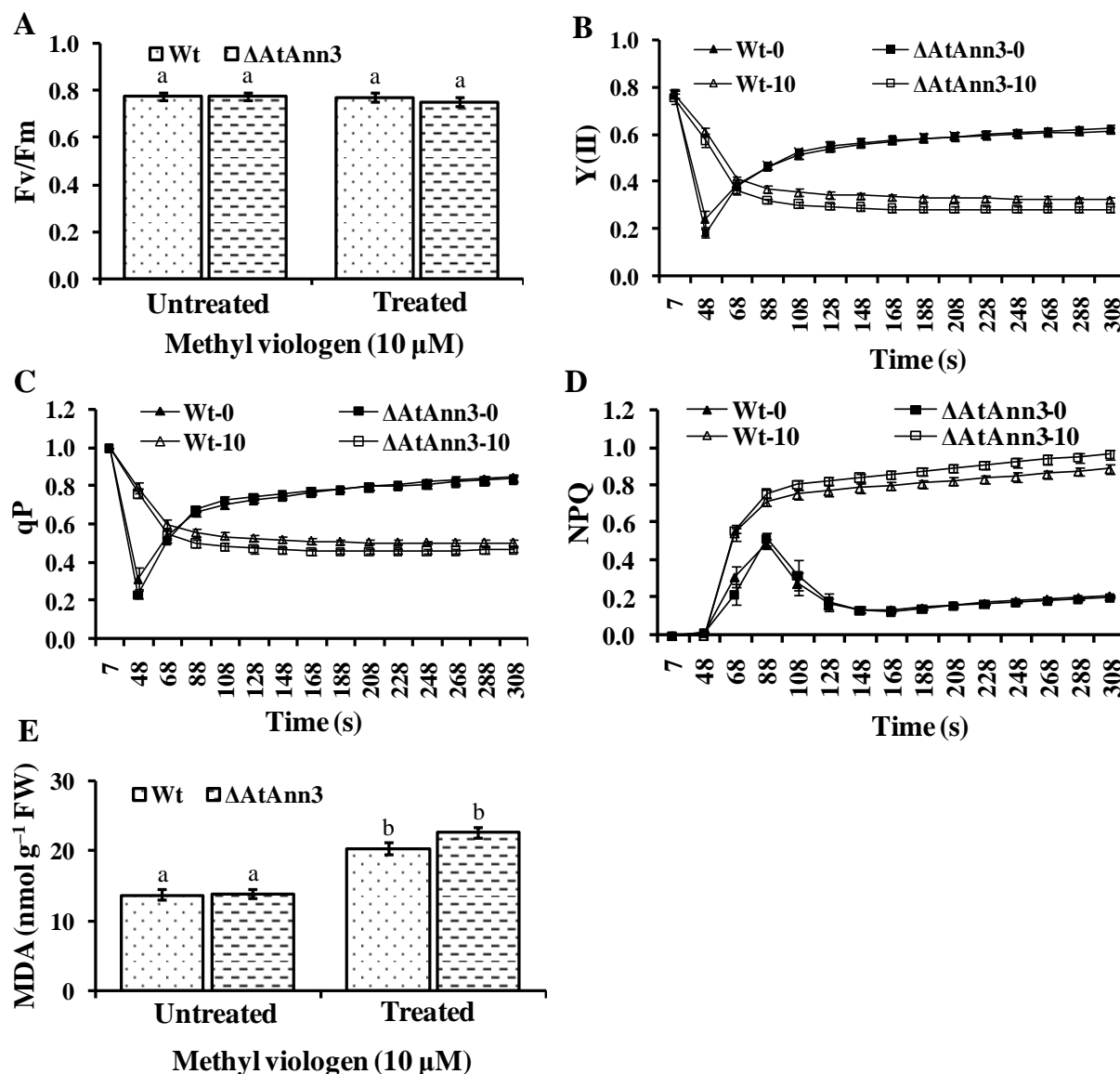


Figure 16 Effect of MV on PSII activity and lipid hydroperoxide levels in wild type and mutant plants. The maximal quantum yield [F_v/F_m] was recorded after the first SP (A). Effective photochemical quantum yield [$Y(II)$] (B), coefficient of photochemical fluorescence quenching [qP] (C) and Stern-Volmer type non-photochemical fluorescence quenching [NPQ] (D) was measured every 20 s over a period of 5 min. Filled and open symbols in line graphs represent untreated and treated samples respectively. Lipid peroxidation was assessed as MDA content (E). Wt and *AtAnn3*-KO represent wild type and *AtAnn3* mutant line respectively. Data represent means of $n=3 \pm SE$. Statistical analysis was carried out in Sigma-Plot11.0 by One-Way ANOVA analysis with Duncan's Multiple Range Test (DMRT). Lowercase letters mark significance of difference ($p < 0.05$). (*) marks significant differences with $p < 0.05$ relative to the like wise treated wild type in line graphs.

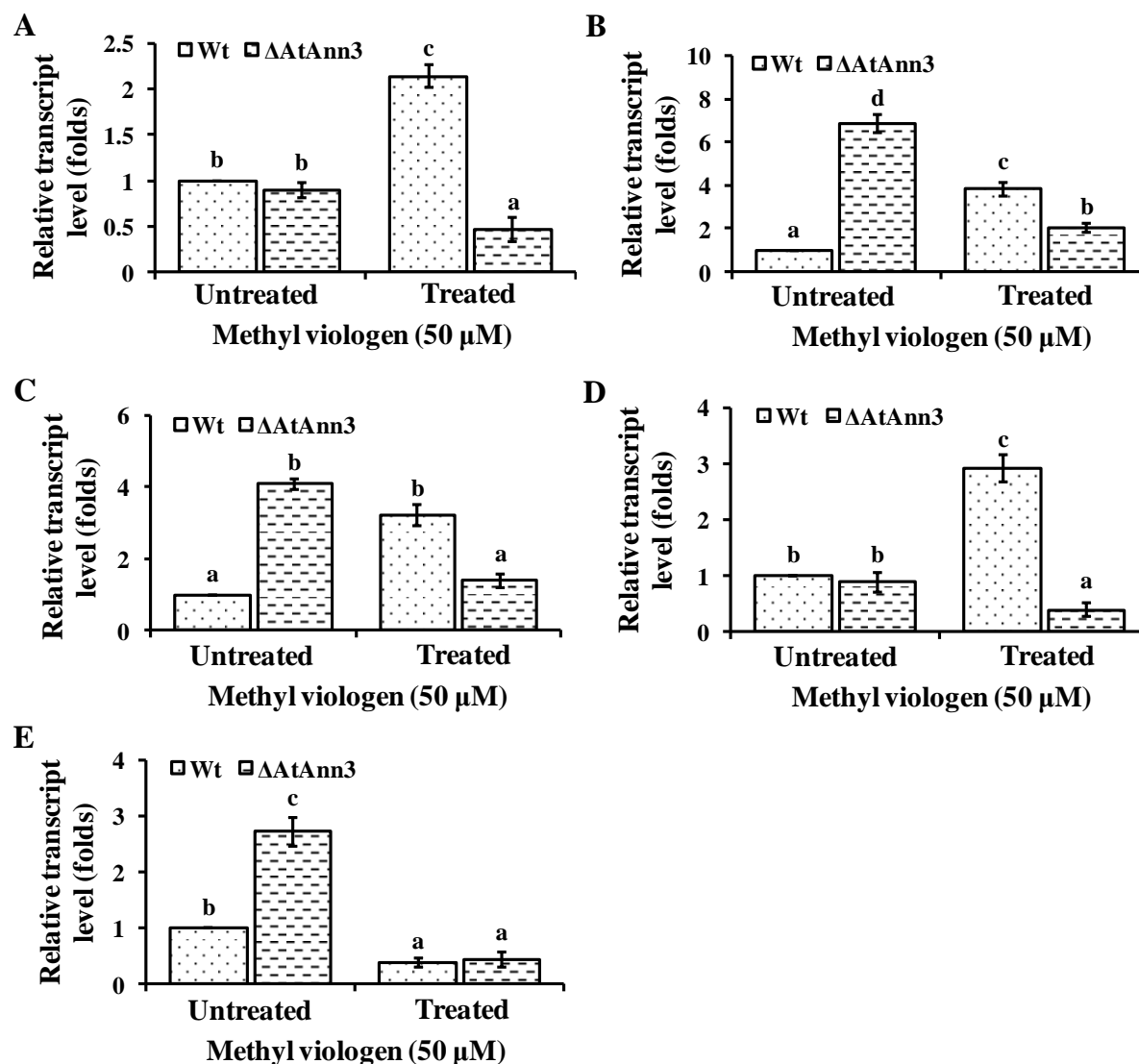


Figure 17 qPCR analysis of mRNA transcripts of some antioxidant enzymes. *sAPX*(A), *tAPX*(B), *APX1*(C), *CSD1*(D) and *FSD1*(E) transcripts were quantified as described above. *18S rRNA* (TAIR: AT2G01010) was used as reference gene. Wt and *AtAnn3*-KO represent wild type and *AtAnn3* mutant line respectively. Data represent means \pm S.E. from 3 measurements. Statistical analysis was carried out in Sigma-Plot11.0 by One-Way ANOVA analysis with Duncan's Multiple Range Test (DMRT). Letters mark significance of difference ($p < 0.05$).

Conclusion

This report characterizes the loss-of-function of AtAnn3 in *A. thaliana* AtAnn3-KO plants. Transcriptional activation of plant annexins have been studied with MV treatment (Jami et al. 2008, 2009). Here it is shown that loss of AtAnn3 has resulted in increased susceptibility of MV-treated knockouts. This necessarily points to the role of AtAnn3 in alleviating MV-mediated oxidative stress in plants. Involvement of AtAnn3 in cellular protection could be direct or indirect. We have shown the role of AtAnn3 in protecting photosynthesis against MV-mediated photo-oxidative damage and preventing MV-mediated plasma membrane damage. This PSII and membrane protection might happen indirectly through cooperation with other cellular antioxidant signaling system. AtAnn3 seems to have a positive role in regulation of most antioxidant transcripts. AtAnn3 showed approximately 95% similarity with BjAnn3 in amino acid level, however, their regulation of antioxidant defense system is very different from each other.

Objective 4

**Role of BjAnn3-cysteines in redox modulation and
oligomerization**

Introduction

Functional proteins whose presence is attributed among almost all organisms and cell types, maintains a basic conserved structure notwithstanding their functional diversity. Significance of such protein counts on from the climatic sphere of the organisms to the core cellular biochemical milieu the protein is exposed to. Beyond a basic similarity in function, their functional divergence is obvious by virtue of the position of organisms across kingdoms or phyla and their disparate habitat. Exposure to inconsistent environment leads to altered cellular homeostasis in plants, attained by a refined harmony of multiple pathways within the cellular compartments (Miller et al. 2010). Uncoupling of different pathways due to stress, results in transfer of electrons with high energy state to molecular oxygen thereby forming ROS (Takahashi and Asada 1988; Mittler et al. 2002). They are generated at minor level during normal metabolic processes (Fridovich et al. 1995; Miller et al. 2010) under optimal growth conditions, however, environmental perturbations result in elevated ROS production, which serves as decisive signaling molecules for protection (Mittler et al. 2002) up to a threshold, beyond which becomes detrimental to the cell.

One of the vital components affected by ROS is lipids (Apel and Hirt 2004) thereby disrupting the structural integrity of phospholipid membranes. Of all other membrane binding proteins, annexins constitute an appreciable fraction and are multifunctional with both calcium dependent and independent membrane binding property (Mortimer et al. 2008; Dabitz et al. 2005). They comprise a multigene family of proteins and are present in almost all organisms except *Saccharomyces* and bacteria. Their expression in various tissues is governed by different abiotic stress factors and signaling molecules (Kovacs et al. 1998; Cantero et al. 2006; Gidrol et al. 1996; Lee et al. 2004; Breton et al. 2000; Jami et al. 2008, 2009; Apel and Hirt 2004). The first annexin protein to be implicated in oxidative stress response was Oxy5 (*AtAnn1*) from *A. thaliana* (Gidrol et al. 1996). The same protein was able to protect mammalian cells from oxidative damage (Janicke et al. 1998; Kush and Sabapathy 2001). Later few more plants annexins which might be involved in antioxidant function came to light (Gorecka et al. 2005; Jami et al. 2008; Laohavisit et al. 2009; Chu et al. 2012).

Peroxidase property of annexins was proposed to be on the basis of two different criteria. Firstly, the histidine residue in the N-terminal region of the protein was hypothesized to bind heme and utilize in the electron transfer reactions (Gidrol et al. 1996) and secondly, the putative S₃ cluster in the first domain that is predicted to function as redox-reactive center involved in electron transfer reactions. This cluster was first observed from the crystal structure of cotton (*Gossypium hirsutum*) annexin (Hofmann et al. 2003) and later from that of AnnAt1 in *A. thaliana* (Protein Data Bank no. At1g35720; 1YCN). Neither any experimental evidence nor structural data supports the possibility of heme binding by plant annexins (Konopka-Postupolska et al. 2011); therefore the first speculation looks inconceivable. Despite lacking experimental validation, the second hypothesis looks promising on the ground of three dimensional crystal structures. Of the three sulfur containing residues responsible for S₃ cluster, two cysteine residues are highly conserved among plant annexins nonetheless the methionine residue has deviated rendering the S₃ cluster into an unconserved feature. Experimental evidence showed that these two cysteine residues are neither responsible for intramolecular nor intermolecular disulfide bridges under non-reducing condition in AnnAt1 and remain free for modifications under biological conditions (Konopka-Postupolska et al. 2009, 2011). Moreover, in AnxGh1 they are known to exist in thiol state however the protein was not under reducing condition, since the torsion angles N-C_α-C_β-S of the two residues and the distance between the two sulfur atoms have not made the dithioether linkage feasible as validated by molecular modeling (Hofmann et al. 2003). However, crystallographic data of a human annexin A2 depicts the involvement of these conserved cysteine residues in disulfide bridge formation under oxidizing conditions (Burger et al. 1996).

Redox-sensitive proteins that experience reversible oxidation/reduction depending upon the cellular redox state, translate the ROS signals into appropriate cellular responses (Shao et al. 2005; Foyer et al. 2006). The sensitivity of proteins to oxidation is intervened by the sulfur atoms within methionine or cysteine. The thiol group (-SH) of cysteine is more reactive compared to the thioether group (-CH₂-S-CH₃) of methionine, although both sulfur species are prone to oxidation. Cysteines undergo various kinds of modifications like disulfide bonds, S-glutathionylation, S-nitrosylation, etc. upon oxidation and helps in

maintaining redox balance in biological systems (Guttmann et al. 2010). Therefore, cysteine residues play critical role in maintaining the redox homeostasis along with other biological activities necessary for cell survival.

From our previous reports, *AnnBj3* was found to be transcriptionally up-regulated under various oxidative stresses (Jami et al. 2009). Earlier objectives have evidenced *AnnBj3* with a protective role in oxidative stress response and also showed antioxidant property of the protein. Moreover, amino acid sequence analysis had confirmed the absence of heme-binding histidine residue as well as well the three residues responsible for S_3 cluster (**Fig. 1**). Thus, this investigation addresses the role of cysteine residues in redox homeostasis.

Results and discussion

This work aimed at understanding the role of cysteines present in BjAnn3 in ROS detoxification/redox sensing and/or oligomerization in response to oxidative stress. Amino acid sequence analysis of BjAnn3 has shown the presence of two more cysteines in addition to two conserved Cys residues of S₃ cluster (**Fig. 1**). As cysteines are widely known to be involved in redox buffering therefore, in order to study their role in BjAnn3 we have generated several mutants. We introduced site-directed mutation into the primary amino acid sequence and produced variants as follows: single cysteine variants BjAnn3_{C114S} and BjAnn3_{C129S}, double cysteine variants BjAnn3_{C129S/C226S} and BjAnn3_{C114S/C242S}, triple cysteine variant BjAnn3_{C114S/C226S/C242S} and tetra cysteine variant BjAnn3_{C114S/C129S/C226S/C242S}. Overexpressed N-terminally His₆-tagged BjAnn3_{WT} and variants were purified by Ni-NTA chromatography (**Fig. 18**) and preceded for subsequent experiments.

Redox dependent electrophoretic mobility of the proteins under oxidizing and reducing conditions

Intermolecular thiol-disulfide transitions results in monomerization-oligomerization of the proteins. Similarly, intramolecular thiol-disulfide transitions often results in altered electrophoretic mobilities. This is due to the formation of a more compact structure by intramolecular disulfide bridge formation. On the contrary to all variants, wild type did not exist as monomer under native condition (**Fig. 19**). Except BjAnn3_{C114S/C129S/C226S/C242S}, all other variants existed in dimers or higher forms along with monomers in native condition. BjAnn3_{C114S}, BjAnn3_{C129S} and BjAnn3_{C129S/C226S} showed shift in electrophoretic mobility. This might have happened due to conformational changes in the proteins because of mutation. Under reducing condition, all proteins showed monomerization. However, under oxidizing condition, all mutations have resulted in monomerization while the wild type existed exclusively in higher oligomeric forms. Except BjAnn3_{C114S/C242S}, BjAnn3_{C114S/C226S/C242S} and BjAnn3_{C114S/C129S/C226S/C242S} all other variants also showed dimerization/oligomerization under oxidizing conditions. BjAnn3_{C114S}, BjAnn3_{C129S} and BjAnn3_{C129S/C226S} showed shift in electrophoretic mobility which may be due to the

formation of intramolecular disulfide bridges. These results suggest a direct role of cysteines in redox modulation through intra and inter molecular disulfide bridge formation.

Determination of redox midpoint potential of BjAnn3_{WT} and its variants

Next we studied the role of cysteines in redox sensing or redox-dependent regulation. We determined the redox midpoint potential which describes the conditions under which its thiols are in the reduced form and could function in ROS detoxification or redox sensing. The E_m -value was determined by gel based assay (**Fig. 20**). E_m -value of BjAnn3_{WT} was between -330 mV and -310 mV which is in line with our previous finding by monobromobimane binding assay where it was approximately -319 mV. As described in objective 2, the thiols of BjAnn3_{WT} will be reduced under regular cytoplasmic redox potentials (Meyer et al. 2007) and might react with H₂O₂. With increasing numbers, mutation has resulted in gradual shifting of the E_m -value towards the more positive end. This indicates that loss of cysteines have resulted in loss of the ability of protein to react with H₂O₂ and contribute to redox homeostasis. These results confirm our previous experiment of the role of cysteines in redox sensing and buffering.

Gel filtration chromatographic study of the role of cysteines in oligomerization

To investigate the effect of mutation on the molecular masses of the protein under native condition, all the proteins were chromatographed on a FPLC gel filtration column with Superose-12 10/300 GL matrix (**Fig. 21**). Molecular masses of the variants were smaller than that of the wild type. All the variants showed a single size except BjAnn3_{C114S}, BjAnn3_{C129S/C226S} and BjAnn3_{C114S/C242S} which showed two slightly different sizes. Though the proteins may behave differently in gel and in solution however, these results suggest that cysteines play important role in oligomerization of plant annexins.

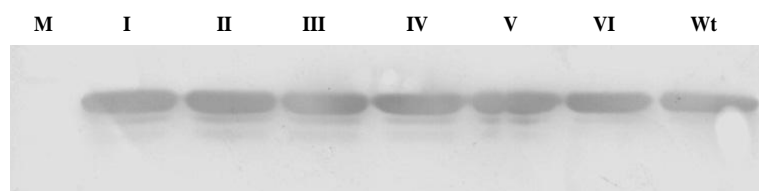


Figure 18 Western blot of recombinant AnnBj3_{WT} protein and its variants. M- Marker; I-BjAnn3_{C114S}; II- BjAnn3_{C129S}; III- BjAnn3_{C129S} and C226S; IV- BjAnn3_{C114S} and C242S; V- BjAnn3_{C114S}, C226S and C242S; VI- BjAnn3_{C114S}, C129S, C226S and C242S; Wt-BjAnn3_{WT}.

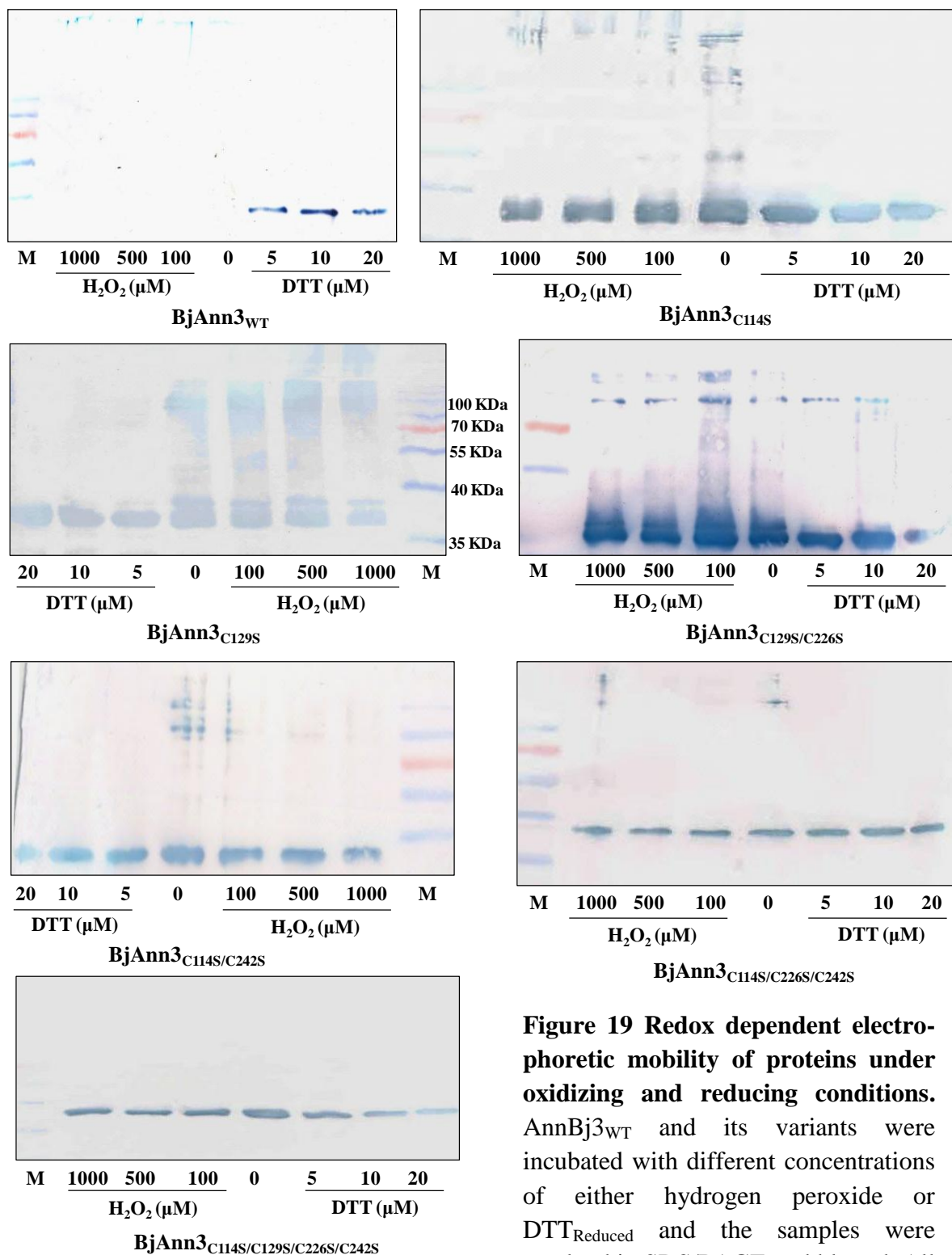


Figure 19 Redox dependent electrophoretic mobility of proteins under oxidizing and reducing conditions. AnnBj3_{WT} and its variants were incubated with different concentrations of either hydrogen peroxide or DTT_{Reduced} and the samples were resolved in SDS/PAGE and blotted. All experiments were repeated at least 3 times.

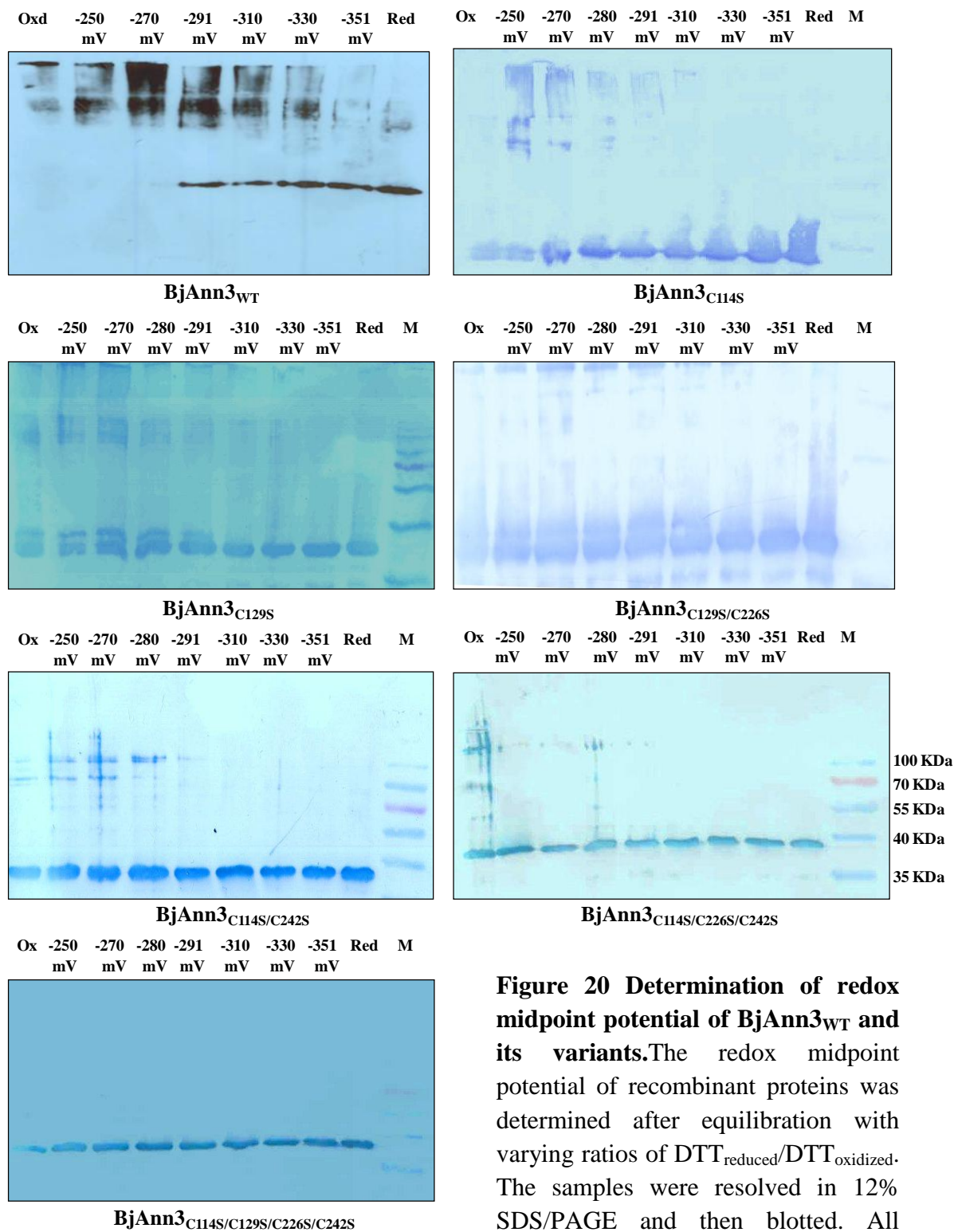


Figure 20 Determination of redox midpoint potential of BjAnn3_{WT} and its variants. The redox midpoint potential of recombinant proteins was determined after equilibration with varying ratios of DTT_{reduced}/DTT_{oxidized}. The samples were resolved in 12% SDS/PAGE and then blotted. All experiments were repeated at least 3 times.

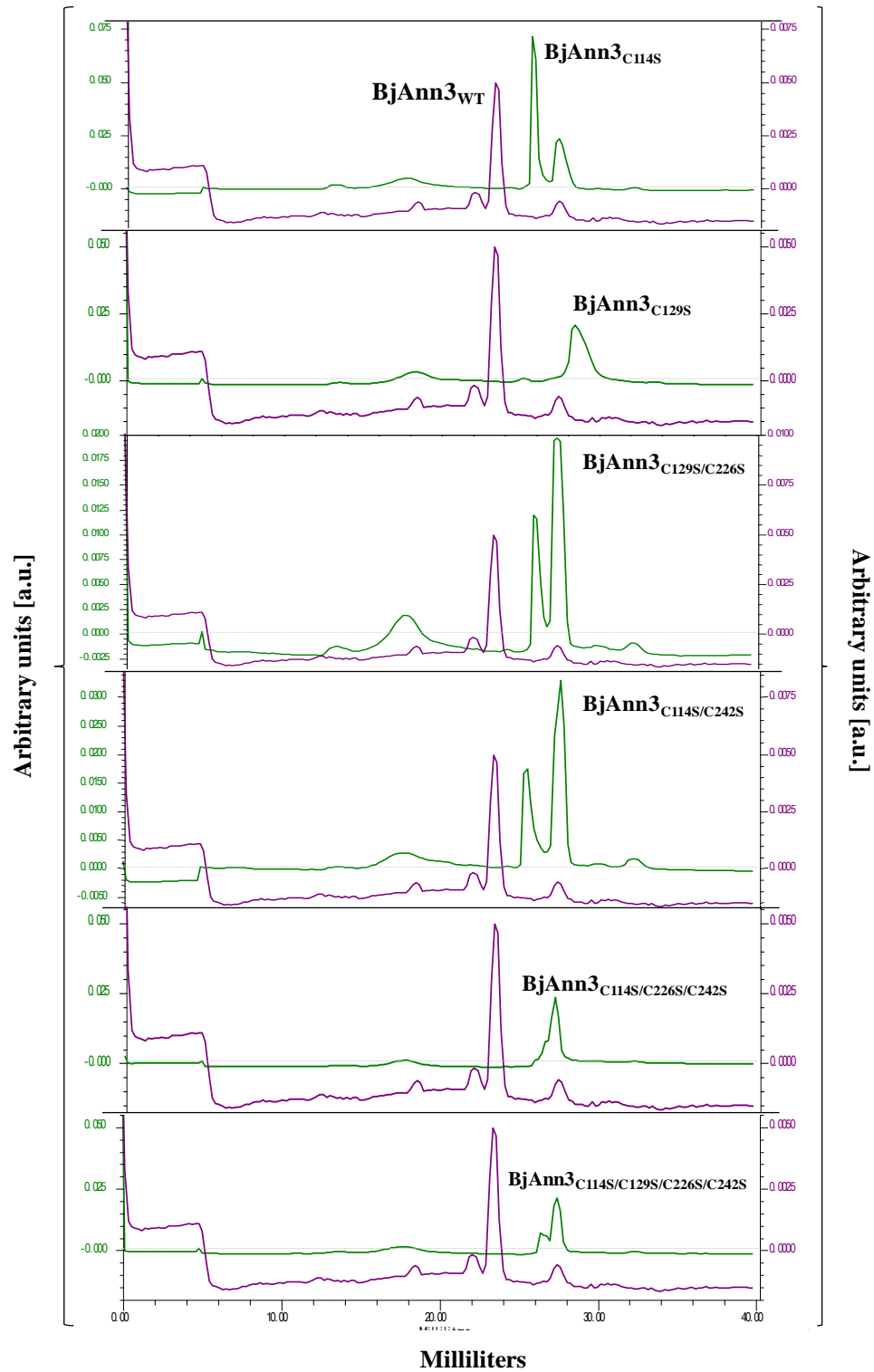


Figure 21 FPLC gel filtration profiles of wild-type and variants on a Superose-12 10/300 GL column. BjAnn3_{WT} profile is compared with that of each variant in each figure. The peaks in each figure are marked with respective protein name. All experiments were repeated at least 3 times.

Conclusion

This report characterizes the role of cysteines in redox modulation and/or oligomerization of BjAnn3 under native and reducing/oxidizing conditions. Loss of Cys residues in BjAnn3 had resulted in altered electrophoretic mobility under oxidizing conditions. This indicates their role in redox modulation by intra and intermolecular disulfide bridge formation in contradiction to earlier reports (Konopka-Postupolska et al. 2009). Cysteine modification (e.g. thiol-disulfide transitions) due to oxidation helps in maintaining redox balance (Guttmann et al. 2010). The role of the cysteine residues in maintaining a negative E_m -value that is in the range of that of the peroxidatic thiol of peroxiredoxins (König et al. 2002) points to their role in BjAnn3-mediated redox buffering.

Summary & Conclusion

Summary and Conclusion

Heterologous expression of plant annexin BjAnn3 protects yeast cells from oxidative stress. Two scenarios are possible: (i) BjAnn3 could either directly detoxify ROS or (ii) positively modulate the endogenous antioxidants and thereby affect ROS accumulation. Expression of BjAnn3 maintained the permeability barrier which could either result from membrane stabilization by binding (Creutz et al. 2012) or from ROS detoxification in a free or membrane-bound state (Mortimer et al. 2009). Again, ROS detoxification may be due to peroxidase activity of BjAnn3 or due to an interaction with native defense system within the cell. The methionine residue is frequently mutated as in BjAnn3, but two cysteine residues of the S₃ cluster remained conserved (Konopka-Postupolska et al. 2009). The absence of both heme-binding histidine residues and S₃ cluster in BjAnn3 might suggest that the conserved Cys residues are involved in ROS detoxification. This hypothesis needs future investigation. Our results indicate that BjAnn3 interferes with other antioxidant genes for ROS modulation. Annexins are also predicted to function as heme-free glutathione peroxidase, a subgroup of peroxiredoxins, using a conserved cysteine to reduce hydroperoxides which act as electron acceptor (Rouhier et al. 2005, Laohavisit et al. 2009 and Dietz 2011). Such a thiol peroxidase activity might be the reason why BjAnn3 complements TSA1-deficient yeast. Their evolutionary significance is well concluded from our results based on their role in transcriptional activation of antioxidant genes and their cross talk with the defense system across kingdom, enabling a cooperative cellular protection.

Overexpressed BjAnn3 alleviates MV-mediated oxidative stress in *Arabidopsis thaliana*. The overexpressing seedlings were more tolerant against MV compared to wild type. BjAnn3 protected photosynthesis against MV-mediated photo-oxidative damage and prevented MV-mediated plasma membrane damage. Three mechanisms may be proposed: (i) BjAnn3 localizes close to the plasma membrane and maintains membrane stability and integrity. This protection may be caused by interaction with lipids, such as direct binding to peroxidized lipids and their decomposition, formation of crystal patches on membranes or membrane resealing (Konopka-Postupolska et al. 2011). (ii) BjAnn3 counteracts ROS accumulation. This may occur either in the free or membrane bound state (Mortimer et al.

2009). BjAnn3 showed a redox potential of approximately -319 mV. This can contribute to the antioxidant property of the protein probably via thiol-based mechanisms. Peroxidase activity confirmed the antioxidant property of the protein. BjAnn3 also resulted in increase of total peroxidase activity in transgenics and showed interference with other cellular antioxidants. BjAnn3 may affect redox buffering at plasma membrane and thereby provide improved cellular protection. (iii) Alternatively BjAnn3 may interfere with cell signaling pathways by molecular interactions involving yet unknown mechanism that may also involve redox reactions (Madureira and Waisman 2013).

Loss of AtAnn3 (a homologue of BjAnn3) has resulted in increased susceptibility of MV-treated knockouts. This necessarily points to the role of AtAnn3 in alleviating MV-mediated oxidative stress in plants. Involvement of AtAnn3 in cellular protection could be direct or indirect. We have shown the role of AtAnn3 in protecting photosynthesis against MV-mediated photo-oxidative damage and preventing MV-mediated plasma membrane damage. This PSII and membrane protection might happen indirectly through cooperation with other cellular antioxidant signaling system. AtAnn3 seems to have a positive role in regulation of most antioxidant transcripts. AtAnn3 showed approximately 95% similarity with BjAnn3 in amino acid level, however, their regulation of antioxidant defense system is very different from each other.

Mutations in the Cys residues of recombinant BjAnn3 had resulted in altered electrophoretic mobility under oxidizing conditions. This indicates their role in redox modulation by intra and intermolecular disulfide bridge formation in contradiction to earlier reports (Konopka-Postupolska et al. 2009). Cysteine modification (e.g. thiol-disulfide transitions) due to oxidation helps in maintaining redox balance (Guttmann et al. 2010). The role of the cysteine residues in maintaining a negative E_m -value that is in the range of that of the peroxidatic thiol of peroxiredoxins (König et al. 2002) points to their role in BjAnn3-mediated redox buffering.

Literature cited

References

- Agrawal GK, Thelen JJ (2006) Large scale identification and quantitative profiling of phosphoproteins expressed during seed filling in oilseed rape. *Mol Cell Proteom* 5:2044–2059.
- Agrimi G, Brambilla L, Frascotti G, Pisano I, Porro D, Vai M, Palmieri L (2011) Deletion or overexpression of mitochondrial NAD⁺ carriers in *Saccharomyces cerevisiae* alters cellular NAD and ATP contents and affects mitochondrial metabolism and the rate of glycolysis. *App Environ Microbiol* 77, 2239–2246.
- Alexandersson E, Saalbach G, Larsson C, Kjellbom P (2004) *Arabidopsis* plasma membrane proteomics identifies components of transport, signal transduction and membrane trafficking. *Plant Cell Physiol* 45:1543–1556.
- Andrew C, Warwicker J, Jones G, Doig A (2002) Effect of phosphorylation on alpha-helix stability as a function of position. *Biochemistry* 41:1897–1905.
- Andrawis A, Solomon M, Delmer DP (1993) Cotton fibre annexins: a potential role in the regulation of callose synthase. *Plant J* 3:763–772.
- Apel K, Hirt H (2004) Reactive oxygen species: Metabolism, oxidative stress, and signal transduction. *Ann Rev Plant Biol* 55:373–399.
- Arisi A-CM, Cornic G, Jouanin L, Foyer CH (1998) Overexpression of iron superoxide dismutase in transformed poplar modifies the regulation of photosynthesis at low CO₂ partial pressures or following exposure to the pro-oxidant herbicide methyl viologen. *Plant Physiol* 117:565–574.
- Asada K (1999) The water-water cycle in chloroplasts: Scavenging of active oxygens and dissipation of excess photons. *Ann Rev Plant Physiol Plant Mol Biol* 50:601–639.
- Babiychuk EB, Monastyrskaya K, Potez S, Draeger A (2009) Intracellular Ca²⁺ operates a switch between repair and lysis of streptolysin O-perforated cells. *Cell Death Different* 16:1126–1134.
- Bai S, Willard B, Chapin LJ, Kinter MT, Francis DM, Stead AD, Jones ML (2010) Proteomic analysis of pollination-induced corolla senescence in petunia. *J Exper Bot* 61:1089–1109.
- Barjaktarović Z, Nordheim A, Lamkemeyer T, Fladerer C, Madlung J, Hampp R (2007) Time-course of changes in amounts of specific proteins upon exposure to hyper-g, 2-D clinorotation, and 3-D random positioning of *Arabidopsis* cell cultures. *J Exper Bot* 58:4357–4363.
- Bassani M, Neumann PM, Gepstein S (2004) Differential expression profiles of growth-related genes in the elongation zone of maize primary roots. *Plant Mol Biol* 56:367–380.

- Baucher M, Lowe YO, Vandeputte OM, Bopopi JM, Moussawi J, Vermeersch M, Pérez-Morga D (2011) *Ntann12* annexin expression is induced by auxin in tobacco roots. *J Exper Bot* 62:4055–4065.
- Bayer EM, Bottrill AR, Walshaw J, Vigouroux M, Naldrett MJ, Thomas CL, Maule AJ (2006) *Arabidopsis* cell wall proteome defined using multidimensional protein identification technology. *Proteomics* 6:301–311.
- Benschop JJ, Mohammed S, O’Flaherty M, Heck AJR, Slijper M, Menke FLH (2007) Quantitative phosphoproteomics of early elicitor signaling in *Arabidopsis*. *Mol Cell Proteom* 6:1198–1214.
- Bindschedler LV, Palmblad M, Cramer R (2008) Hydroponic labeling of entire plants (HILEP) for quantitative plant proteomics; an oxidative stress case study. *Proteomics* 69:1962–1972.
- Bianchi MW, Damerval C, Vartanian N (2002) Identification of proteins regulated by cross-talk between drought and hormone pathways in *Arabidopsis* wild-type and auxin-insensitive mutants, *axr1* and *axr2*. *Funct Plant Biol* 29:55–61.
- Bianco L, Lopez L, Scalone AG, Di Carli M, Desiderio A, Benvenuto E, Perrotta G (2009) Strawberry proteome characterization and its regulation during fruit ripening and in different genotypes. *J Proteom* 72:586–607.
- Björkman O, Demmig B (1987) Photon yield of O₂ evolution and chlorophyll fluorescence characteristics at 77 K among vascular plants of diverse origins. *Planta* 170:489–504.
- Blackbourn HD, Walker JH, Battey NH (1991) Calcium-dependent phospholipid binding proteins in plants. Their characterisation and potential for regulating cell growth. *Planta* 184:67–73.
- Blackbourn HD, Barker PJ, Huskisson NS, Battey NH (1992) Properties and partial protein sequence of plant annexins. *Plant Physiol* 99:864–871.
- Blackbourn HD, Battey NH (1993) The control of exocytosis in plant cells. *New Phytol* 125:307–338.
- Boustead C, Smallwood M, Small H, Bowles D, Walker JH (1989) Identification of Ca²⁺-dependent phospholipid-binding proteins in higher plant cells. *FEBS Lett* 244:456–460.
- Bowler C, Slooten L, Vandenbranden S, De Rycke R, Botterman J, Sybesma C, Montagu MV, Inzé D (1991) Manganese superoxide dismutase can reduce cellular damage mediated by oxygen radicals in transgenic plants. *EMBO J* 10:1723–1732.
- Boyer JS (1982) Plant productivity and environment. *Science* 218:443–448.

- Breton G, Vazquez-Tello A, Danyluk J, Sarhan F (2000) Two novel intrinsic annexins accumulate in wheat membranes in response to low temperature. *Plant Cell Physiol* 41:177–184.
- Buitink J, Leger JJ, Guisle I, Vu BL, Wuillème S, Lamirault G, Le Bars A, Le MN, Becker A, Leger KH, Guisle JJ, et al. (2006) Transcriptome profiling uncovers metabolic and regulatory processes occurring during the transition from desiccation-sensitive to desiccation-tolerant stages in *Medicago truncatula* seeds. *Plant J* 47:735–750.
- Burger A, Berendes R, Liemann S, Benz J, Hofmann A, Göttig P, Huber R, Gerke V, Thiel C, Römisch J, Weber K (1996) The crystal structure and ion channel activity of human annexin II, a peripheral membrane protein. *J Mol Biol* 257:839–847.
- Cantero A, S. Barthakur TJ, Bushart S, Chou RO, Morgan MP, Fernandez GB, Clark SJ, Roux (2006) Expression profiling of the *Arabidopsis* annexin gene family during germination, de-etiolation and abiotic stress. *Plant Physiol Biochem* 44:13–24.
- Camp W, Van K, Capiou M, Montagu V, Inze D, Slooten L (1996) Enhancement of oxidative stress tolerance in transgenic tobacco plants overproducing Fe-superoxide dismutase in chloroplasts. *Plant Physiol* 112:1703–1714.
- Calvert CM, Gant SJ, Bowles DJ (1996) Tomato annexins p34 and p35 bind to F-actin and display nucleotide phosphodiesterase activity inhibited by phospholipid binding. *Plant Cell* 8:333–342.
- Carletti P, Masi A, Spolaore B, De Laureto PP, De Zorzi M, Turetta L, Ferretti M, Nardi S (2008) Protein expression changes in maize roots in response to humic substances. *J Chem Ecol* 34:804–818.
- Carroll AD, Moyon C, Van Kesteren P, Tooke F, Battey NH, Brownlee C (1998) Ca^{2+} , annexins, and GTP modulate exocytosis from maize root cap protoplasts. *Plant Cell* 10:1267–1276.
- Chandran D, Inada N, Hather G, Kleindt CK, Wildermuth MC (2010) Laser microdissection of *Arabidopsis* cells at the powdery mildew infection site reveals site-specific processes and regulators. *PNAS, USA* 107:460–465.
- Chapin FS (1991) Effects of multiple environmental stresses on nutrient availability and use. Mooney HA, Winner WE, Pell EJ (Eds). *Response of plants to multiple stresses*. San Diego, Academic Press, pp 67–88.
- Choi HW, Kim YJ, Lee SC, Hong JK, Hwang BK (2007) Hydrogen peroxide generation by the pepper extracellular peroxidase CaPO₂ activates local and systemic cell death and defense response to bacterial pathogens. *Plant Physiol* 145:890–904.

- Chu P, Chen H, Zhou Y, Li Y, Ding Y, Jiang L, Tsang ET, Wu K, Huang S (2012) Proteomic and functional analyses of *Nelumbo nucifera* annexins involved in seed thermotolerance and germination vigor. *Planta* 235:1271–1288.
- Clamp M, Cuff J, Searle SM, Barton GJ (2004) The Jalview Java Alignment Editor. *Bioinformatics* 20:426–427.
- Clark GB, Cantero-Gracia A, Butterfield T, Dauwalder M, Roux SJ (2005a) Secretion as a key component of gravitropic growth: implications for annexin involvement in differential growth. *Gravit Space Biol* 18:113–114.
- Clark GB, Dauwalder M, Roux SJ (1998) Immunological and biochemical evidence for nuclear localization of annexin in peas. *Plant Physiol Biochem* 36:621–627.
- Clark GB, Konopka-Postupolska D, Hennig J, Roux S (2010) Is annexin 1 a multifunctional protein during stress responses? *Plant Signal Behav* 5:303–307.
- Clark GB, Lee DW, Dauwalder M, Roux SJ (2005b) Immunolocalization and histochemical evidence for the association of two different *Arabidopsis* annexins with secretion during early seedling growth and development. *Planta* 220:621–631.
- Clark GB, Morgan RO, Fernandez M-P, Roux SJ (2012) Evolutionary adaptation of plant annexins has diversified their molecular structures, interactions and functional roles, *New Phytol* 196:695–712.
- Clark GB, Rafati DS, Bolton RJ, Dauwalder M, Roux SJ (2000) Redistribution of annexin in gravi-stimulated pea plumules. *Plant Physiol Biochem* 38:937–947.
- Clark GB, Sessions A, Eastburn DJ, Roux SJ (2001) Differential expression of members of the *Annexin* multigene family in *Arabidopsis*. *Plant Physiol* 126:1072–1084.
- Clark GB, Turnwald S, Tirlapur UK, von der Mark K, Roux SJ, Scheuerlein R (1995) Induction and polar distribution of annexin-like proteins during phytochrome-mediated rhizoid initiation and growth in spores of the ferns *Dryopteris* and *Anemia*. *Planta* 197:376–384
- Clarke B, Liang R, Morell MK, Bird AR, Jenkins CLD, Li Z. 2008. Gene expression in a starch *Ila* mutant of barley: changes in the level of gene transcription and grain composition. *Functional and Integrative Genomics* 8: 211–221.
- Clough SJ, Bent AF (1998) Floral dip: a simplified method for *Agrobacterium*-mediated transformation of *Arabidopsis thaliana*. *Plant J* 16:735–743.
- Cramer GR, Urano K, Delrot S, Pezzotti M, Shinozaki K (2011) Effects of abiotic stress on plants: a systems biology perspective. *BMC Plant Biol* 11:163.
- Creutz CE, Hira JK, Gee VE, Eaton JM (2012) Protection of the membrane permeability barrier by annexins. *Biochemistry* 51:9966–9983.

- Dabitz N, Hu N-J, Yusof AM, Tranter N, Winter A, Daley M, Zschörnig O, Brisson A, Hofmann A (2005) Structural determinants for plant annexin-membrane interactions. *Biochemistry* 44:16292–16300.
- Dai S, Lei L, Chen T, Chong K, Xue Y, Wang T (2006) Proteomic analyses of *Oryza sativa* mature pollen reveal novel proteins associated with pollen germination and tube growth. *Proteomics* 6:2504–2529.
- de Carvalho-Niebel F, Lescure N, Cullimore JV, Gamas P (1998) The *Medicago truncatula* *MtAnn1* gene encoding an annexin is induced by nod factors and during the symbiotic interaction with *Rhizobium meliloti*. *Mol Plant Microbe Inter* 11:504–513.
- de Carvalho-Niebel F, Timmers ACJ, Chabaud M, Defaux-Petras A, Barker DG (2002) The Nod factor-elicited annexin MtAnn1 is preferentially localized at the nuclear periphery in symbiotically activated root tissues of *Medicago truncatula*. *Plant J* 32:343–352.
- del Río LA, Sandalio LM, Corpas FJ, Palma JM, Barroso JB (2006) Reactive oxygen species and reactive nitrogen species in peroxisomes. Production, scavenging, and role in cell signaling. *Plant Physiol* 141:330–335.
- Delmer DP, Potikha TS (1997) Structures and functions of annexins in plants. *Cell Mol Life Sci* 53:546–553
- Demasi APD, Pereira GAG, Netto LES (2001) Cytosolic thioredoxin peroxidase I is essential for the antioxidant defense of yeast with dysfunctional mitochondria. *FEBS Letters* 509:430–434.
- Demasi APD, Pereira GAG, Netto LES (2006) Yeast oxidative stress response. Influences of cytosolic thioredoxin peroxidase I and of the mitochondrial functional state. *FEBS J* 273:805–816.
- Dietz KJ (2011) Peroxiredoxins in plants and *Cyanobacteria*. *Antioxid Redox Signal* 15: 1129–1159.
- Divya K, Jami SK, Kirti PB (2010) Constitutive expression of mustard annexin, *AnnBj1* enhances abiotic stress tolerance and fiber quality in cotton under stress. *Plant Mol Biol* 73:293–308.
- Doyle J, Doyle J (1990) Isolation of plant DNA from fresh tissue. *Focus* 12:13–15.
- Faurobert M, Mihr C, Bertin N, Pawlowski T, Negroni L, Sommerer N, Causse M (2007) Major proteome variations associated with cherry tomato pericarp development and ripening. *Plant Physiol* 143:1327–1346.
- Feng YM, Wei XK, Liao WX, Huang LH, Zhang H, Liang SC, Peng H (2013) Molecular analysis of the annexin gene family in soybean. *Biol Planta* 1–8.

- Fischer T, Lu L, Haigler HT, Langen R (2007) Annexin B12 is a sensor of membrane curvature and undergoes major curvature-dependent structural changes. *J Biol Chem* 282:9996–10004.
- Foyer, Christine H, Trebst A, Noctor G (2006) Signaling and integration of defense functions of tocopherol, ascorbate and glutathione. Photoprotection, photoinhibition, gene regulation and environment. Springer Netherlands, pp 241–268.
- Franklin-Tong VE, Gourlay CW (2008) A role for actin in regulating apoptosis/programmed cell death: evidence spanning yeast, plants and animals. *Biochem J* 413:389–404.
- Fridovich I (1995) Superoxide radical and superoxide dismutases. *Annu Rev Biochem* 64:97–112.
- Friso G, Giacomelli L, Ytterberg AJ, Peltier J-B, Rudella A, Sun Q, Van Wijk KJ (2004) In-depth analysis of the thylakoid membrane proteome of *Arabidopsis thaliana* chloroplasts: new proteins, new functions, and a plastid proteome database. *Plant Cell* 16:478–499.
- Fujibe T, Saji H, Arakawa K, Yabe N, Takeuchi Y, Yamamoto KT (2004) A methyl viologen-resistant mutant of *Arabidopsis*, which is allelic to ozone-sensitive *rcd1*, is tolerant to supplemental ultraviolet-B irradiation. *Plant Physiol* 134:275–285.
- Fukao Y, Hayashi M, Hara-Nishimura I, Nishimura M (2003) Novel glyoxysomal protein kinase, GPK1, identified by proteomic analysis of glyoxysomes in etiolated cotyledons of *Arabidopsis thaliana*. *Plant Cell Physiol* 44:1002–1012.
- Gallardo K, Le Signor C, Vandekerckhove J, Thompson RD, Burstin J (2003) Proteomics of *Medicago truncatula* seed development establishes the time frame of diverse metabolic processes related to reserve accumulation. *Plant Physiol* 133:664–682.
- Garrido EO, Grant CM (2002) Role of thioredoxins in the response of *Saccharomyces cerevisiae* to oxidative stress induced by hydroperoxides. *Mol Microbiol* 43:993–1003.
- Gay C, Collins J, Gebicki JM (1999) Hydroperoxide assay with the ferric-xylenol orange complex. *Analy Biochem* 273:149–155.
- Gerke V, Moss SE (2002) Annexins: from structure to function. *Physiol Rev* 82:331–71.
- Gerke V, Creutz CE, Moss SE (2005) Annexins: linking Ca^{2+} signalling to membrane dynamics. *Nature Rev Mol Cell Biol* 6:449–461.
- Gidrol X, Sabelli PA, Fern YS, Kush AK (1996) Annexin-like protein from *Arabidopsis thaliana* rescues delta *oxyR* mutant of *Escherichia coli* from H_2O_2 stress. *PNAS, USA* 93:11268–11273.
- Godbold DL (1998) Stress concepts and forest trees. *Chemosphere* 36:859–864.

- Gorantla M, Babu PR, Lachagari VBR, Feltus FA, Paterson AH, Reddy AR (2005) Functional genomics of drought-stress response in rice: transcript mapping of annotated unigenes of an indica rice (*Oryza sativa* L. cv. Nagina 22). *Curr Sci* 89: 496–514.
- Gorecka KM, Thouverey C, Buchet R, Pikula S (2007) Potential role of annexin AtANN1 from *Arabidopsis thaliana* in pH-mediated cellular response to environment stimuli. *Plant Cell Physiol* 48:792–803.
- Gorecka KM, Konopka-Postupolska D, Hennig J, Buchet R, Pikula S (2005) Peroxidase activity of annexin 1 from *Arabidopsis thaliana*. *Biochem Biophys Res Comm* 336: 868–875.
- Göring H (1982) Reaktionen der Pflanzen auf extreme physikalische und chemische Umweltbedingungen. *Umwelt Stress. Wiss. Beitr. Martin-Luther-Univ.*, 35, 17. Halle, Wittenberg, pp 152–160.
- Grime JP (1993) Stress, competition, resource dynamics and vegetation processes. In: Fowden L, Mansfield T, Stoddart J (Eds). *Plant adaptation to environmental stress*. London, Chapman and Hall, pp 45–65.
- Gupta AS, Heinen JL, Holaday AS, Burke JJ, Allen RD (1993) Increased resistance to oxidative stress in transgenic plants that overexpress chloroplastic Cu/Zn superoxide dismutase. *PNAS, USA* 90:1629–1633.
- Guttmann RP (2010) Redox regulation of cysteine-dependent enzymes. *J Animal Sci* 88:1297–1306.
- Hashimoto M, Toorchi M, Matsushita K, Iwasaki Y, Komatsu S (2009) Proteome analysis of rice root plasma membrane and detection of cold stress responsive proteins. *Protein Pept Lett* 16:685–697.
- Heath RL, Packer L (1968) Phytoperoxidation in isolated chloroplast. Kinetics and stoichiometry of fatty acid peroxidation. *Arch Biochem Biophys* 125:189–198.
- Hirasawa M, Schürmann P, Jacquot J-P, Manieri W, Jacquot P, Keryer E, Hartman FC, Knaff DB (1999) Oxidation-reduction properties of chloroplast thioredoxins, ferredoxin: thioredoxin reductase, and thioredoxin f-regulated enzymes. *Biochem* 38:5200–5205.
- Hofmann A (2004) Annexins in the plant kingdom: perspectives and potentials. *Annexins* 1:51–61.
- Hofmann A, Benz J, Liemann S, Huber R (1997) Voltage-dependent binding of annexin V, annexin VI and annexin VII-Core to acidic phospholipid membranes. *Biochim et Biophys Acta* 1330:254–264.

- Hofmann A, Delmer DP, Wlodawer A (2003) The crystal structure of annexin *Gh1* from *Gossypium hirsutum* reveals an unusual S₃ cluster. *Europ J Biochem* 270:2557–2564.
- Hofmann A, Ruvinov S, Hess S, Schantz R, Delmer DP, Wlodawer A (2002) Plant annexins form calcium-independent oligomers in solution. *Protein Sci* 11:2033–2040.
- Hoshino D, Hayashi A, Temmei Y, Kanzawa N, Tsuchiya T (2004) Biochemical and immunohistochemical characterization of *Mimosa* annexin. *Planta* 219:867–875.
- Hoshino T, Mizutani A, Chida M, Hidaka H, Mizutani J (1995) Plant annexins form homodimer during Ca²⁺-dependent liposome aggregation. *Biochem Mol Biol Intern* 35:749–755.
- Hu N-J, Yusof AM, Winter A, Osman A, Reeve AK, Hofmann A (2008) The crystal structure of calcium-bound annexin Gh1 from *Gossypium hirsutum* and its implications for membrane binding mechanisms of plant annexins. *J Biol Chem* 283:18314–18322.
- Hu SQ, Brady SR, Kovar DR, Staiger CJ, Clark GB, Roux SJ, Muday GK (2000) Identification of plant actin-binding proteins by F-actin affinity chromatography. *Plant J* 24:127–137.
- Huang Y, Wang J, Zhang L, Zuo K (2013) A cotton annexin protein AnxGb6 regulates fiber elongation through its interaction with actin 1. *PLoS One* 8:e66160.
- Huh SM, EK, Noh HG, Kim BW, Jeon K, Bae H-C, Hu JM, Kwak OK, Park (2010) *Arabidopsis* Annexins AnnAt1 and AnnAt4 interact with each other and regulate drought and salt stress responses. *Plant Cell Physiol* 51:1499–1514.
- Ito J, Heazlewood JL, Millar AH (2006) Analysis of the soluble ATP binding proteome of plant mitochondria identifies new proteins and nucleotide triphosphate interactions within the matrix. *J Proteome Res* 5:3459–3469.
- Jacob S, Dietz KJ (2009) Systematic analysis of superoxide-dependent signaling in plant cells. Usefulness and specificity of methyl viologen application. In: Hirt H (Eds). *Plant stress biology: from genomics to systems biology*, Wiley VCH, Weinheim, pp. 179–196.
- Jänicke RU, Porter AG, Kush A (1998) A novel *Arabidopsis thaliana* protein protects tumor cells from tumor necrosis factor-induced apoptosis. *BBA- Mol Cell Res* 1402:70–78.
- Jami SK, Clark GB, Turlapati SA, Handley C, Roux SJ, Kirti PB (2008) Ectopic expression of an annexin from *Brassica juncea* confers tolerance to abiotic and biotic stress treatments in transgenic tobacco. *Plant Physiol Biochem* 46:1019–1030.
- Jami SK, Dalal A, Divya K, Kirti PB (2009) Molecular cloning and characterization of five annexin genes from Indian mustard (*Brassica juncea* L. Czern and Coss). *Plant Physiol Biochem* 47:977–990.

- Jami S, Clark G, Ayele B, Roux S, Kirti PB (2012) Identification and characterization of annexin gene family in rice. *Plant Cell Rep* 31:813–825.
- Jami SK, Hill RD, Kirti PB (2010) Transcriptional regulation of annexins in Indian mustard, *Brassica juncea* and detoxification of ROS in transgenic tobacco plants constitutively expressing *AnnBj1*. *Plant Signal Behav* 5:618–621.
- Jaspers P, Kangasjärvi J (2010) Reactive oxygen species in abiotic stress signaling. *Physiol Planta* 138:405–413.
- Johnson GN, Young AJ, Scholes JD, Horton P (1993) The dissipation of excess excitation energy in British plant species. *Plant Cell Environ* 16:673–679.
- Kamada M, Higashitani A, Ishioka N (2005) Proteomic analysis of *Arabidopsis* root gravitropism. *Biol Sci Space* 19:148–154.
- Katori T, Ikeda A, Iuchi S, Kobayashi M, Shinozaki K, Maehasji KJ, Sakata Y, Tanaka S, Taji T (2010) Dissecting the genetic control of natural variation in salt tolerance of *Arabidopsis thaliana* accessions. *J Exper Bot* 65:1125–1138.
- Kiba T, Naitou T, Koizumi N, Yamashino T, Sakakibara H, Mizuno T (2005) Combinatorial microarray analysis revealing *Arabidopsis* genes implicated in cytokinin responses through the His->Asp phosphorelay circuitry. *Plant Cell Physiol* 46:339–355.
- Klein P, Seidel T, Stöcker B, Dietz K-J (2012) The membrane-tethered transcription factor ANAC089 serves as redox-dependent suppressor of stromal ascorbate peroxidase (sAPX) gene expression. *Frontiers Plant Sci* 3.
- König J, Baier M, Horling F, Kahmann U, Harris G, Schürmann P, Dietz K-J (2002) The plant-specific function of 2-Cys peroxiredoxin-mediated detoxification of peroxides in the redox-hierarchy of photosynthetic electron flux. *PNAS, USA* 99:5738–5743.
- Konopka-Postupolska D (2007) Annexins: putative linkers in dynamic membrane–cytoskeleton interactions in plant cells. *Protoplasma* 230:203–215.
- Konopka-Postupolska D, Clark G, Goch G, Debski J, Floras K, Cantero A, Fijolek B, Roux S, Hennig J (2009) The role of Annexin 1 in drought stress in *Arabidopsis*. *Plant Physiol* 150:1394–1410.
- Konopka-Postupolska D, Clark G, Hofmann A (2011) Structure, function and membrane interactions of plant annexins: An update. *Plant Sci* 181:230–241.
- Kovács I, Ayaydin F, Oberschall A, Ipacs I, Bottka S, Pongor S, Dudits D, Tóth ÉC (1998) Immunolocalization of a novel annexin-like protein encoded by a stress and abscisic acid responsive gene in alfalfa. *Plant J* 15:185–197.
- Kung C-CS, Huang W-N, Huang Y-C, Yeh K-C (2006) Proteomic survey of copper-binding proteins in *Arabidopsis* roots by immobilized metal affinity chromatography and mass spectrometry. *Proteomics* 6:2746–2758.

- Kush A, Sabapathy K (2001) Oxy5, a novel protein from *Arabidopsis thaliana*, protects mammalian cells from oxidative stress. *Inter J Biochem Cell Biol* 33:591–602.
- Kwon H-K, Yokoyama R, Nishitani K (2005) A proteomic approach to apoplastic proteins involved in cell wall regeneration in protoplasts of *Arabidopsis* suspension-cultured cells. *Plant Cell Physiol* 46:843–857.
- Laohavisit A, Brown AT, Cicuta P, Davies JM (2010) Annexins- components of the calcium and reactive oxygen signaling network. *Plant Physiol* 152:1824–1829.
- Laohavisit A, Davies JM (2011) Annexins. *New Phytol* 189:40–53.
- Laohavisit A, Mortimer JC, Demidchik V, Coxon KM, Stancombe MA, Macpherson N, Brownlee C, Hofmann A, Webb AAR, Miedema H, Battey NH, Davies JM (2009) *Zea mays* Annexins modulate cytosolic free Ca^{2+} and generate a Ca^{2+} -permeable conductance. *Plant Cell Online* 21:479–493.
- Laohavisit A, Shang Z, Rubio L, Cuin TA, Véry A-A, Wang A, Mortimer JC, Macpherson N, Coxon KM, Battey NH, Brownlee C, Park OK, Sentenac H, Shabala S, Webb AAR, Davies JM (2012) *Arabidopsis* Annexin1 mediates the radical-activated plasma membrane Ca^{2+} - and K^{+} -permeable conductance in root cells. *Plant Cell Online* 24:1522–1533.
- Larcher W (1980) *Physiological plant ecology*. New York, Springer-Verlag.
- Larkin MA, et al. (2007) Clustal W and clustal X version 2.0. *Bioinformatics* 23:2947–2948.
- Lascano HR, Gomez LD, Casano LM, Trippi VS (1998) Changes in glutathione reductase activity and protein content in wheat leaves and chlloplasts exposed to photooxidative stress. *Plant Physiol Biochem* 36:321–329.
- Lascano HR, Antonicelli GE, Luna CM, Melchiorre MN, Racca RW, Trippi VS, Casano LM (2001) Antioxidant system response of different wheat cultivars under drought: field and *in vitro* studies. *Funct Plant Biol* 28:1095–1102.
- Lascano HR, Melchiome MN, Luna CM, Trippi VS (2003) Effect of photooxidative stress induced by paraquat in two wheat cutivars with differential tolerance to water stress, *Plant Sci* 164:841–846.
- Laskar S, Bhattacharyya MK, Shankar R, Bhattacharyya S (2011) *HSP90* controls *SIR2* mediated gene silencing. *PLoS One* 6:e23406.
- Laxa M, König J, Dietz KJ, Kandlbinder A (2007) Role of the cysteine residues in *Arabidopsis thaliana* cyclophilin CYP20-3 in peptidyl-prolyl *cis-trans* isomerase and redox-related functions. *Biochem J* 401:287–97.
- Lee J, He K, Stolz V, Lee H, Figueroa P, Gao Y, Tongprasit W, Zhao H, Lee I, Deng XW (2007) Analysis of transcription factor HY5 genomic binding sites revealed its hierarchical role in light regulation of development. *Plant Cell* 19:731–749.

- Lee KH, Kim Y-S, Park C-M, Kim H-J (2008) Proteomic identification of differentially expressed proteins in *Arabidopsis* mutant *ntm1-D* with disturbed cell division. *Mol Cells* 25:70–77.
- Lee S, Lee EJ, Yang EJ, Lee JE, Park AR, Song WH, Park OK (2004) Proteomic identification of annexins, calcium-dependent membrane binding proteins that mediate osmotic stress and abscisic acid signal transduction in *Arabidopsis*. *Plant Cell Online* 16:1378–1391.
- Lefebvre B, Furt F, Hartmann M-A, Michaelson LV, Carde J-P, Sargueil-Boiron F, Rossignol M, Napier JA, Cullimore J, Bessoule J-J, Mongrand S (2007) Characterization of lipid rafts from *Medicago truncatula* root plasma membranes: a proteomic study reveals the presence of a raft-associated redox system. *Plant Physiol* 144:402–418.
- Levin EJ, Kondrashov DA, Wesenberg GE, Phillips GN (2007) Ensemble refinement of protein crystal structures: validation and application. *Structure* 15:1040–1052.
- Levitt J (1980) Responses of plant to environmental stress. Vol. 1. New York, Academic Press.
- Levitt J (1982) Stress terminology. In: Turner NC, Kramer PJ (Eds). Adaptation of plants to water and high temperature stress. New York, Wiley-Interscience, pp 437–439.
- Li B, Li DD, Zhang J, Xia H, Wang XL, Li Y, Li XB (2013) Cotton AnnGh3 encoding an annexin protein is preferentially expressed in fibers and promotes initiation and elongation of leaf trichomes in transgenic *Arabidopsis*. *J Integrat Plant Biol*.doi: 10.1111/jipb.12063.
- Li BQ, Tian SP (2006) Effects of trehalose on stress tolerance and biocontrol efficacy of *Cryptococcus laurentii*. *J App Microbiol* 100:854–861.
- Liemann S, Benz J, Burger A, Voges D, Hofmann A, Huber R, Göttig P (1996) Structural and functional characterisation of the voltage sensor in the ion channel human annexin V. *J Mol Biol* 258:555–561.
- Lim EK, Roberts MR, Bowles DJ (1998) Biochemical characterization of tomato annexin p35-independence of calcium binding and phosphatase activities. *J Biol Chem* 273: 34920–34925.
- Lin Y, Seals DF, Randall SK, Yang Z (2001) Dynamic localization of Rop *GTPase* to the tonoplast during vacuolar development. *Plant Physiol* 125:241–251.
- Lindermayr C, Saalbach G, Durner J (2005) Proteomic identification of δ -nitrosylated proteins in *Arabidopsis*. *Plant Physiol* 137:921–930.

- Lu Y, Ouyang B, Zhang J, Wang T, Lu C, Han Q, Zhao S, Ye Z, Li H (2012) Genomic organization, phylogenetic comparison and expression profiles of annexin gene family in tomato (*Solanum lycopersicum*). *Gene* 499:14–24.
- Madureira PA, Hill R, Miller VA, Giacomantonio C, Lee PWK, Waisman DM (2011) Annexin A2 is a novel cellular redox regulatory protein involved in tumorigenesis. *Oncotarget* 2:1075–1093.
- Madureira P, Waisman D (2013) Annexin A2: the importance of being redox sensitive. *Inter J Mol Sci* 14:3568–3594.
- Maffey KG, Keil LB, DeBari VA (2001). The influence of lipid composition and divalent cations on annexin V binding to phospholipid mixtures. *Annals Clinical Lab Sci* 31: 85–90.
- Marathe R, Guan Z, Anandalakshmi R, Zhao H, Dinesh-Kumar SP (2004) Study of *Arabidopsis thaliana* in response to cucumber mosaic virus infection using whole genome microarray. *Plant Mol Biol* 55: 501–520.
- Marmagne A, Ferro M, Meinel T, Bruley C, Kuhn L, Garin J, Barbier- Brygoo H, Ephritikhine G (2007) A high content in lipid-modified peripheral proteins and integral receptor kinases features in the *Arabidopsis* plasma membrane proteome. *Mol Cellul Proteom* 6:1980–1996.
- Mc Clung AD, Carroll AD, Battey NH (1994) Identification and characterization of ATPase activity associated with maize (*Zea mays*) annexins. *Biochem J* 303:709–712.
- Meijer HJG, van de Vondervoot PJI, Yin QY, de Koster CG, Klis FM, Govers F, de Groot PWJ (2006) Identification of cell wall-associated proteins from *Phytophthora ramorum*. *Mol Plant Microbe Inter* 18:1348–1358.
- Megli FM, Russo L, Sabatini K (2005) Oxidized phospholipids induce phase separation in lipid vesicles. *FEBS Lett* 579:4577–4584.
- Megli FM, Sabatini K (2003) EPR studies of phospholipid bilayers after lipoperoxidation: 1. inner molecular order and fluidity gradient. *Chem Physics Lipids* 125:161–172.
- Meyer AJ, Brach T, Marty L, Kreye S, Rouhier N, Jacquot J-P, Hell R (2007) Redox-sensitive GFP in *Arabidopsis thaliana* is a quantitative biosensor for the redox potential of the cellular glutathione redox buffer. *Plant J* 52:973–986.
- Mikosch M, Homann U (2009) How do ER export motifs work on ion channel trafficking? *Curr Opinion Plant Biol* 12:685–689.
- Miller GAD, Suzuki N, Ciftci-Yilmaz S, ULTAN, Mittler RON (2010) Reactive oxygen species homeostasis and signaling during drought and salinity stresses. *Plant Cell Environ* 33:453–467.

- Mittler R (2002) Oxidative stress, antioxidants and stress tolerance. *Trends Plant Sci* 7:405–410.
- Morano KA, Grant CM, Moye-Rowley WS (2012) The response to heat shock and oxidative stress in *Saccharomyces cerevisiae*. *Genetics* 190:1157–1195.
- Morgan RO, Fernandez MP (1997) Annexin gene structures and molecular evolutionary genetics. *Cellu Mol Life Sci* 53:508–515.
- Morgan RO, Martin-Almedina S, Garcia M, Jhoncon-Kooyip J, Fernandez MP (2006) Deciphering function and mechanism of calcium-binding proteins from their evolutionary imprints. *Biochim et Biophys Acta* 1763:1238–1249.
- Mortimer JC, Coxon KM, Laohavisit A, Davies JM (2009) Heme independent soluble and membrane-associated peroxidase activity of a *Zea mays* annexin preparation. *Plant Signal Behav* 4:428–430.
- Mortimer JC, Laohavisit A, Macpherson N, Webb A, Brownlee C, Battey NH, Davies JM (2008) Annexins: multifunctional components of growth and adaptation, *J Exper Bot* 59:533–544.
- Müller R, Morant M, Jarmer H, Nilsson L, Nielsen TH (2007) Genome wide analysis of the *Arabidopsis* leaf transcriptome reveals interaction of phosphate and sugar metabolism. *Plant Physiol* 143:156–171.
- Myouga F, Hosoda C, Umezawa T, Iizumi H, Kuromori T, Motohashi R, Shono Y, Nagata N, Ikeuchi M, Shinozaki K (2008) A heterocomplex of iron superoxide dismutases defends chloroplast nucleoids against oxidative stress and is essential for chloroplast development in *Arabidopsis*. *Plant Cell Online* 20:3148–3162.
- Nilsen ET, Orcutt DM (1996) The physiology of plants under stress: abiotic factors. New York, John Wiley & Sons. 689 pp.
- Oelze M-L, Vogel MO, Alsharafa K, Kahmann U, Viehhauser A, Maurino VG, Dietz K-J (2012) Efficient acclimation of the chloroplast antioxidant defence of *Arabidopsis thaliana* leaves in response to a 10- or 100-fold light increment and the possible involvement of retrograde signals. *J Exper Bot* 63:1297–1313.
- Pabla R, Pawar V, Zhang H, Siede W (2006) Characterization of checkpoint responses to DNA damage in *Saccharomyces cerevisiae*: basic protocols. *Methods Enzymol* 409:101–117.
- Park SG, Cha M-K, Jeong W, Kim I-H (2000) Distinct physiological functions of thiol peroxidase isoenzymes in *Saccharomyces cerevisiae*. *J Biol Chem* 275:5723–5732.
- Pfannschmidt T, Ogrzewalla K, Baginsky S, Sickmann A, Meyer HE, Link G (2000) The multisubunit chloroplast RNA polymerase A from mustard (*Sinapsis alba* L.).

- Integration of a prokaryotic core into a larger complex with organelle-specific functions. *Eur J Biochem* 267:253–264.
- Proust J, Houlne G, Schantz M-L, Schantz R (1996) Characterization and gene expression of an annexin during fruit development in *Capsicum annum*. *FEBS Lett* 383:208–212.
- Proust J, Houlne G, Schantz ML, Shen WH, Schantz R (1999) Regulation of biosynthesis and cellular localization of Sp32 annexins in tobacco BY2 cells. *Plant Mol Biol* 39:361–372.
- Punwani JA, Rabiger DS, Drews GN (2007) MYB98 positively regulates a battery of synergid-expressed genes encoding filiform apparatus localized proteins. *Plant Cell* 19:2557–2568.
- Raynal P, Pollard HB (1994) Annexins: the problem of assessing the biological role for a gene family of multifunctional Ca^{2+} and phospholipid-binding proteins. *Biochim Biophys Acta* 1197:63–93.
- Renault J, Hausman J-F, Weisniewski ME (2006) Proteomics and low temperature studies: bridging the gap between gene expression and metabolism. *Physiol Planta* 126:97–109.
- Repetto O, Bestel-Corre G, Dumas-Gaudot E, Berta G, Gianinazzi-Pearson V, Gianinazzi S. 2003. Targeted proteomics to identify cadmium-induced protein modifications in *Glomus mosseae*-inoculated pea roots. *New Phytol* 157:555–567.
- Rhee HJ, Kim GY, Huh JW, Kim SW, Na DS (2000) Annexin I is a stress protein induced by heat, oxidative stress and a sulfhydryl-reactive agent. *Eur J Biochem* 267:3220–3225.
- Riewe D, Grosman L, Fernie AR, Wucke C, Geigenberger P (2008) The potato-specific apyrase is apoplastically localized and has influence on gene expression, growth, and development. *Plant Physiol* 146:1579–1598.
- Rizhsky L, Davletova S, Liang H, Mittler R (2004) The zinc finger protein Zat12 is required for cytosolic ascorbate peroxidase 1 expression during oxidative stress in *Arabidopsis*. *J Biol Chem* 279:11736–11743.
- Rohila JS, Chen M, Chen S, Chen J, Cerny R, Dardick C, Canlas P, Xu X, Gribskov M, Kanrar S et al. (2006) Protein-protein interactions of tandem affinity purification-tagged protein kinases in rice. *Plant Journal* 46:1–13.
- Rouhier N, Jacquot J-P (2005) The plant multigenic family of thiol peroxidases. *Free Radic Biol Med* 38:1413–1421.
- Rudella A, Friso G, Alonso JM, Ecker JR, van Wijk KJ (2006) Down regulation of *ClpR2* leads to reduced accumulation of the *ClpPRS* protease complex and defects in chloroplast biogenesis in *Arabidopsis*. *Plant Cell* 18:1704–1721.

- Sacre SM, Moss SE (2002) Intracellular localization of endothelial cell annexins is differentially regulated by oxidative stress. *Exp Cell Res* 274:254–263.
- Sagi M, Fluhr R (2006) Production of reactive oxygen species by plant NADPH oxidases. *Plant Physiol* 141:336–340.
- Sambrook J, Fritsch EF, Maniatis T (1989) Molecular cloning: a laboratory manual, 2nd edition. Cold spring Harbor Laboratory Press.
- Santoni V, Rouquie D, Doumas P, Mansion M, Boutry M, Degand H, Dupree P, Packman L, Sherrier J, Prime T et al. (1998) Use of a proteome strategy for tagging proteins present at the plasma membrane. *Plant Journal* 16:633–641.
- Schmitt ME, Brown TA, Trumpower BL (1990) A rapid and simple method for preparation of RNA from *Saccharomyces cerevisiae*. *Nucleic Acids Res* 18:3091–3092.
- Schubert R (Ed) (1985) Bioindikation in terrestrischen Ökosystemen. Jena, Gustav Fischer Verlag. 327 pp.
- Seals DF, Parrish ML, Randall SK (1994) A 42-kilodalton annexin-like protein is associated with plant vacuoles. *Plant Physiol* 106:1403–1412.
- Seals DF, Randall SK (1997) A vacuole-associated annexin protein, VCaB42, correlates with the expansion of tobacco cells. *Plant Physiol* 115:753–761.
- Seigneurin-Berny D, Rolland N, Dorne AJ, Joyard J (2000) Sulfolipid is a potential candidate for annexin binding to the outer surface of chloroplast. *Biochem Biophys Res Comm* 272:519–524.
- Shao HB, Liang ZS, Shao MA, Sun Q, Hu ZM (2005) Investigation on dynamic changes of photosynthetic characteristics of 10 wheat (*Triticum aestivum* L.) genotypes during two vegetative-growth stages at water deficits. *Biointerfaces* 43:221–227.
- Sheffield J, Taylor N, Fauquet C, Chen S (2006) The cassava (*Manihot esculenta* Crantz) root proteome: protein identification and differential expression. *Proteomics* 6:1588–1598.
- She YM, Narindrasorasak S, Yang S, Spitale N, Roberts EA, Sarkara B (2003) Identification of metal-binding proteins in human hepatoma lines by immobilized metal affinity chromatography and mass spectrometry. *Mol Cellul Proteom* 2:1306–1318.
- Shin HS, Brown RM (1999) GTPase activity and biochemical characterization of a recombinant cotton fiber annexin. *Plant Physiol* 119:925–934.
- Soler M, Serra O, Molinas M, Huguet G, Fluch S, Figueras M (2007) A genomic approach to suberin biosynthesis and cork differentiation. *Plant Physiol* 144:419–431.
- Stepien P, Johnson GN (2009) Contrasting responses of photosynthesis to salt stress in the glycophyte *Arabidopsis* and the halophyte *Thellungiella*: role of the plastid terminal oxidase as an alternative electron sink. *Plant Physiol* 149:1154–1165.

- Szilak L, Moitra J, Krylov D, Vinson C (1997) Phosphorylation destabilizes-helices. *Nat Struct Biol* 4:112–114.
- Takahashi M, Asada K (1988) Superoxide production in aprotic interior of chloroplast thylakoids. *Arch Biochem Biophys* 267:714–722.
- Talukdar T, Gorecka KM, de Carvalho-Niebel F, Downie JA, Cullimore J, Pikula S (2009) Annexins- calcium- and membrane-binding proteins in the plant kingdom. Potential role in nodulation and mycorrhization in *Medicago truncatula*. *Acta Biochim Polon* 56:199–210.
- Tang L, Bhat S, Petracek ME (2003) Light control of nuclear gene mRNA abundance and translation in tobacco. *Plant Physiol* 133:1979–1990.
- Thonat C, Mathieu C, Crevecoeur M, Penel C, Gaspar T, Boyer N (1997) Effects of a mechanical stimulation on localization of annexin-like proteins in *Bryonia dioica* internodes. *Plant Physiol* 114:981–988.
- Truman W, Bennett MH, Kubigsteltig I, Turnbull C, Grant M (2007) *Arabidopsis* systemic immunity uses conserved defense signaling pathways and is mediated by jasmonates. *PNAS, USA* 104:1075–1080.
- Tuomainen M, Tervahauta A, Hassinen V, Schat H, Koistinen KM, Lehesranta S, Rantalainen K, Häyrinen J, Auriola S, Anttonen M et al. (2010) Proteomics of *Thlaspi caerulescens* accessions and an interaccession cross segregating for zinc accumulation. *J Exper Bot* 61:1075–1087.
- Vaahtera L, Brosché M (2011) More than the sum of its parts- how to achieve a specific transcriptional response to abiotic stress. *Plant Sci* 180:421–430.
- Vandeputte O, Lowe YO, Burssens S, van Raemdonck D, Hutin D, Boniver D, Geelen D, El Jaziri M, Baucher M (2007) The tobacco *Ntann12* gene, encoding an annexin, is induced upon *Rhodococcus fascians* infection and during leafy gall development. *Mol Plant Pathol* 8:185–194.
- Vanhoudt N, Vandenhove H, Horemans N, Wannijn J, Bujanic A, Vangronsveld J, Cuypers A (2010) Study of oxidative stress related responses induced in *Arabidopsis thaliana* following mixed exposure to uranium and cadmium. *Plant Physiol Biochem* 48:879–886.
- Vellosillo T, Martínez M, López MA, Vicente J, Cascón T, Dolan L, Hamberg M, Castresana C (2007) Oxylipins produced by the 9-lipoxygenase pathway in *Arabidopsis* regulate lateral root development and defense responses through a specific signaling cascade. *Plant Cell* 19:831–846.
- Waller F, Riemann M, Nick P (2002) A role for actin-driven secretion in auxin-induced growth. *Protoplasma* 219:72–81.

- Wang Y, Ohara Y, Nakayashiki H, Tosa Y, Mayama S (2005) Microarray analysis of the gene expression profile induced by the endophytic plant growth-promoting rhizobacteria *Pseudomonas fluorescens* FPT9601-T5 in *Arabidopsis*. *Mol Plant Microbe Inter* 18:385–396.
- Watkinson JJ, Sioson AA, Vasquez-Robinet C, Shukla M, Kumar D, Ellis M, Heath LS, Ramakrishnan N, Chevone B, Watson LT et al. (2003) Photosynthetic acclimation is reflected in specific patterns of gene expression in drought-stressed loblolly pine. *Plant Physiol* 133:1702–1716.
- Weber M, Trampczynska A, Clemens S (2006) Comparative transcriptome analysis of toxic metal responses in *Arabidopsis thaliana* and the Cd²⁺-hypertolerant facultative metallophyte *Arabidopsis halleri*. *Plant Cell Environ* 29:950–963.
- Wienkoop S, Saalbach G (2003) Proteome analysis. Novel proteins identified at the peribacteroid membrane from *Lotus japonicus* root nodules. *Plant Physiol* 131:1080–1090.
- Wong C-M, Zhou Y, Raymond WM Ng, Kung H-fu, Jin D-Y (2002) Cooperation of yeast peroxiredoxins *Tsa1p* and *Tsa2p* in the cellular defense against oxidative and nitrosative stress. *J Biol Chem* 277:5385–5394.
- Xiao F, Tang X, Zhou J-M (2001) Expression of 35S::Pto globally activates defense-related genes in tomato plants. *Plant Physiol* 126:1637–1645.
- Xin Z, Zhao Y, Zheng Z-L (2005) Transcriptome analysis reveals specific modulation of abscisic acid signaling by ROP10 small GTPase in *Arabidopsis*. *Plant Physiol* 139:1350–1365.
- Yan Y, Stolz S, Chételat A, Reymond P, Pagni M, Dubugnon L, Farmer EE (2007) A downstream mediator in the growth repression limb of the jasmonate pathway. *Plant Cell* 19:2470–2483.
- Yang P, Li X, Wang X, Chen H, Chen F, Shen S (2007) Proteomic analysis of rice (*Oryza sativa*) seeds during germination. *Proteomics* 7:3358–3368.
- Yang S, Zeng X, Li T, Liu M, Zhang S, Gao S, Wang Y, Peng C, Li L, Yang C (2012) AtACD1, an ABC1-like kinase gene, is involved in chlorophyll degradation and the response to photooxidative stress in *Arabidopsis*. *J Experl Bot* 63:3959–3973.
- Yang Y-W, Bian SM, Yao Y, Liu YJ (2008) Comparative proteomic analysis provides new insights into the fiber elongating process in cotton. *J Proteom Res* 7:4623–4637.
- Zhang Y, Wang Q, Zhang X, Liu X, Wang P, Hou Y (2011) Cloning and characterization of an annexin gene from *Cynanchum komarovii* that enhances tolerance to drought and *Fusarium oxysporum* in transgenic cotton. *J Plant Biol* 54:303–313.

- Zhou L, Duan J, Wang X-M, Zhang H-M, Duan M-X, Liu J-Y (2011) Characterization of a novel annexin gene from cotton (*Gossypium hirsutum* cv CRI 35) and antioxidative role of its recombinant protein. *J Inte Plant Biol* 53:347–357.
- Zhou M-L, Yang X-B, Zhang Q, Zhou M, Zhao E-Z, Tang Y-X, Zhu X-M, Shao J-R, Wu Y-M (2013) Induction of annexin by heavy metals and jasmonic acid in *Zea mays*. *Funct Inte Genom* 13:241–251.

Prominent achievements

Presented a talk in Indo-German Grand Science Slam organized by German House for Research & Innovation (DWIH, New Delhi) in collaboration with DFG held on 27th October 2012 at the Indo-German Urban Mela in New Delhi.

Selected for presentation in Gordon Research Conference on “Salt and water stress in Plants” held from June 24, 2012 to June 29, 2012 at the Chinese University of Hong Kong, Hong Kong, China.

Invited as Visiting Scholar in Prof. Karl-Josef Dietz group, Department of Biochemistry and Physiology of Plants, University of Bielefeld, Germany, with scholarship awarded by The Collaborative Research Center SFB 613 (Physics of Single molecule processes and molecular recognition in organic systems) from June 2011 to August 2011.

Presented in Keystone symposia on “Plant Abiotic Stress Tolerance Mechanisms, Water and Global Agriculture” held from January 17, 2011 to January 22, 2011 at Keystone, Colorado, USA.

Awarded Keystone Symposia Scholarship associated with the meeting on “Plant Abiotic Stress Tolerance Mechanisms, Water and Global Agriculture” held from January 17, 2011 to January 22, 2011 at Keystone, Colorado, USA.

Qualified “General Course on Intellectual Property” organized by World Intellectual Property Organization (WIPO) held from October 1, 2010 to November 15, 2010.

Selected in DST-DAAD project in collaboration between University of Hyderabad and University of Gießen to work with the group of Prof. Dr. Karl-Heinz Kogel, Institute of Phytopathology and Applied Zoology, University of Gießen, Germany, from February’ 2010 to March’ 2010.

Awarded “DAAD Short term fellowship For PhD Registered Scholars”, 2008, to work under the supervision of Dr. Andrea Viehhauser in Department of Biochemistry and Physiology of Plants, University of Bielefeld, Germany, from June’ 09 to November’ 09 [Desk No. 425, Code No. A/08/74472].
